29th Annual Fall Field *Frolic!!*

Department of Geological Sciences
California State University Northridge
August 24-27, 2011

Tuweep, or not Tuweep, that is the question…

Zion N.P | Coral Pink Sand | Tuweep, AZ

Campsites:

Wednesday Aug. 24 – Zion National Park, Utah

Thursday Aug. 25 – Coral Pink Sand Dunes State Park, Utah

Friday Aug. 26 – Tuweep (a.k.a. Toroweap), Grand Canyon National Park, 3000 vertical feet above the Colorado River!

Rough itinerary: Depart 8 a.m. on the 24th, return late afternoon of the 27th. Highlights include Zion Narrows hike (weather permitting); coral… pink… sand… dunes!!!; Lava falls, Grand Canyon stratigraphic section, and much more!

Trip Leaders: R. Heermance, D. Liggett, and D. Yule

Contact Mari Flores (mari.flores@csun.edu; 818-677-3541) by Aug. 1, 2011 to reserve a spot. A $25 deposit is required.

Field Frolic 2011 Table of Contents

To Weep or not Tuweep. Field Frolic Itinerary 2011

The 2011 Fall Field Frolic will travel ~1000 miles from Los Angeles into the southwestern corner of the Colorado Plateau. During our travels, we will observe Paleozoic and Mesozoic strata, Quaternary volcanoes and faults, and impressive sand dunes and canyons.

ITINERARY (subject to change)

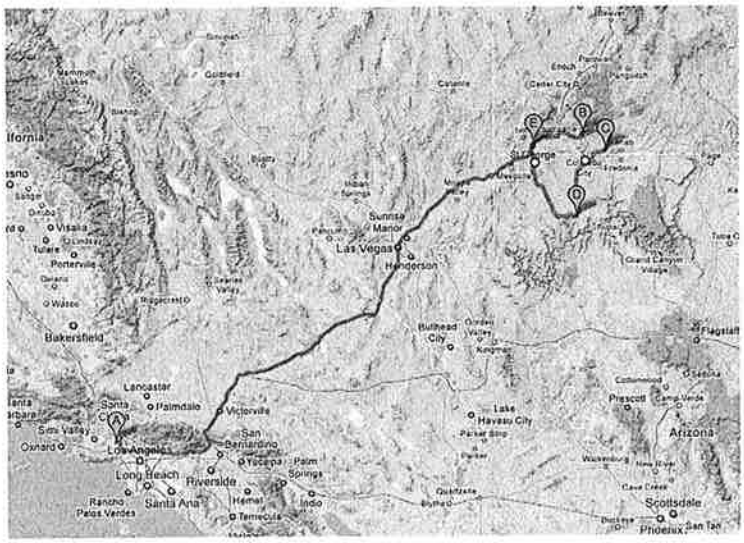

DAY 1 (Wed, Aug 24):

Depart CSUN (A) at 8 AM and drive east on 210 along the southern edge of the San Gabriel Mts. Turn north on I-15 and cross the San Andreas Fault just south of Cajon Pass between the San Gabriel and San Bernardino Mts. We will continue across the Mojave Desert, stopping for lunch in Baker, CA. After lunch we will continue on I-15 through Las Vegas and St. George, arriving in Zion National Park (B) in the late afternoon. The afternoon and evening can be spent walking in the Zion Narrows, swimming in the Virgin River, visiting the Zion Visitor Center, or hanging out at camp.

DAY 2 (Th, Aug 25):

Return to Zion Canyon to discuss the stratigraphy and formation of the area. If time allows, we will take one of the many hikes within Zion Canyon. ~11 AM we will drive towards the eastern park entrance and stop for lunch at Checkerboard Mesa. After lunch, we will continue on towards Mt. Carmel Junction, stopping to investigate Cretaceous strata along the way. We will arrive Coral Pink Sand Dunes State Park (C) in the mid-afternoon in time to explore the area.

DAY 3 (Fr, Aug 26):

Drive south from the sand dunes towards Tuweep (D) on the inner gorge of the Grand Canyon. The plan is to arrive in the late morning, and spend the day exploring the Quaternary volcanoes, viewing the stratigraphy of the Grand Canyon, and discussing the complex (and controversial) history of the area.

DAY 4 (Sat, Aug 27):

Drive to St. George, UT (E), with a stop at the Hurricane Fault. We'll stop for lunch outside of St. George, and depart for home in the early afternoon.

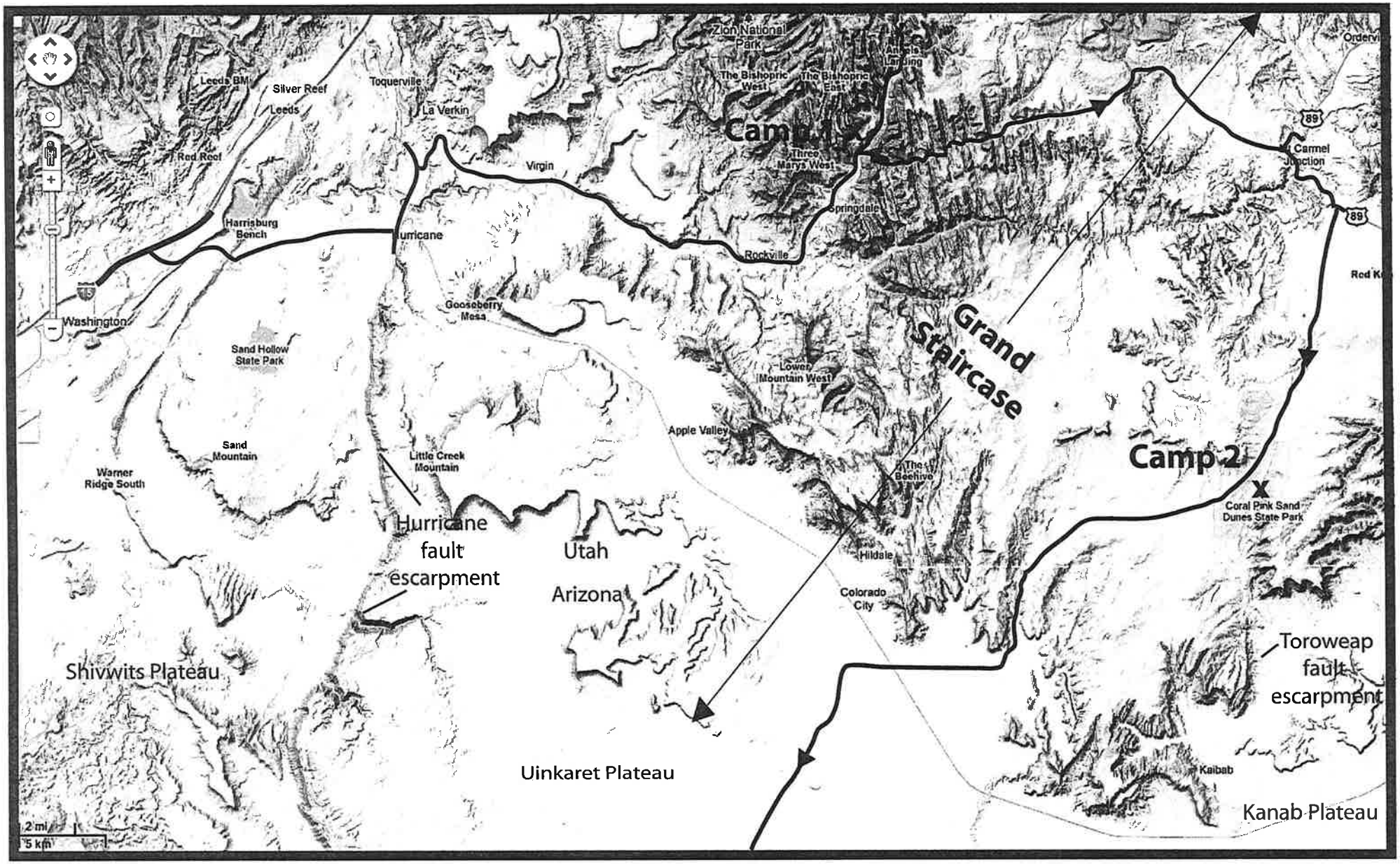
Zion National Park
The Bishopric West
The Bishopric East
Camp 1
Three Marys West
Springdale
Rockville
Virgin
Leeds BM
Silver Reef
Leeds
Toquerville
La Verkin
Red Reef
Harrisburg Bench
Hurricane
Washington
Gooseberry Mesa
Sand Hollow State Park
Sand Mountain
Warner Ridge South
Little Creek Mountain
Hurricane fault escarpment
Utah
Arizona
Shivwits Plateau
Uinkaret Plateau
Grand Staircase
Lower Mountain West
Apple Valley
The Beehive
Camp 2
Coral Pink Sand Dunes State Park
Hildale
Colorado City
Toroweap fault escarpment
Kaibab
Kanab Plateau
Camel Junction
89
2 mi
5 km

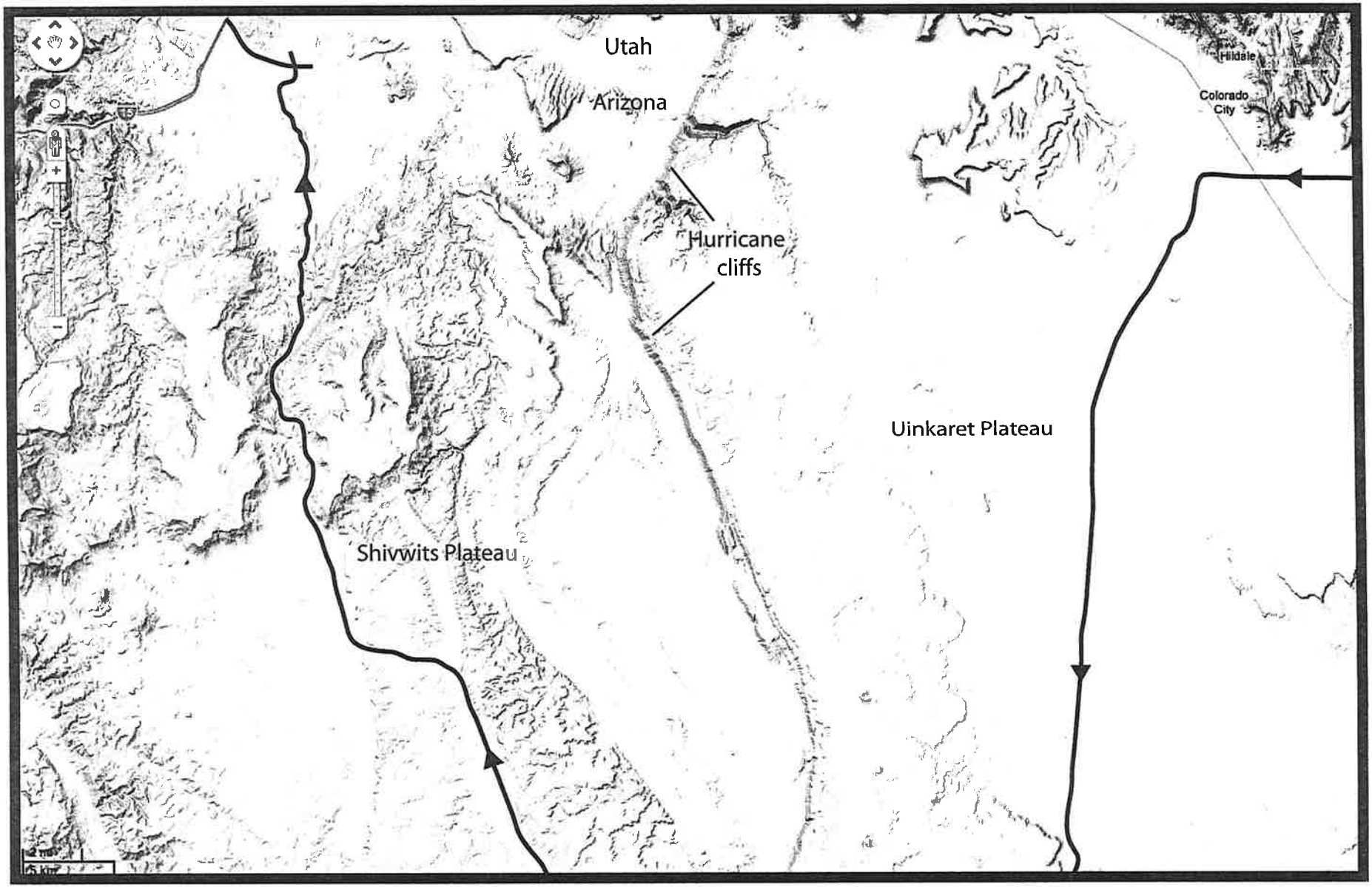
Utah
Arizona
Hildale
Colorado City
Hurricane cliffs
Uinkaret Plateau
Shivwits Plateau

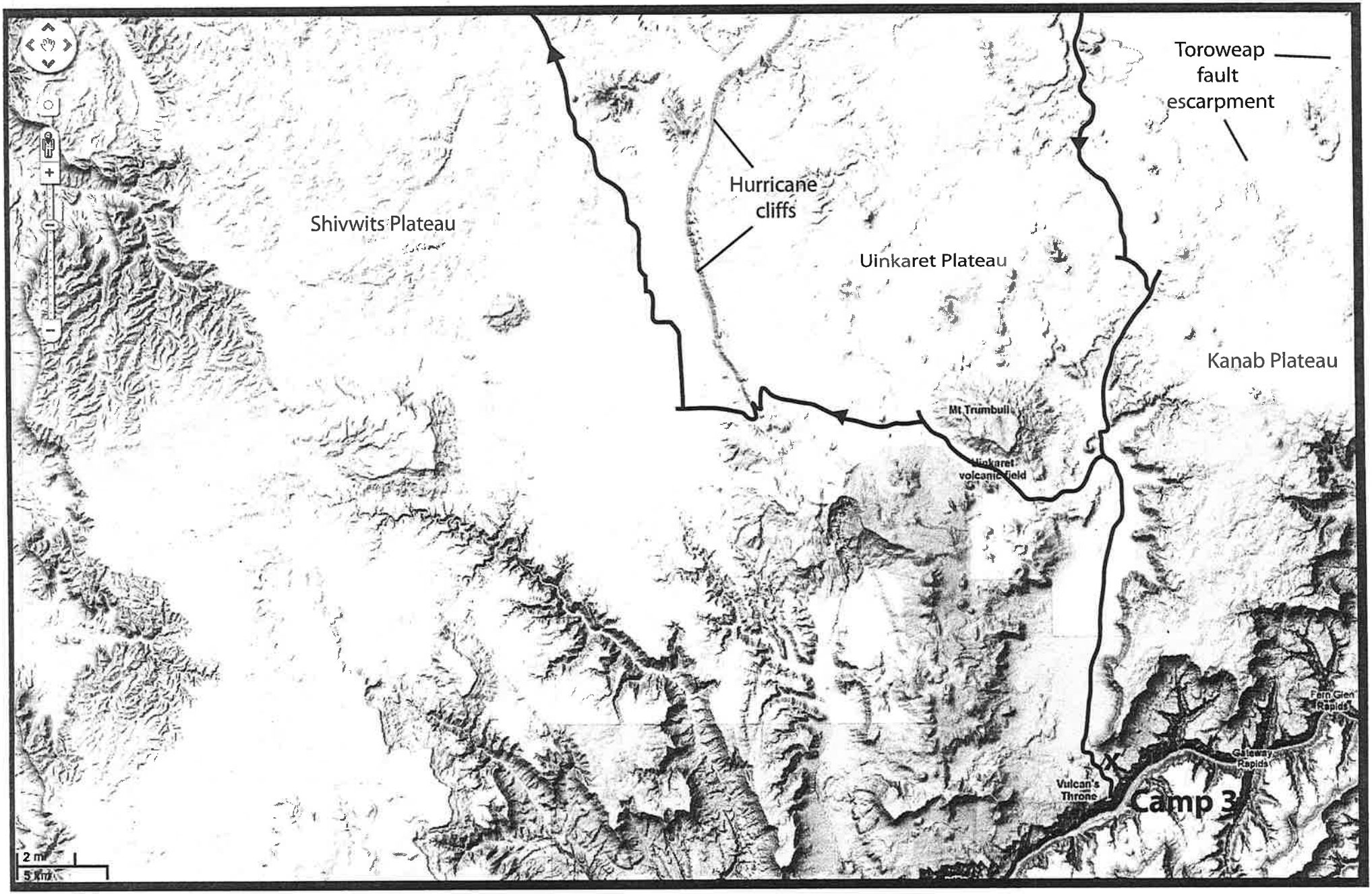
Toroweap
fault
escarpment
Hurricane
cliffs
Shivwits Plateau
Uinkaret Plateau
Kanab Plateau
Mt Trumbull
Uinkaret
volcanic field
Fern Glen
Rapids
Gateway
Rapids
Vulcan's
Throne
Camp 3
2 mi
5 km

Figure 9–11. Topography of the Basin and Range Province, western United States, part of a shaded-relief image prepared by Thelin and Pike (1991) by digitizing elevation values at intervals of 805 m and illuminating the resulting digital elevation model from the west-northwest, 25° above the horizon. North is approximately toward the top of page. Vertical exaggeration 2×. Black area at upper right is Great Salt Lake; flat area farther north is Snake River Plain (cf. Fig. 9–12). Basin and Range Province extends from Wasatch fault, east of Great Salt Lake, to eastern front of Sierra Nevada (lower left corner). Albers Equal-Area Conic Projection.

Virgin River Gorge; Boundary between the Colorado Plateau and the Great Basin in northwestern Arizona

R. L. Langenheim, Jr., Department of Geology, 245 NHB, 1301 West Green Street, University of Illinois, Urbana, Illinois 61801
M. K. Schulmeister, Illinois State Water Survey, 101 Island Avenue, Batavia, Illinois 60510

LOCATION

The Virgin River Gorge and one of its tributaries are traversed by I-15 between milepost 12, about 13 mi (21 km) east of Mesquite, Nevada, and Milepost 28, about 12 mi (19 km) west of St. George, Utah (Fig. 1). Geologic features are readily observable from the road and from a scenic viewpoint in the Virgin River Canyon Recreation Area, which is entered from an interchange between mileposts 18 and 19. The site is in the northern half of the Purgatory Canyon, Arizona, 7½-minute Quadrangle and in the northeastern quarter of the Littlefield, Arizona, 15-Minute Quadrangle.

SIGNIFICANCE

The Virgin River crosses the boundary between the Colorado Plateau and the Basin and Range physiographic province in a deep gorge separating the Beaverdam Mountains and Virgin Mountains (Fig. 1). Little-deformed, nearly flat-lying rocks of the westernmost plateau are well exposed east of the "Narrows." The gorge cuts across a broad anticline broken by numerous basin-and-range–type faults. The Grand Wash fault, the western boundary of the Colorado Plateau, is not obvious from the road, but is well exposed. The Beaver Dam–Virgin Mountain block is separated from the intermountain valley containing Beaverdam Wash and the Virgin River by a major range-front fault at the lower end of the Narrows. Late Cambrian through Middle Permian rocks exposed in the gorge (Fig. 1) are characteristic of the transition from miogeosynclinal deposition, dominant to the northwest, and platform deposits on the plateau to the east. In addition, the Narrows is a fine example of the results of accelerated erosion that accompanied elevation of the Colorado Plateau and extensional deformation in the Basin and Range during the late Tertiary and Quaternary. Ancient channel and terrace deposits are prominent in the gorge. Classic alluvial fans, basin-filling deposits, and caliche crusts border the west face of the Beaver Dam-Virgin Mountains and the intermontane valley to the west.

SITE DESCRIPTION

Late and Middle Cambrian Bonanza King Dolomite, Dunderberg Shale, and Nopah Dolomite, Late Devonian Muddy Peak Limestone, Mississippian Monte Cristo Group, and Mississippian-Pennsylvanian Callville Limestone crop out along the road in the Narrows between milepost 12.8 at the western end of the gorge and milepost 17.3, where the Sullivans Canyon and Cedar Wash faults cross the highway (Fig. 1).

The Cambrian Bonanza King Dolomite and Nopah Dolomite crop out in steep rounded cliffs and benches and the intervening Dunderberg Shale forms the most prominent of the benches between mileposts 13.5 and 16.8 (Figs. 1, 2). The Bonanza King Dolomite in the vicinity of the gorge is brown-weathering, fine- to medium-grained dolomite with 33 ft (9 m) of interbedded limestone and dolomite resting on a notably glauconitic layer near the top (Steed, 1980). The glauconitic layer forms a notable bench and is exposed in a road cut at milepost 15.8. The Dunderberg Shale, thinly interbedded green shale and dolomite, is cleanly exposed in roadcuts near mileposts 13.9 and 16.8. The Nopah Dolomite is mostly very fine-grained, light-gray dolomite, and weathers somewhat ligher brown than the underlying Bonanza King Dolomite.

Cambrian rocks of the Virgin Gorge are at the southeastern limit of characteristic Middle and Late Cambrian miogeosynclinal or carbonate platform deposits. The same formations crop out in the Mormon Mountains, the first range to the northwest, where the mostly Middle Cambrian Bonanza King Dolomite is 1,914 ft (580 m) thick and the Late Cambrian Nopah Dolomite is 627 ft (190 m) thick (Wernicke and others, 1984). Farther northwest, these units are two or three times as thick. Cambrian rocks to the east on the platform differ greatly; they consist of the basal Tapeats Sandstone, a middle Bright Angel Shale, and an upper argillaceous Muav Limestone along the Grand Canyon (McKee and Resser, 1945). The Grand Canyon rocks, however, are all older than those in the Virgin Gorge; late-Middle Cambrian and Late Cambrian rocks have been removed by erosion at the canyon.

The hiatus at the post-Nopah Dolomite unconformity in the Virgin Gorge is represented by some of the uppermost Nopah Dolomite, the Ordovician Pogonip Dolomite, Eureka Quartzite, Ely Springs Dolomite, and, probably, part of the basal Devonian sequence in the Mormon Mountains—more than 1,221 ft (370 m) of rock (Wernicke and others, 1984). Farther west, in the Arrow Canyon Range, 649.5 ft (197 m) of Silurian Laketown Dolomite and Early and Middle Devonian Piute Formation intervene between the Ely Springs Dolomite and Late Devonian rocks. All of these rocks are absent along the Grand Canyon to the southeast.

Late Devonian Muddy Peak Limestone crops out in the slope of ledges and cliffs just below the high, sheer cliffs of the Monte Cristo Group on the north wall of the Narrows between mileposts 13.5 and 16.8 (Figs. 1, 2, 3). On the south wall of the canyon the Muddy Peak Limestone outcrop, as well as that of the Monte Cristo Group, is visible from the road between milepost 13.5 and 14.3. The lower part of the Muddy Peak Limestone is

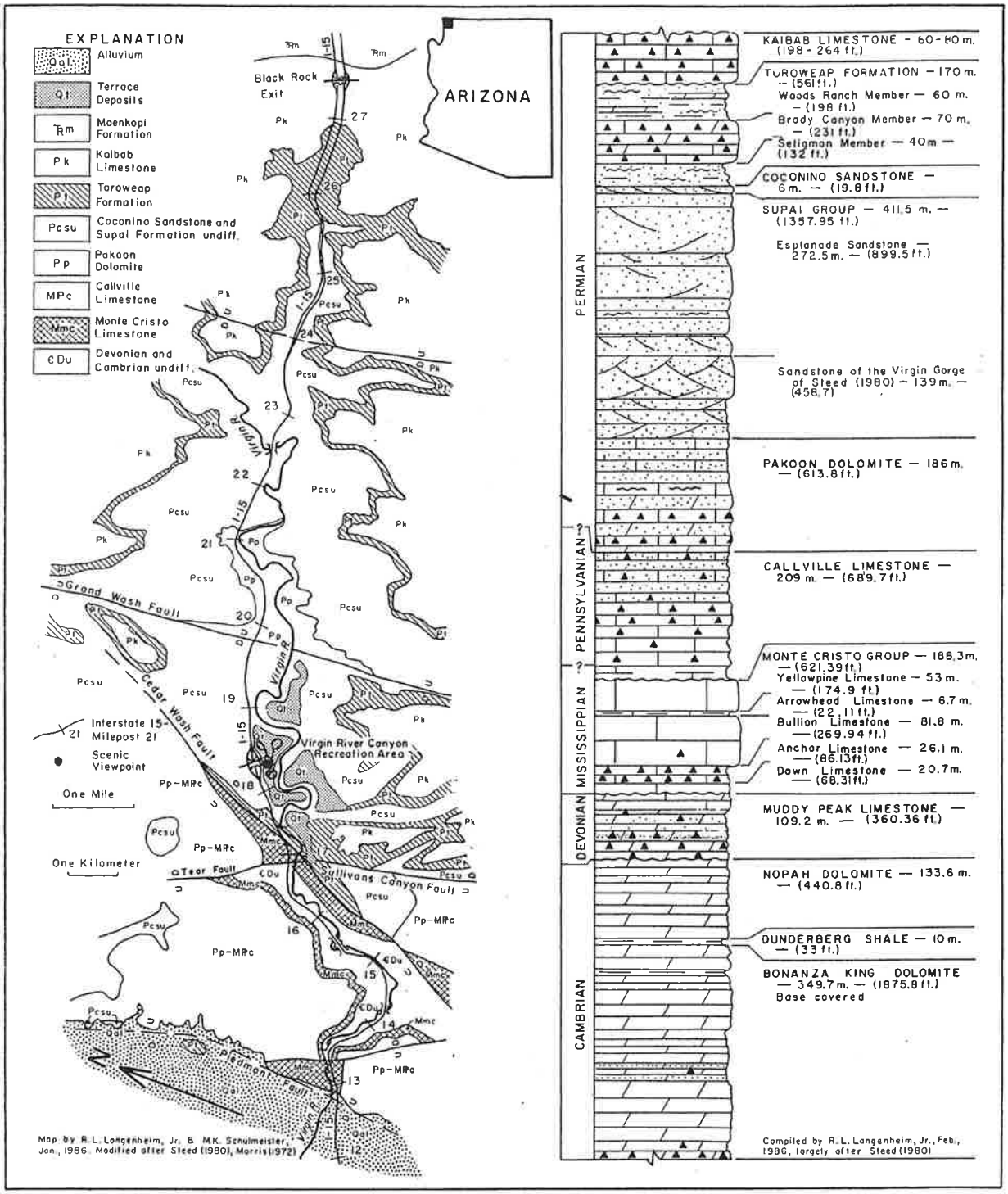

Figure 1. Geologic map and columnar section of rocks exposed along I-15 between mileposts 12 and 27, Arizona.

almost entirely medium-grained dolomite, but includes fairly prominent nodular layers of flint and rusty-weathering quartzite (Steed, 1980). The flint and quartzite distinguish the formation from the underlying Nopah Dolomite. The upper part of the Muddy Peak Limestone is lighter colored, includes substantial amounts of limestone, and is, in part, fine grained (Steed, 1980).

Devonian rocks thin on the platform to the southeast and only scattered remnants of Temple Butte Limestone occur in the eastern part of the Grand Canyon. To the northwest, Devonian rocks thicken substantially and Early and Middle Devonian sed-

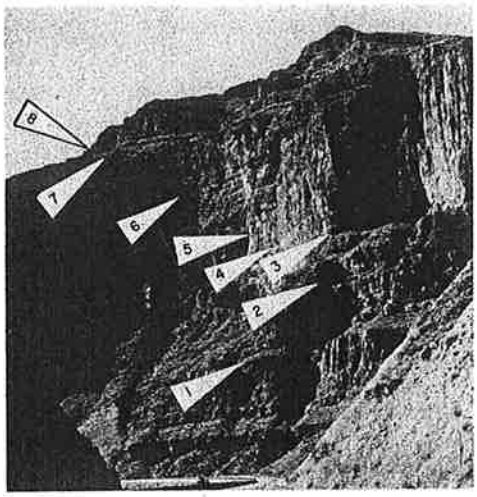

Figure 2. Late Cambrian through Early Pennsylvanian rocks, view down the canyon from milepost 17. 1 = bench formed by Dunderberg Shale, 2 = base of Muddy Peak Limestone, 3 = base of Dawn Limestone, 4 = base of Anchor Limestone, 5 = base of Bullion Limestone, 6 = Arrowhead Limestone, 7 = base of Callville Limestone, and 8 = top of shaley basal part of Callville Limestone.

Figure 3. View west-southwest across the Cedar Wash fault from "Scenic Viewpoint" in the Virgin River Recreation Area. The Esplanade Sandstone, Coconino Sandstone, and the Brushy Canyon and Seligman Members of the Toroweap Formation are exposed in the foreground and in the prominent butte in the middle of the picture. Cliffs behind are on the upthrown block of the Cedar Wash fault and expose Cambrian through Mississippian rocks. The Callville Limestone and Permian rocks crop out along the skyline. 1 = base of Toroweap Formation. The Coconino Sandstone is the thin, white, cliffy ledge just below the contact. 2 = base of Monte Cristo Group, 3 = base of shaley bench in lowermost Callville Limestone, and 4 = base of ledge and cliff sequence in the Callville Limestone. Smooth slopes rising to the top of the ridge on the right include Pakoon Dolomite and Supai Group outcrops.

iments are also present. Wernicke and others (1984) reported 726 ft (220 m) of Sultan Limestone in the Mormon Mountains, and Langenheim and others (1962) cited 1970 ft (597 m) of Devonian rocks in the Arrow Canyon Range.

The Early and Middle Mississippian Monte Cristo Group crops out in a high, sheer cliff that rises precipitously above the ledge and slope exposures of the Muddy Peak Limestone (Figs. 1, 2, 3). The Yellowpine, Arrowhead, and Bullion Limestones are cleanly exposed in a roadcut from milepost 12.8 through 13.4. Prominent coral biostromes crop out in the vicinity of milepost 13. The lowermost Dawn Limestone is dominantly medium- to coarse-grained limestone with minor interbedded dolomite (Steed, 1980). The formation is chert free, and rests unconformably on the underlying Muddy Peak Limestone. The Anchor Limestone is sharply delineated by abundant nodular chert interbedded with fine- to coarse-grained bioclastic limestone. The chert weathers dark brown or black, and the unit forms either an indentation in the Monte Cristo cliff or a minor bench. The overlying Bullion Limestone is predominantly very thick-bedded, coarse-grained, bioclastic limestone and comprises most of the sheer cliff. The Arrowhead Limestone is composed of thin nodular bioclastic limestone beds separated by shale breaks. It is readily identified from a distance because it crops out as a light-colored, narrow stripe two-fifths of the way down the brown, sheer cliff. The uppermost formation of the Monte Cristo Group, the Yellowpine Limestone, is thick-bedded, medium- to coarse-grained limestone in the lower half and very fine-grained, somewhat thinner bedded limestone in the upper portion. The formation makes up the upper two-fifths of the sheer cliff and is abruptly succeeded by bench-forming basal Callville Limestone.

The Dawn Limestone correlates with the Whitmore Wash Member of the Redwall Limestone on the platform to the southeast. The Anchor Limestone correlates with the Thunder Springs Member, the Bullion Limestone with the Mooney Falls Member, and the Arrowhead and Yellowpipe Limestones with the Horseshoe Mesa Member. These units are strikingly uniform and continuous across the miogeosynclinal-platform boundary, in marked contrast to patterns in the pre-Mississippian sequence and in the Carboniferous and pre-Toroweap Limestone rocks above the Monte Cristo or Redwall Limestone. The Redwall Limestone thins from about 490.5 ft (148.6 m) in the eastern Grand Canyon (McKee and Gutschick, 1969) and the Monte Cristo Group thickens to 924 ft (280 m) in the Mormon Mountains (Wernicke and others, 1984).

The Late Mississippian and Pennsylvanian Callville Limestone is not exposed at the roadside, but crops out above the Monte Cristo Group north of the highway from the lower entrance of the Narrows to the Cedar Wash fault (Fig. 1), and south of the highway from the lower entrance of the Narrows to milepost 14.4. The basal 62.7 ft (19 m) of the Callville Limestone crops out in a well-defined bench separating the cliff of the Monte Cristo Limestone from the markedly cyclic low cliff and bench succession above. This covered slope is underlain by interbedded thin limestone and argillaceous beds (Steed, 1980). Very fine-grained limestone, with chert in nodules and nodular layers, in-

JOURNAL OF GEOPHYSICAL RESEARCH, VOL. 108, NO. B4, 2199, doi:10.1029/2001JB000682, 2003

Comparison of geodetic and geologic data from the Wasatch region, Utah, and implications for the spectral character of Earth deformation at periods of 10 to 10 million years

Anke M. Friedrich,[1] Brian P. Wernicke, and Nathan A. Niemi[2]
Division of Geological and Planetary Sciences, California Institute of Technology, Pasadena, California, USA

Richard A. Bennett and James L. Davis
Smithsonian Astrophysical Observatory, Harvard University, Cambridge, Massachusetts, USA

Received 22 June 2001; revised 2 June 2002; accepted 21 November 2002; published 15 April 2003.

[1] The Wasatch fault and adjacent fault zones provide an opportunity to compare present-day deformation rate estimates obtained from space geodesy with geologic displacement rates over at least four temporal windows, ranging from the last millennium up to 10 Myr. The three easternmost GPS sites of the Basin and Range Geodetic Network (BARGEN) at this latitude define a ~130-km-wide region spanning three major normal faults extending east-west at a total rate of 2.7 ± 0.4 mm/yr, with an average regional strain rate estimated to be 21 ± 4 nstrain/yr, about twice the Basin and Range average. On the Wasatch fault, the vertical component of the geologic displacement rate is 1.7 ± 0.5 mm/yr since 6 ka, <0.6 mm/yr since 130 ka, and 0.5–0.7 mm/yr since 10 Ma. However, it appears likely that at the longest timescale, rates slowed over time, from 1.0 to 1.4 mm/yr between 10 and 6 Ma to 0.2 to 0.3 mm/yr since 6 Ma. The cumulative vertical displacement record across all three faults also shows time-variable strain release ranging from 2 to 4 mm/yr since 10 ka to <1 mm/yr averaged over the past 130 kyr. Conventional earthquake recurrence models ("Reid-type" behavior) would require an accordingly large variation in strain accumulation or loading rate on a 10-kyr timescale, for which there appears to be no obvious geophysical explanation. Alternatively, seismic strain release, given a wide range of plausible constitutive behaviors for frictional sliding, may be clustered on the 10-kyr timescale, resulting in the high Holocene rates, with comparatively low, uniform strain accumulation rates on the 100-kyr timescale ("Wallace-type" behavior). The latter alternative, combined with observations at the million-year timescale and the likelihood of a significant contribution of postseismic transients, implies maxima of spectral amplitude in the velocity field at periods of ~10 Myr (variations in tectonic loading), ~10 kyr (clustered strain release), and of 100 years (postseismic transients). If so, measurements of strain accumulation and strain release may be strongly timescale-dependent for any given fault system. *INDEX TERMS:* 1208 Geodesy and Gravity: Crustal movements—intraplate (8110); 1243 Geodesy and Gravity: Space geodetic surveys; 7209 Seismology: Earthquake dynamics and mechanics; 8107 Tectonophysics: Continental neotectonics; 8109 Tectonophysics: Continental tectonics—extensional (0905); *KEYWORDS:* geodetic, geologic, fault slip rate, normal fault, timescale, earthquake cycle

Citation: Friedrich, A. M., B. P. Wernicke, N. A. Niemi, R. A. Bennett, and J. L. Davis, Comparison of geodetic and geologic data from the Wasatch region, Utah, and implications for the spectral character of Earth deformation at periods of 10 to 10 million years, *J. Geophys. Res.*, *108*(B4), 2199, doi:10.1029/2001JB000682, 2003.

1. Introduction

[2] Geodetic data and geological displacement rate data are the observational basis for physical models of the earthquake deformation cycle and the assessment of seismic hazards. In the simplest model, the elastic strain energy accumulated across locked faults is periodically released during earthquakes of relatively uniform slip and recurrence interval, each of which releases the strain energy accumulated since the last earthquake (Figure 1a) [*Reid*, 1910; *Savage and Burford*, 1973; *Scholz*, 1990]. In this model, far-field displacement, which is proportional to strain accumulation, occurs at a uniform rate and is equal to the displacement rate recorded by earthquakes on the fault.

[1]Now at Institute of Geosciences, Potsdam University, Golm, Germany.
[2]Now at Institute for Crustal Studies, University of California, Santa Barbara, California, USA.

0148-0227/03/2001JB000682$09.00

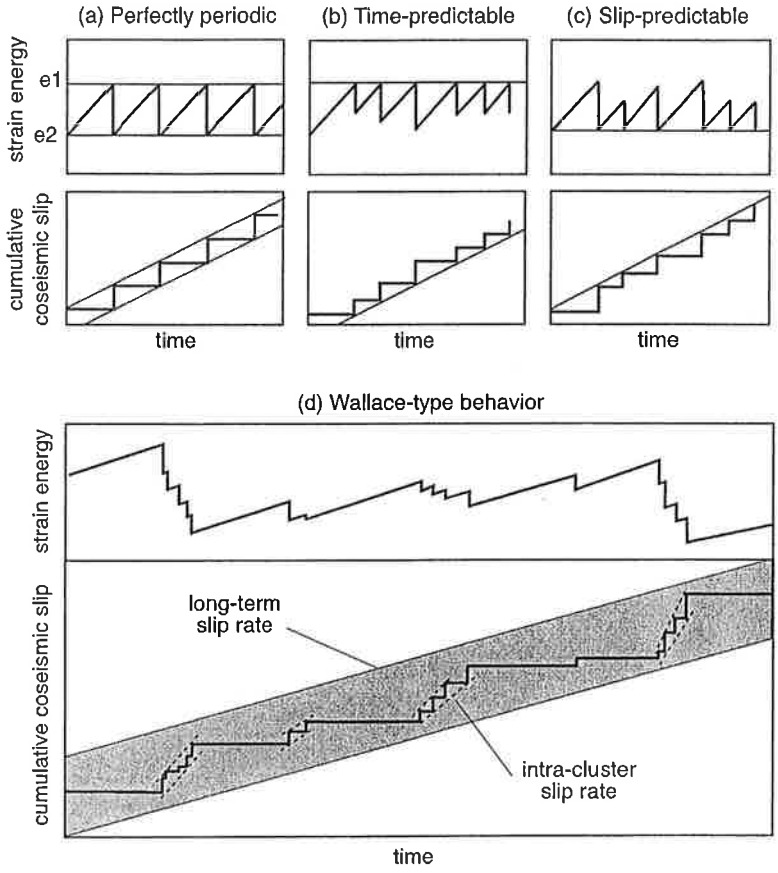

Figure 1. Strain release models for earthquakes (Figures 1a–1c are redrawn after *Scholz* [1990]). (a) Perfectly periodic model [*Reid*, 1910], (b) time-predictable model where the size of the last earthquake predicts the time of the next earthquake [*Shimazaki and Nakata*, 1980], and (c) slip-predictable model where the time since the last earthquake predicts the size of the next earthquake [e.g., *Shimazaki and Nakata*, 1980]. (d) Clustered strain release and uniform, low strain accumulation, modified after *Wallace* [1987]. See color version of this figure in the HTML.

This model was modified to account for the fact that the interseismic interval and the size of earthquakes on a particular fault are not perfectly periodic [e.g., *Shimazaki and Nakata*, 1980]. One variant is the "time-predictable" model where each event occurs when a critical amount of strain energy has accumulated (Figure 1b). In this model, the slip rate and the size of the last earthquake predict the time, but not the size, of the next earthquake. Another variant is the "slip-predictable" model where for any given event, all strain energy accumulated since the last earthquake is released. In this model, the slip rate and the time since the last earthquake are combined to predict the size, but not the time, of the next event (Figure 1c).

[3] In terms of both earthquake physics and hazards analysis, models such as these beg the question [*Wallace*, 1987; *Ward*, 1998]: Is the strain release rate of some small number of earthquakes equal to the long-term strain accumulation rate applied to faults? All three models assume a constant rate of far-field displacement and strain accumulation, and therefore predict that well-constrained slip histories, determined over several earthquake cycles, will agree with contemporary interseismic measurements of far-field displacement. The question is complicated, however, by the fact that it is not clear to what degree both strain accumulation and release are influenced by local stress diffusion within a viscous or viscoelastic substrate due to each event [e.g., *Foulger et al.*, 1992; *Hager et al.*, 1999; *Kenner and Segall*, 2000; *Wernicke et al.*, 2000]. Here we evaluate these issues through comparison of recently acquired geodetic data with displacement rates derived from paleoseismic and other geologic data for the Wasatch and related faults, which are among the best characterized Quaternary fault systems in the world [e.g., *Machette et al.*, 1992a].

[4] For the Wasatch and a number of other fault zones, an important consideration in comparing deformation rates on different timescales is that strain release may occur during "clusters" of earthquakes, wherein recurrence intervals are as much as an order of magnitude shorter than during quiescent periods between clusters [*Wallace*, 1987; *Swan*, 1988; *Sieh et al.*, 1989; *McCalpin and Nishenko*, 1996; *Grant and Sieh*, 1994; *Marco et al.*, 1996; *Zreda and Noller*, 1998; *Rockwell et al.*, 2000]. Clustering is consistent with the time-predictable and slip-predictable behavior. However, because slip per event for most well-documented fault segments does not appear to be highly variable [e.g., *Schwartz and Coppersmith*, 1984], these models require

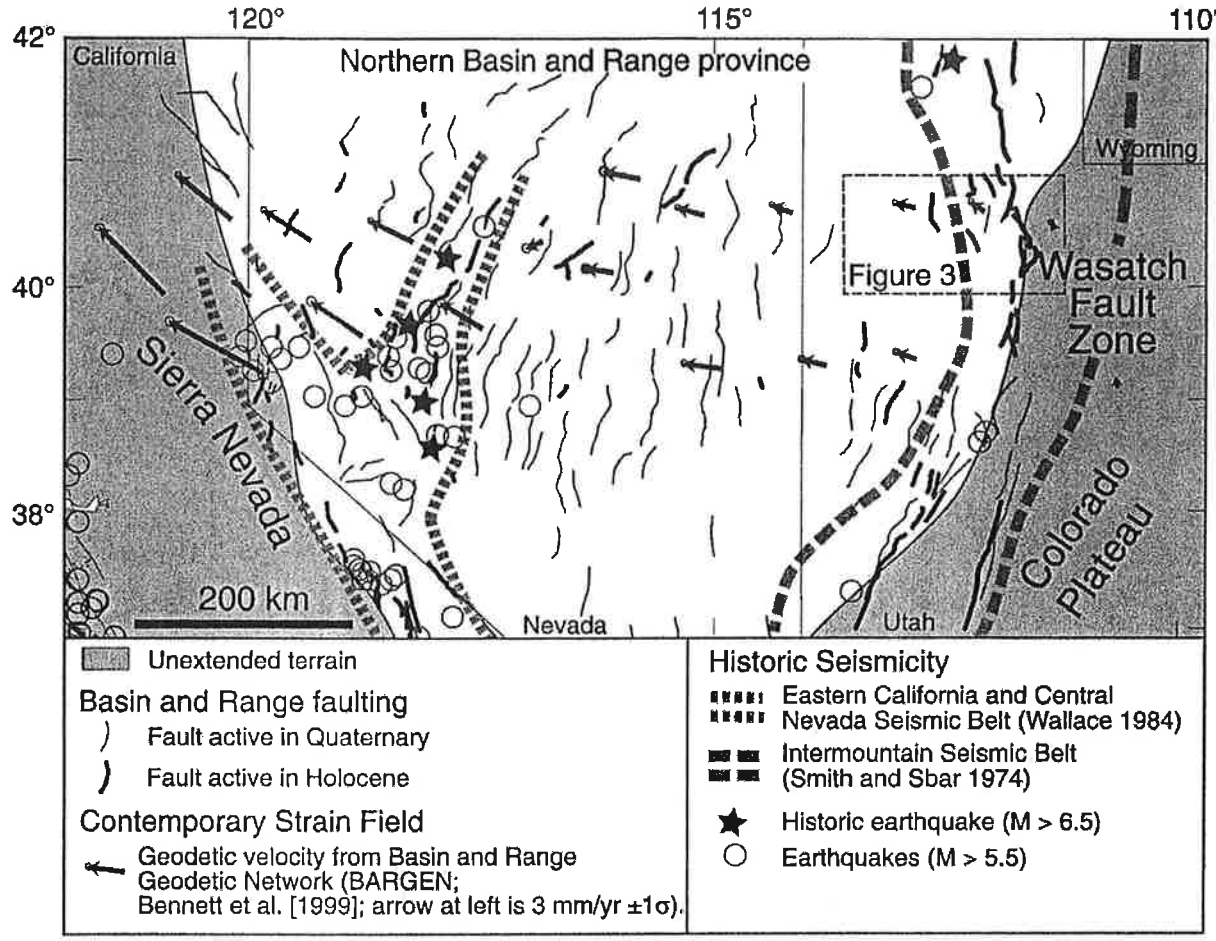

Figure 2. Simplified tectonic map of the northern Basin and Range province, located between the Sierra Nevada and the Colorado plateau. The BARGEN geodetic velocities [e.g., *Bennett et al.*, 1999] and the distribution of active normal faults and historic earthquakes are shown. See color version of this figure in the HTML.

that strain accumulation (via changes in either the far-field or local processes mentioned above) would vary markedly, on the same timescale as the clusters. In this event, at any given time strain accumulation inferred from geodesy and strain release inferred from paleoseismology should be the same. On the other hand, far-field strain accumulation may be constant, generally being lower than seismic strain release rates during clusters, and higher in between clusters. In this case, strain release would bear no relation to either a critical level of strain energy required for slip (time-predictable model), nor the amount of strain energy accumulated since the previous earthquake (slip-predictable model) (Figure 1d) [*Wallace*, 1987].

[5] The Wasatch fault zone is ideally suited for comparisons of strain accumulation and release because the slip histories of most or all segments of the fault are well known, and there are good constraints on the longer term slip history [e.g., *Machette et al.*, 1992a, 1992b; *McCalpin and Nishenko*, 1996; *McCalpin and Nelson*, 2000; *Parry and Bruhn*, 1987; *Ehlers et al.*, 2001]. In this paper we present new geodetic data from the Basin and Range Geodetic Network (BARGEN) from 1996 to 2000 across the eastern Basin and Range-Colorado Plateau transition region at the latitude of Salt Lake City and compare them with a synthesis of published geological displacement rates across the same region at the 1-kyr, 100-kyr, 1-Myr, and 10-Myr timescales.

2. Neotectonic Setting

[6] The northern Basin and Range province, bounded on the west by the Sierra Nevada and on the east by the Colorado Plateau (Figure 2), is a wide (~750 km) region of extended continental crust. Extension initiated in the Oligocene and peaked during mid to late Miocene time (~15–10 Ma [*Stockli*, 2000]) with a maximum displacement rate near 20 mm/yr [*Wernicke and Snow*, 1998], resulting in the formation of range front faults spaced ~30 km apart, separating ~15-km-wide basins from mountain ranges. Since ~10 Ma the overall rate of deformation has slowed to about half the maximum value and includes a major component of right-lateral shear along the western margin of the province [*Bennett et al.*, 1998, 1999; *Thatcher et al.*, 1999].

[7] Most range-bounding faults in Nevada and western Utah have been active in Quaternary time [*Dohrenwend et al.*, 1996; *Hecker*, 1993]. Regions of modern seismicity, however, are restricted to three narrow belts, the Eastern

Field Guide to Permian Rocks of Grand Canyon and Sedona Areas, North-Central Arizona

Ronald C. Blakey *Department of Geology, Northern Arizona University, Flagstaff, AZ 86011*

Larry T. Middleton *Department of Geology, Northern Arizona University, Flagstaff, AZ 86011*

INTRODUCTION AND REGIONAL SETTING

Permian rocks of the southern Western Interior of the United States occupied the west-central margin of the supercontinent Pangea (Fig. 1) in an area that was part of a vast arid climate zone (Parrish and Peterson, 1988). The culmination of the assembly of Pangea resulted in the extensive Marathon-Ouachita-Appalachian mountain chain 800 km south and southeast of the study area. Stresses from continental collisions caused fracturing and local uplift of the North American craton including the Ancestral Rocky Mountains (Kluth and Coney, 1981), adjacent to and east of the study area (Fig. 2). Meanwhile, the long-established passive margin of western North America was evolving into the active Cordilleran margin. Thus, the southern Western Interior formed a southwest-tapered extension of cratonic North America bordered to the southeast, south, and west by active tectonic terranes and to the east by uplift on the craton. The field area escaped strong tectonism but was the site of minor tectonic and epeirogenic movements in the form of upwarps/arches and intervening basins (Armin, 1987). Late Paleozoic glacially controlled eustatic cycles (Ross and Ross, 1988) were superimposed on this complex tectonic and arid climatic regime.

The arid climate and abundant clastic sediment sources contributed to the widespread eolian deposition. Eolian deposits formed in environments that ranged from eolian sand sheets and coastal dune fields to vast coastal and inland ergs (eolian sand seas). Tectonic and eustatic controls strongly influenced the details of eolian sediment dispersal, distribution, geometry, and preservation (Blakey, 1988; 1996; Blakey et al., 1988). Eolian deposits are intimately interbedded with fluvial, sabkha, coastal-plain, and shallow marine deposits.

Permian rocks of the field area (Fig. 3), though sparsely fossiliferous and subject to abrupt facies changes, have been correlated in moderate detail based on locally excellent and continuous exposures and detailed stratigraphic analysis (Figs. 4,5). The correlations and nomenclature presented in this paper follow those of Blakey (1988), Blakey et al. (1988), Blakey and Knepp (1989), and Blakey (1990a).

Blakey (1996) recognized and correlated four widespread and prominent unconformities (Fig. 6). The unconformities are given letter designations as follows: P-O (base of Permian), P-sc (base of Schnebly Hill Formation or Coconino Sandstone), P-tw (base of Toroweap Formation or White Rim Sandstone), P-k (base of Kaibab Formation).

Modern sedimentological studies have been published on each of the Permian deposits in the study area. A summary of these studies and their interpretations is briefly summarized in Figure 6.

PERMIAN ROCKS IN GRAND CANYON

Permian strata are exposed throughout Grand Canyon and, and with coeval strata in the Sedona - Oak Creek Canyon area, record a complex interplay of eolian, fluvial, and nearshore marine processes. The Permian succession comprises the Esplanade Sandstone of the Supai Group, Hermit Formation, Coconino Sandstone, and the Toroweap and Kaibab Formations. The latter forms the prominent cap rock throughout Grand Canyon. This part of the field trip will focus on the Coconino, Toroweap, and Kaibab formations. We will examine sedimentological characteristics of each unit and discuss their significance with respect to depositional settings and regional paleogeography. Each of the units exhibit major features that developed in response to regional climatic, eustatic, and tectonic events.

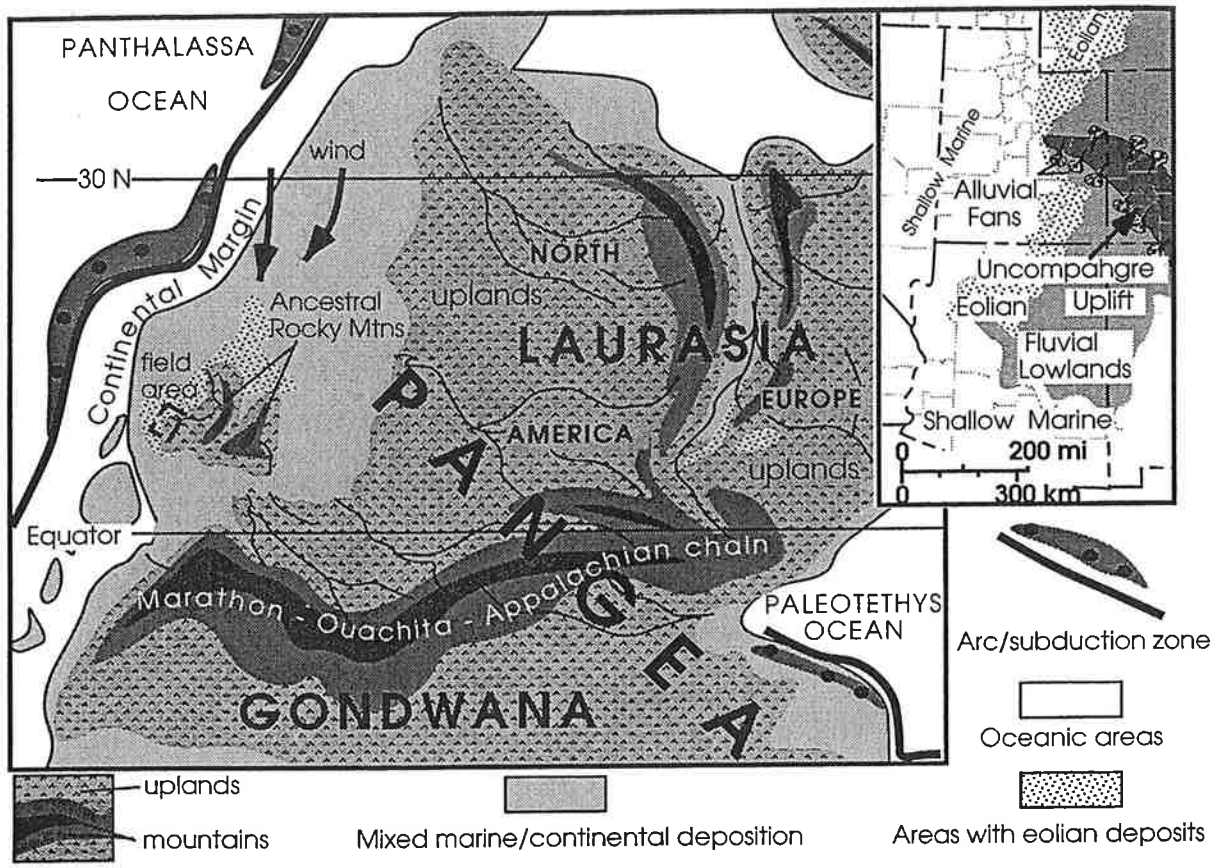

Figure 1. Generalized Permian paleogeographic and tectonic map of North America.

Esplanade Sandstone

The Esplanade Sandstone of the Supai Group crops out throughout Grand Canyon where it forms a prominent cliff beneath the less resistant Hermit Formation and in western Grand Canyon forms broad platforms, hence the name esplanade (Fig. 7). Although the thickness of the Esplanade varies throughout the Grand Canyon, the unit averages about 280 ft (92 m) thick (McKee, 1982).

In the Grand Canyon the basal third of the formation comprises slope-forming, fine-grained units that are overlain by a thick, cliff-forming, sandstone-dominated sequence (Fig. 8). The basal slope-forming sequence is heterogeneous, consisting of reddish, thinly bedded sandstones, mudstones and subordinate carbonates. The prominent cliff-forming sandstone contains abundant sedimentary structures including upward-coarsening ripple laminae, avalanche deposits (sand-flow strata) and small-large-scale trough and planar-tabular cross stratification that indicate a complex depositional arena.

The depositional settings in which the Esplanade accumulated include both nearshore marine and continental environments (McKee, 1982). The slope-forming basal part of the Esplanade likely was deposited in shallow shelf areas, although little work has been done on the unit . Stratification styles within the upper cliff-forming sandstone, however, strongly indicate deposition in eolian settings (Blakey, 1990a). These include the upward-coarsening laminae that are the products of wind ripple migration (Hunter, 1977), presence of down-foreset tapering of sand flows, that represent avalanche deposits, and rare suspension-deposited laminae (grain fall deposits). Other features such as wavy laminae and disrupted laminae suggest periodic flooding and reworking of these windblown deposits. Thus, the upper sandstones in the Esplanade likely record deposition in a coastal dune complex that experienced episodic flooding of dune and interdunal areas. An increase in plant fragments and vertebrate tracks and trails in outcrops in central parts of the Grand Canyon (McKee, 1982) and also in Marble Canyon likewise attest to deposition in

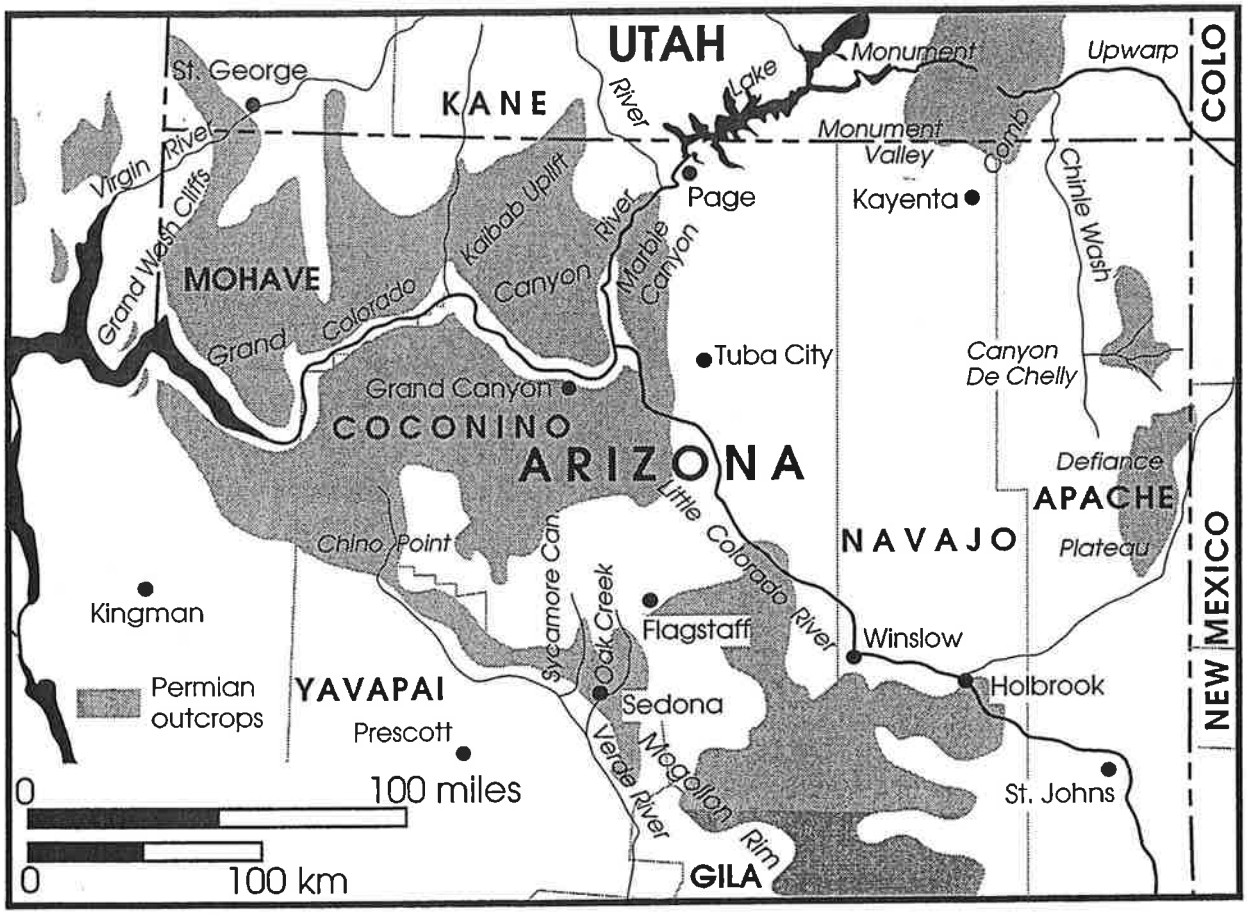

Figure 3. Permian outcrops (gray) in northern Arizona

westward thickening with sections in western Grand Canyon up to 1000 feet (300 m) thick (Beus, 1987).

In the Grand Canyon the Hermit comprises red-brown mudstones and subordinate, intercalated, thin-bedded sandstone (McKee, 1982). Deposition occurred in broad, shallow channels that likely were ephemeral to well established, channelized high sinuosity streams. The ephemeral nature of many channel complexes is indicated by the presence of planar bedded sandstone and presence of rip-up, intraformational mudstone clasts. Presence of large-scale inclined strata containing both trough and ripple cross stratification indicate that some of the Hermit stream systems were localized incised, of high sinuosity, and perennial. The latter represent the deposits of side and point bars. The best examples of these are seen in the Sedona area (Day 2). Many of the channelized sandstone deposits contain pedogenetically modified overbank fine-grained siliciclastics and carbonates. The carbonates occur as discrete nodules at the base of many sandstones and reflect prolonged periods of channel stability and a semi-arid environment. There are numerous intraformational carbonate conglomerates in the Hermit Formation composed of carbonate clasts that indicate the erosion of bank-margin calcic paleosols. These will be best be seen in the stops in the Oak Creek Canyon. Few other indicators of arid climatic conditions have been reported from the Hermit Formation. Blakey (1990b), however, reports wind ripple laminae from sandstones near the base of the Hermit Formation, indicating the onset of increasingly arid environments.

The upper contact of the Hermit with the Coconino Sandstone in Grand Canyon is sharp and represents a prolonged hiatus in deposition and also erosion preceding the southward incursion of the Coconino sand sea.

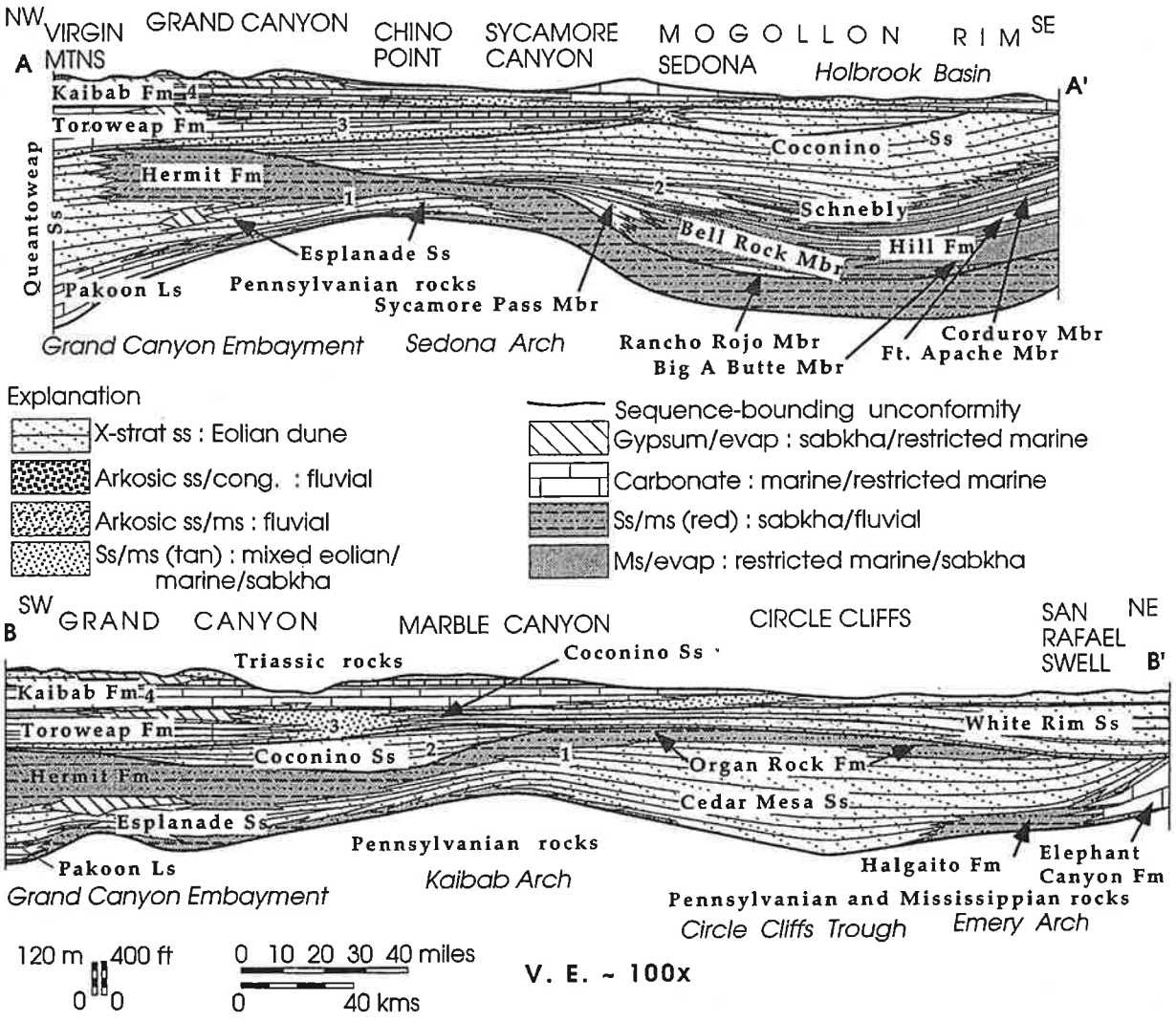

Figure 4. Stratigraphic cross sections of Permian strata on Colorado Plateau. Numbers 1 - 4 refer to sequences and locations of cross sections are shown on Figure 2.

Coconino Sandstone

One of the most distinctive units in the Grand Canyon is the early Permian (Leonardian) Coconino Sandstone (Fig. 10). Extraordinary exposures occur throughout the Grand Canyon region and extend into central Arizona (Fig. 11). The large-scale cross stratified sandstone is easily identifiable along the canyon walls and forms a pronounced marker horizon in the Permian succession. Regional stratigraphic relationships have been established by McKee (1933), Blakey and Knepp (1989), Blakey et al. (1988), and Blakey (1996). Surprisingly, comparatively few sedimentologic analyses have been conducted (McKee, 1933; Middleton et al., 1990).

Thickness of the Coconino is variable across the outcrop belt, thinning to the west in Grand Canyon and thickening to the south in the Sedona - Oak Creek Canyon area. The Coconino is 600 feet (180 m) thick in the eastern part of Grand Canyon thinning to 65 feet (20 m) near Lake Mead and to 60 feet (18 m) in Marble Canyon. The Coconino pinches out near the Arizona - Utah border. Along the Mogollon Rim in the Sedona area the formation is at least 1000 feet (305 m) thick (McKee, 1933). The increase in thickness of the Coconino to the south is related to increased rates of subsidence but also might reflect intertonguing of the Toroweap Formation with the Coconino.

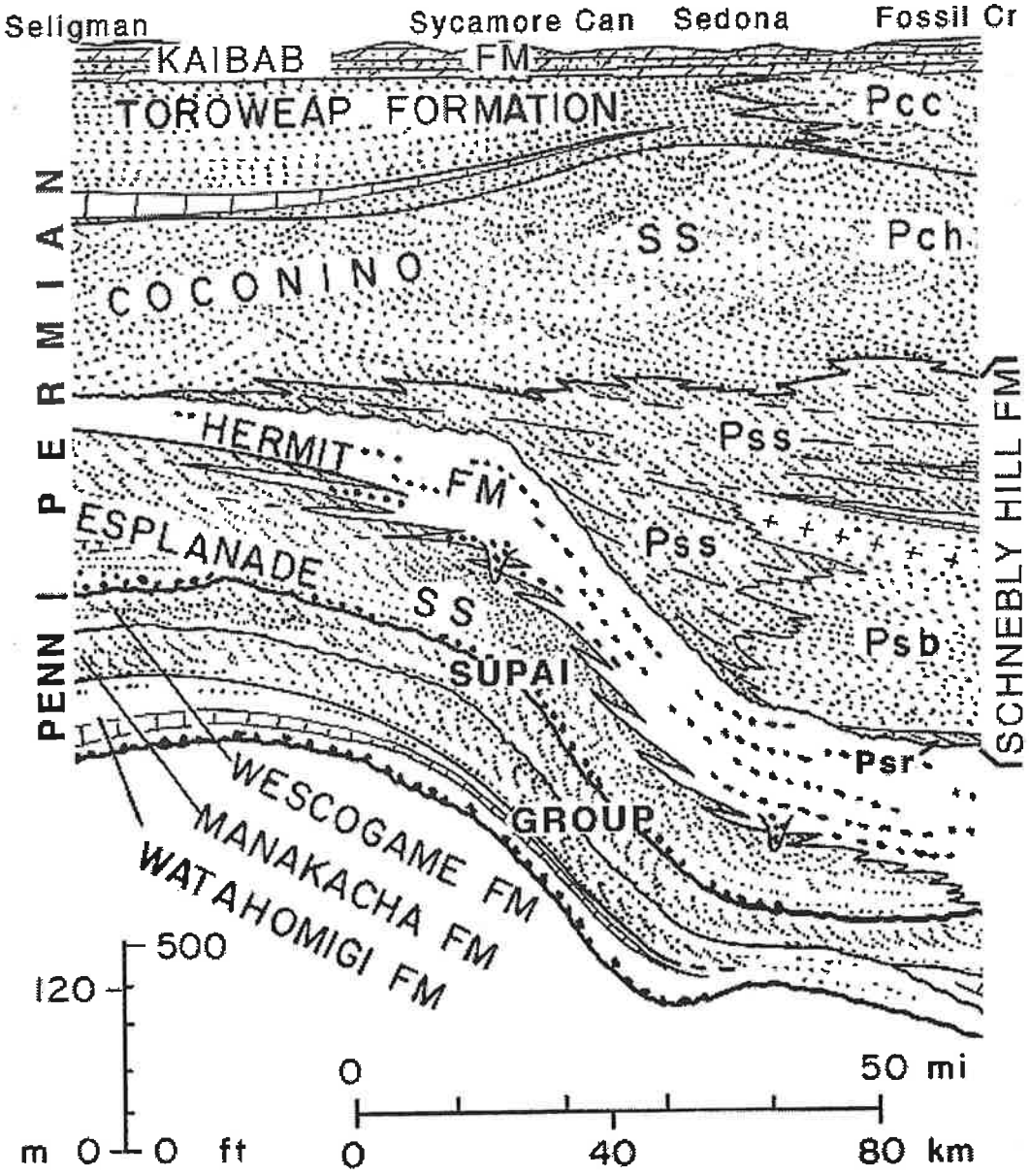

Figure 5. Lithologic and thickness relations of Penn-Permian strata in north-central Arizona.

Facies changes in both formations are similar and hence differentiation between the two is difficult. Blakey and Knepp (1989) proposed that these thickness variations are controlled to some extent by regional tectonic elements most notably the Sedona Arch and Holbrook basin (Fig. 2). An eolian origin for the Coconino Sandstone has been supported by sedimentologic and stratigraphic analyses (McKee 1933; Middleton et al., 1990). Middleton et al. (1990) provide a comprehensive discussion of the depositional systems. The Coconino is composed of well rounded and well sorted, fine- to medium-grained sand. Mineralogically, the unit is a quartz arenite with minor amounts of potassium feldspar. Although this degree of textural and mineralogic maturity is attainable in high energy, nearshore environments, facies sequences and regional stratigraphic patterns indicate that the Coconino represents a widespread sand sea or erg; the first major sand sea to develop during the Phanerozoic on the

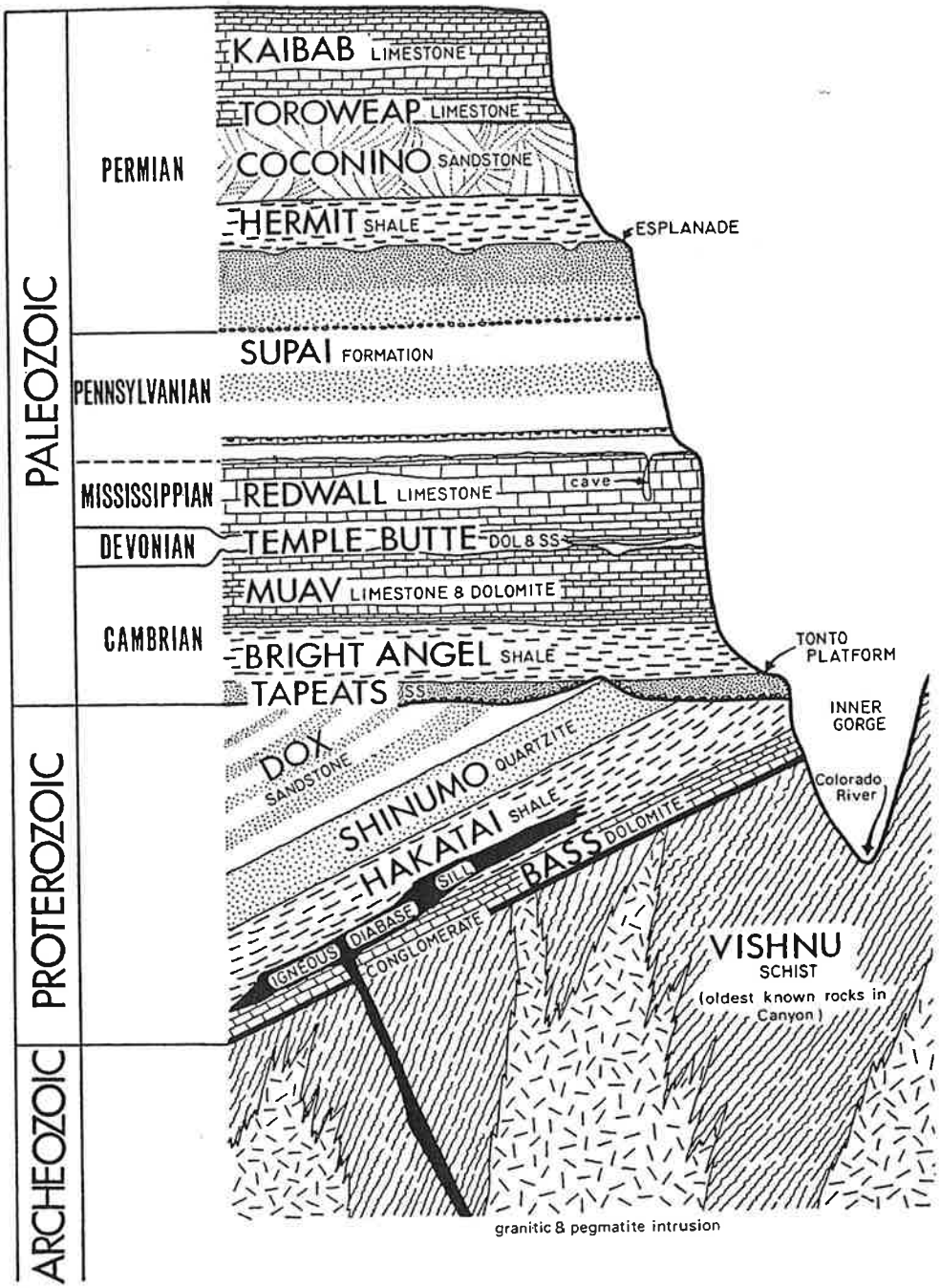

Figure 13. Cross section of crystalline and sedimentary rocks of Proterozoic age and the Paleozoic succession in eastern Grand Canyon. A pronounced unconformity separates younger Precambrian strata of the Unkar Group from the overlying Cambrian (from Breed and Roat, 1974).

EARLY AND MIDDLE JURASSIC PALEOGEOGRAPHY AND VOLCANOLOGY OF ARIZONA AND ADJACENT AREAS

Nancy R. Riggs and Ronald C. Blakey
Department of Geology
Northern Arizona University
Flagstaff, AZ 86011

ABSTRACT

Early to Middle Jurassic sedimentary rocks and their bounding unconformities on the Colorado Plateau in northern Arizona and southern Utah can be divided into six major sequences. These sequences, when coupled with coeval volcanic successions in the magmatic arc of southern and western Arizona and eastern California, provide a basis for tectonic interpretation of arc and back-arc regions.

Sequence 1 (Lower Jurassic Wingate Sandstone and Dinosaur Canyon member of the Moenave Formation) overlies the J-0 unconformity. Eolian and fluvial strata were deposited on a broad plain inclined gently from uplifted areas in the early magmatic arc.

The lower part of Sequence 2 (lower Kayenta Formation and Springdale Sandstone member of the Moenave Formation) overlies the sub-Kayenta unconformity. The Mogollon slope may have been close to the Colorado Plateau during deposition of Sequence 2, and the sources of streams draining into the Colorado Plateau were within a monsoonal belt as the Colorado Plateau drifted in an arid climate.

The upper part of Sequence 2 (upper Kayenta Formation and Navajo Sandstone) is overlain by the J-1 unconformity. Pronounced subsidence in the western Utah-Idaho trough contributed to preservation of tremendous thicknesses of eolian sandstone, and sand was driven as far south as the magmatic arc in southern Arizona. Widespread volcanic deposits of a similar age in southern Arizona reflect deposition in an extensional or transtensional environment. Numerous red bed deposits in these ranges may reflect periods of relative quiescence in arc activity, although the correlation of several units in southern Arizona is not confirmed.

Sequence 3 (Middle Jurassic Temple Cap Sandstone) lies between the J-1 and J-2 unconformities. The presence of numerous bentonite horizons within this eolian-sabkha unit indicates active volcanism, although fewer isotopic dates on volcanic rocks correspond to this time than to other sequences.

Sequence 4 (Lower Page Sandstone and Carmel Formation) was deposited in a time when volcanic activity may have reached a maximum. Bentonite horizons probably derived from explosive eruptions throughout the Mojave and Sonoran deserts are common in the Page Sandstone and Carmel Formation, and some uplift of the area south of the Colorado Plateau is indicated.

Sequence 5 (Upper Page Sandstone and Carmel and Entrada Formations) reflects a complex series of uplift and subsidence events across the Colorado Plateau and Utah-Idaho trough. Volcanism in the magmatic arc persisted well into this period.

Sequence 6 (Curtis Formation and Summerville and Romana Sandstones) reflects drying upward sequences that represent transgression and regression. Sequence 6 is truncated by the J-5 unconformity, which separates Middle from Upper Jurassic strata.

INTRODUCTION

The Mesozoic Cordilleran magmatic arc was originally referred to as an "Andean" arc (Burchfiel and Davis, 1972), evoking images of high-standing volcanic edifices, a well-developed fold-and-thrust belt, convergent tectonics, and a topographic barrier between arc and back-arc. Increasing evidence suggests that from Late Triassic or Early Jurassic time through at least early Middle Jurassic time, the northeastern portions of the arc were low-standing and occupied an extensional or transtensional regime.

We summarize here data from Arizona and southern Utah that form the basis of a paleogeographic reconstruction of the arc and back-arc during Late Triassic to Middle Jurassic time (Fig. 1). We have confined our synthesis of the magmatic arc to exposures west of approximately 110°30'. Controversies and debate are active in the following topics concerning paleogeography and tectonic reconstruction: 1) the height and continuity of the magmatic arc: low lying and discontinuous vs. high-standing and continuous topographic barrier; 2) the nature of the landscape between the arc and the present Jurassic outcrops on the Colorado Plateau: low featureless plains or gentle slopes vs. rugged highlands that strongly influenced streams in the back-arc area; 3) the distance between the magmatic arc and the back-arc area now represented by exposures on the Colorado Plateau: modern-day configuration vs. significant translation owing to late Mesozoic and Cenozoic tectonism; 4) the cor-

In Dunn, G., and McDougall, K., eds.,1993,
Mesozoic Paleogeography of the Western United States-II
Pacific Section SEPM, Book 71, p. 347-375

Figure 1. Map of the southern Colorado Plateau and adjacent Basin and Range showing locations referred to in text, line of sections in Figure 4, and restorations (after Marzolf, 1990; 1991) of selected ranges in southern Nevada and eastern California to pre-Cenozoic positions. Shaded line shows present approximate southern margin of Jurassic outcrops on the Colorado Plateau.

relation of rock units between the relatively stable back-arc and the active magmatic arc: correlation of discrete formations and unconformities vs. tenuous correlations hampered by controversial lithostratigraphic and geochronologic dating.

We propose that the sequences we describe in general reflect drying-upward cycles. Drying and wetting refer here to sedimentological, not climatological, trends (e.g. Clemmensen and others, 1989). A sequence that dries upward contains, for example, sabkha deposits overlain by dune deposits, or perennial stream deposits overlain by ephemeral stream deposits or dunes.

Paleogeographic reconstruction of this part of the Mesozoic orogen contributes to an understanding of the tectonic forces active in the arc and backarc regions, and how patterns of sedimentation across the region were affected by these forces.

Early and Middle Jurassic Time Scales

Controversy surrounding correlation of stratigraphic units, especially eolianites, between the magmatic arc province and Colorado Plateau may stem in part from uncertainties in the various chronostratigraphic time scales. The time scales of Haq and others (1988) and Harland and others (1990) are very similar for Lower and Middle Jurassic time (Fig. 2), but deviate considerably for Upper Jurassic time. We have therefore adopted the Harland and others (1990) scale throughout this paper. Biostratigraphic zones of Imlay (1980) are shown and correlated with the chronostratigraphic scale of Harland and others (1990; Fig. 1).

Additional precision is added to the Middle Jurassic portion of the time scale by $^{40}Ar/^{39}Ar$ dates by Everett and others (1989) on bentonite ash from the Judd Hollow Member of the Carmel Formation (Co-op Creek Member of Doelling and others, 1989). Limestone beds containing several ash beds in the Judd Hollow Member contain Bajocian/Bathonian marine fauna (Imlay, 1980).

REGIONAL STRATIGRAPHY

Mesozoic volcanic and sedimentary rocks were deposited on a basement of Proterozoic metamorphic and plutonic rocks overlain by Paleozoic stable-margin platform/shelf sedimentary rocks. The northeast-trending passive margin was truncated in late Paleozoic time (Walker, 1988; Stone and Stevens, 1988), and a superposed northwest trend dominated the configuration of the continental margin during Jurassic time and has been maintained to present time. This northwest trend strongly affected tectonic elements (Fig. 3) that in turn controlled certain aspects of sedimentation, including loci of deposition and source areas.

Lower and Middle Jurassic Strata, Colorado Plateau and Vicinity

Introduction

The correlation and depositional history of the Lower Jurassic Glen Canyon Group and the Middle Jurassic San Rafael Group has received thorough recent examination (Peterson and Pipiringos, 1979; Pipiringos and O'Sullivan, 1979; Blakey, 1988, 1989; Blakey and others, 1988; Peterson, 1988a). We briefly review these studies and focus on the interpretation of the several depositional sequences and the unconformities. The sequences, their internal lithostratigraphic composition, and bounding unconformities are shown on Figure 4.

Lower Glen Canyon Group [J-0 to J-sub-Kayenta (J-sub-Kay) unconformities].

J-0 Unconformity

The J-0 unconformity (Pipiringos and O'Sullivan, 1979) marks the base of the Glen Canyon Group (as restricted by Dubiel, 1989) across the southern Colorado Plateau.

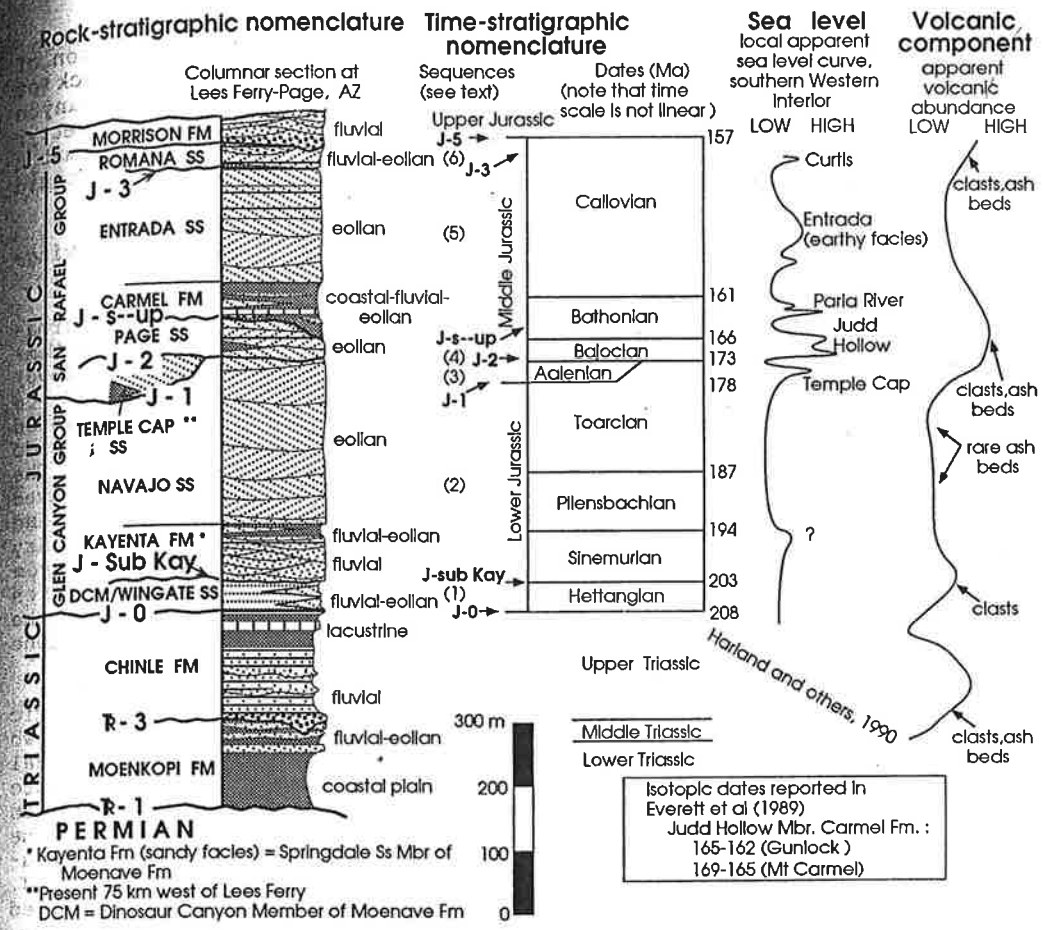

Figure 2. Rock- and time-stratigraphic nomenclature, apparent sea-level curve, and known volcanic components of Triassic and Jurassic rocks, southern Colorado Plateau.

Because strata in the overlying Moenave Formation contain Early Jurassic palynomorphs and the underlying Chinle Formation is considered entirely Late Triassic in age, the J-0 is believed to mark the Triassic-Jurassic boundary in this region (Peterson and Pipiringos, 1979).

The J-0 is regionally a low-angle unconformity (Blakey, 1990; Marzolf, 1991; Fig. 5). As much as 24 m of basal conglomerate in the Moenave-Kayenta formation (undivided) overlies the J-0 unconformity west of the present Colorado Plateau near Las Vegas, and Marzolf (1991) has traced it into the arc terrane of southeastern California where it overlies Paleozoic rocks in the Cowhole Mountains (Fig. 1). Reynolds and others (1989) reported that Jurassic rocks in the Buckskin-Harquahala area of western Arizona rest unconformably on rocks ranging from Proterozoic to Middle(?) Triassic in age. In general, the low-angle discordance of the J-0 across the Colorado Plateau suggests gentle epeirogenic up-to-the-southwest tilting of the region (Blakey, 1990). A few tens of kilometers off the west and southwest edges of the present Colorado Plateau, however, the J-0 represents sharp orogenic uplift (Marzolf, 1991; Reynolds and others, 1989). This tectonic activity may represent upwarping associated with the early stages of construction of the Mesozoic Cordilleran arc.

Wingate Sandstone and Dinosaur Canyon Member

The lower Glen Canyon Group comprises the eolian Wingate Sandstone (Blakey and others, 1988; Nation, 1990) and coeval ephemeral stream deposits of the Dinosaur Canyon Member of the Moenave Formation (Clemmensen and others, 1989). The two units are coeval facies that intertongue along a northwest-trending alignment roughly coincident with the Zuni lineament (Blakey, 1988). Northwest-flowing streams followed broad open terrain defined by remnants of the pre-J-0 uplift to the southwest and Wingate ergs to the northeast. The streams were deflected northward into the southern Utah-Idaho trough in southwestern Utah. Northerly to westerly winds deflated the stream courses and transported fine sand into the western and southern portions of the Wingate erg. The nearly opposite paleocurrent flow of the fluvial-eolian transportation systems probably trapped much of the sediment on the south-central Colorado Plateau (Blakey and others, 1992). Northwest-moving fluvial sediment was blown back to the southeast and sand that escaped the Wingate erg was recycled northward by Moenave streams (Fig. 6).

North of Flagstaff, Arizona, volcanic granules occur in the Dinosaur Canyon Member. Although these grains have been neither dated isotopically nor studied petrographically, paleocurrent data in fluvial deposits suggest that they were derived from volcanic rocks to the south.

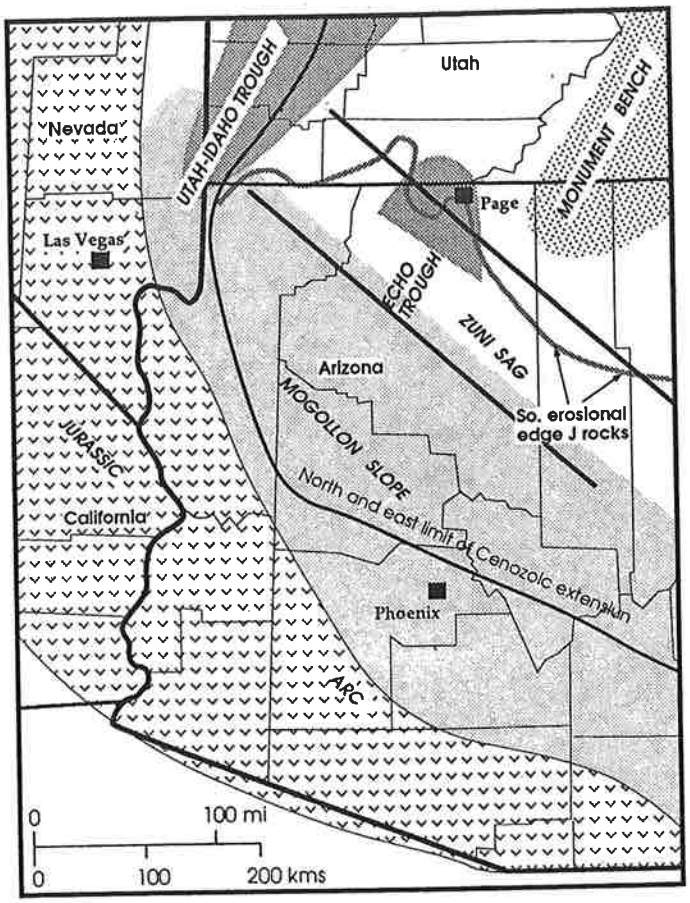

Figure 3. Generalized Early and Middle Jurassic tectonic elements. Northeastern extent of arc reconstruction after Marzolf (1990, 1991). The north and east limit of Cenozoic extension theoretically marks the maximum possible northeastward extent of the arc as no known Jurassic intrusions occur in non-extended rocks.

Upper Glen Canyon Group (J-sub-Kayenta to J-1 unconformities)

Sub-Kayenta Unconformity

Nation (1990) and Clemmensen and others (1989) document that appreciable erosion affected the top of the Wingate Sandstone - Moenave Formation sequence. This contact has local relief of up to 15 m but lacks any angular discordance (Fig. 4). Evidence supporting an unconformity includes the presence of silcrete with extensive burrows, roots, tree trunks, and soil horizons northeast of Flagstaff (Edwards, 1985). The unconformity is present across most of the Colorado Plateau; its extent to the west is unknown, and eastward it is truncated by younger unconformities. According to F. Peterson (pers. communication, 1993), there is no evidence indicating an unconformity at this stratigraphic position in the Uinta Mountains of northern Utah.

The sub-Kayenta unconformity represents a period of downcutting of unknown, but probably short, duration following deposition of the lower Glen Canyon Group. The lack of angularity (the Wingate-Dinosaur Canyon isopach has a irregular, sheet-like geometry) suggests a fall in base level or climatic changes rather than significant tectonic uplift.

Kayenta Formation (sandy facies) and Springdale Sandstone

The sandy facies of the Kayenta Formation and equivalent Springdale Sandstone Member of the Moenave Formation (Blakey, 1990) define a widespread sandy perennial to locally ephemeral stream system that flowed west to northwest across much of the Colorado Plateau (Luttrell, 1985; Bromley, 1991). The large, mature, perennial streams were derived well east of the Colorado Plateau, and entrained sediment from older sedimentary rocks as well as Precambrian clasts from small remnants of the Ancestral Rockies (Luttrell, 1985). The upper contact of the Kayenta Formation with the Navajo Sandstone is gradational and intertonguing.

It is paradoxical that a mature dynamic fluvial system would be encased between two major eolian deposits. Scoured erosional features at the top of the underlying Wingate Sandstone, together with sandstone clasts in the Kayenta Formation likely derived from the Wingate Sandstone, strongly suggest cementation of the older eolian deposits (M.J. Nation, personal commun., 1992). Coupled with recognition of the sub-Kayenta unconformity, this suggests that Kayenta streams flowed across bedrock and did not erode through loose sand.

As Kayenta streams flowed westward across the porous Wingate Sandstone and across a semi-arid to arid region, water loss downstream contributed to more ephemeral structural characteristics such as smaller and fewer cross beds and an increase in planar (upper flow regime) stratification. The last remnants of the Springdale Sandstone occur near the edge of the Colorado Plateau at St. George, Utah (Fig. 7). Only the southern margin of the Kayenta/Springdale system is clearly defined. South of the pinchout near Tuba City, Arizona, the sub-Kayenta unconformity is marked by extensive silcrete deposits.

The cause of the great influx of perennial fluvial systems onto the Colorado Plateau during the arid Jurassic Period is unknown but we speculate a climatic cause. During the break-up of Pangea, the Colorado Plateau "drifted" northward through the monsoonal belt several degrees north of the equator (Late Triassic Megamonsoon of Dubiel and others, 1991). The Plateau was under the arid influence of the subtropical high during most of Jurassic time (Parrish, 1992). Areas to the south and east, however, may still have been under the monsoonal belt. Perhaps the western tilt of the Colorado Plateau (as documented by paleostream flow) during this time coupled with undocumented tectonic tilting southeast of the study area (rejuvenation

immediately south of the restored transect in the Buckskin Mountains (Reynolds and others, 1989).

SYNTHESIS

Introduction and Terminology

The six Lower and Middle Jurassic sedimentary sequences and their bounding unconformities provide the foundation for a tectonic synthesis. For each of these sequences, we have established: 1) a regional tilt, 2) distribution of volcanic ash and clasts, 3) general paleoenvironmental setting, and 4) relation between preserved sedimentary and volcanic rocks and tectonic elements. These factors, isotopic dates from arc rocks, distribution (and reconstruction) of arc rocks, and petrographic and structural data from the arc, can be synthesized into a comprehensive analysis of the western Colorado Plateau and adjacent arc terrane (Figs. 21, 22). The details gleaned from the tectonic interpretation of rocks on the Colorado Plateau provide a basis for the extrapolation of tectonic events into the structurally complex and less well understood arc terrane. We have attempted to keep tectonic terminology to a minimum. Although a number of tectonic elements have been named and recognized as being active during Jurassic time (Peterson, 1988a, 1988b; Blakey, 1988), the following were most influential and are used in the ensuing synthesis, and are shown on Figure 3.

1) The Utah-Idaho trough was a strongly topographically negative area in which subsidence rates either matched or exceeded sedimentation rates. The trough provided the pathway for several marine transgressions into dominantly continental sequences, and during continental episodes of sedimentation it was a locus of north-directed stream deposition.

2) The Mogollon slope (Bilodeau, 1986) was apparently a gently inclined buttress along the southern margin of the Colorado Plateau. At times a gentle slope confined northwesterly flowing streams that entered the Colorado Plateau from the south. More rarely, the slope was steeper, and vigorous streams that drained mountainous terrain to the south or southeast flowed across it. During times in which an extensional arc terrain is envisioned, we speculate that Mogollon slope was a topographic rift shoulder or a low arch between the arc graben-depression and the back arc or Colorado Plateau region. Before establishment of the extensional/transtensional regime, the southward termination of the Mogollon slope may have been primary volcanic highlands. The slope was not a hindrance to ergs that periodically migrated southward into the arc (Bilodeau, 1986).

3) The Monument bench subsided at a slower rate than areas to the south and west. Throughout lower Middle Jurassic time, younger deposits onlapped the gentle west-dipping plain (manifested as the J-2 erosion surface) and eventually buried it in early Callovian time (Fig. 20).

4) The Echo trough (King and Blakey, 1991) was a rapidly subsiding feature in Middle Jurassic time. Present-day erosion truncates the Page Sandstone and upper member of the Carmel Formation, but isopach studies show a continuing thickening of these forma-

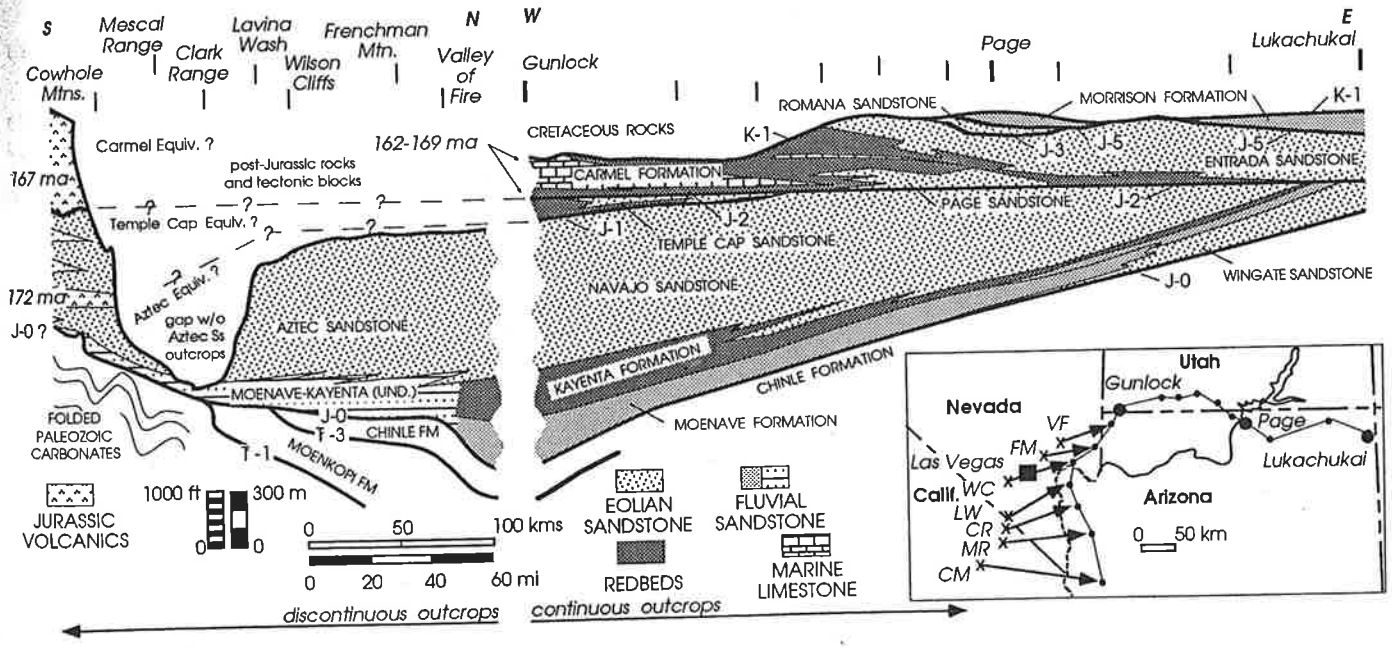

Figure 20. Restored and partly idealized cross section of Jurassic rocks from the Cowhole Mountains to Fort Defiance, Arizona. Correlation in the discontinuous outcrops south and west of the Colorado Plateau partly after Marzolf (1990, 1991); however, correlation of post-172 ma rocks in Cowhole Mountains to rocks on Colorado Plateau follows our suggestions discussed in text.

LATE CRETACOUS PALEOGEOGRAPHY OF THE SOUTHERN SEVIER FORELAND, SOUTHWEST UTAH, SOUTHERN NEVADA, AND NORTHWEST ARIZONA

Robert P. Fillmore
Department of Geology
University of Kansas
Lawrence, Kansas

ABSTRACT

Late Cretaceous sedimentary rocks in southwest Utah, southern Nevada, and northwest Arizona were deposited in a continental setting, in the proximal reaches of the southern sector of the Sevier foreland basin. These strata record deformation in the Sevier fold and thrust belt to the west, and provide insight into the evolution of this part of the foreland basin.

Sedimentologic and compositional data indicate that basal conglomerate throughout the study area was deposited on a regional pediment surface of Jurassic rock by east-flowing, bedload-dominated, braided fluvial systems. Abundant quartzite clasts suggest a provenance in the Wheeler-Gass Peak thrust system in the south, and the Wah Wah thrust in the north. In the northern part of the study area, at Three Peaks, Utah, north-flowing, mudflow-dominated fan deposits that interfinger with east-directed, quartzose fluvial deposits are interpreted to reflect incipient movement on the Iron Springs thrust.

Claystone, bentonitic tuff, fine-grained sandstone, and carbonate that overlie the basal conglomerate indicate a change to low-energy fluvial and paludal environments. The preservation of these deposits in a proximal foreland setting suggests continued subsidence and sediment starvation.

The last phase of Cretaceous basin evolution is marked by the eastward advancement of the thrust belt, and a change in regional drainage patterns. The change in drainage from an earlier east-flowing, transverse system to a north-northeast flowing system, parallel to the orogenic front, is attributed to increased subsidence caused by thrust loading. Compositional data from sandstone and conglomerate indicate erosion of Paleozoic carbonate rocks suggesting that eastward thrust migration was manifested by development of the Summit-Willow Tank and Muddy Mountain thrusts in the south, and the Blue Mountain and Escalante thrusts in the north.

INTRODUCTION

Late Cretaceous strata in southwest Utah, southern Nevada, and northwest Arizona were deposited in the proximal reaches of an extensive foreland basin that reached from northern Canada to southern Nevada (Fig. 1). These continental strata were deposited in the southernmost sector of the foreland, adjacent to the east-vergent Sevier fold and thrust belt that lay to the west and were a source for clastic material (Armstrong, 1968). Thus, these sediments provide a record of Late Cretaceous contractional deformation and associated basin evolution.

Previous studies of proximal Sevier foreland deposits have concentrated on strata to the north (e.g. Wiltschko and Dorr, 1983; Lawton, 1983, 1985, 1986; Dickinson and others, 1986; DeCelles, 1988). The southern sector, however, remained largely unstudied except for regional stratigraphic and structural studies (e.g. Bissell, 1952; Bohannon, 1983).

Strata in the study area include the Dakota and Iron Springs Formations, southwest Utah (Mackin, 1947; Fillmore and Middleton, 1989; Fillmore, 1991), the Willow Tank Formation and Baseline Sandstone in the Muddy Mountains of southern Nevada (Longwell, 1949; Fleck, 1970; Bohannon, 1983), and the Jacobs Ranch and Cottonwood Wash Formations of northwest Arizona (Moore, 1972) (Fig. 2). Correlations between these formations are dominantly based on stratigraphic position and lithologic character, in addition to radiometric and biostratigraphic data.

In this paper stratigraphic and sedimentologic data, including sediment dispersal patterns, and provenance of clastic facies, are used to reconstruct the regional paleogeography of the southern sector of the foreland. This paper builds on previous work on the Dakota and Iron Springs Formations (Fillmore and Middleton, 1989; Fillmore, 1991) with new data on Cretaceous strata in Nevada and Arizona to provide an expanded view of the regional paleogeography.

STRATIGRAPHY

Southwest Utah - Dakota Conglomerate and Iron Springs Formation

The study area in southwest Utah includes the Beaver Dam Mountains to the south, near the town of Gunlock, and the Three Peaks area (Fig. 2). Throughout this area upper Cretaceous strata rest unconformably on various members of the Jurassic Carmel Formation with up to 60 m of erosional relief (Hintze, 1986; Fig. 3). At Gunlock, conglomerate of the basal Dakota Formation ranges from 0 to 15 m in thickness and is separated from the overlying Iron Springs Formation by a 7-m-thick bentonitic

In Dunn, G., and McDougall, K., eds.,1993,
Mesozoic Paleogeography of the Western United States-II
Pacific Section SEPM, Book 71, p. 417-432.

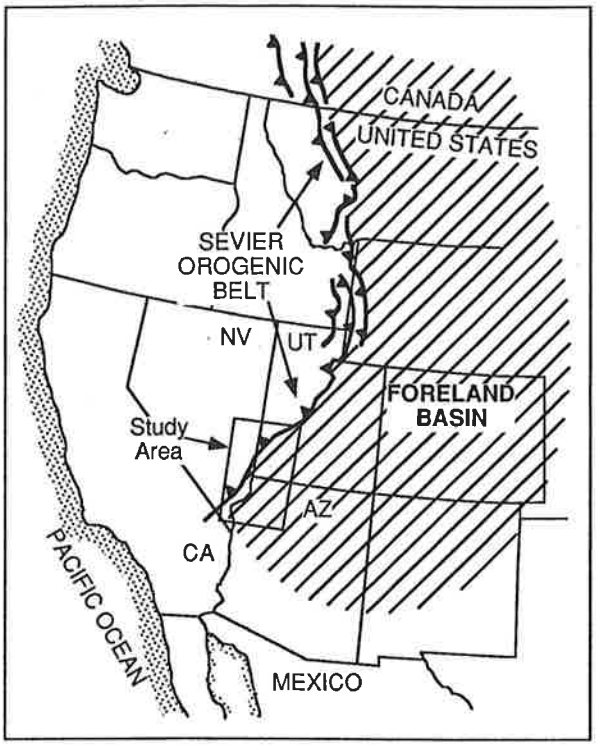

Figure 1. Map of western North America showing the study area and the extent of the Cretaceous Sevier orogenic belt and associated foreland basin.

tuff bed (Hintze, 1986). The sandstone-dominated Iron Springs Formation ranges to ~1000 m in thickness and grades upwards into, and intertongues with, the upper Cretaceous(?)-Paleocene(?) Grapevine Wash Formation (Wiley, 1963; Goldstrand, 1992), which is overlain by the Lower Tertiary Claron Formation.

At Three Peaks no Dakota Formation is recognized; the Iron Springs Formation is up to 830 m thick and consists of sandstone, siltstone, and conglomerate (Fillmore, 1991). Basal conglomeratic strata at Three Peaks, however, are interpreted to be correlative to the Dakota at Gunlock (Fillmore, 1991). The Iron Springs Formation is unconformably overlain by the Claron Formation (Mackin, 1947; Mackin and Rowley, 1976; Goldstrand, 1992).

Although the previously assigned Late Cretaceous age for these strata, based on stratigraphic correlation, was correct (Bissell, 1952; Van de Graff, 1963), recent data have provided significantly tighter constraints. A Cenomanian age for the fluviatile Dakota Formation in southwest Utah is based on correlation with fossiliferous fluvial and marine Dakota strata to the east, in south-central Utah (am Emde, 1991; Eaton, 1991). At Gunlock, Hintze (1986) reported an 80+/-10 Ma zircon fission track age from the bentonitic tuff that lies between the Dakota and Iron Springs Formations. Only the upper range of error for this fission track age fits the Cenomanian to Turonian age that is indicated by palynomorphs from lower Iron Springs strata at Gunlock (Hintze, 1986). Vertebrate fossils from the upper part of the formation, in the Pine Valley Mountains immediately east of Gunlock (Fig. 2), indicate a Santonian age (Eaton, 1992). No age data from the Three Peaks area have been obtained.

Southern Nevada - Willow Tank Formation and Baseline Sandstone.

In the Muddy Mountains, southern Nevada, the Willow Tank Formation lies unconformably on an erosional surface cut into the Jurassic Carmel Formation and Aztec Sandstone (Longwell, 1949; Bohannon, 1983). The Willow Tank Formation is ~80 m thick and consists of a basal conglomerate and a relatively thick sequence of claystone, siltstone, and carbonaceous shale. In the conformably overlying Baseline Sandstone three members are recognized (Fig. 3). The sandstone-dominated basal white member is conformably overlain by the red member, which is defined by its red color. To the north, in the North Muddy Mountains, the red member interfingers with the Overton Conglomerate Member. The Overton Conglomerate, over most of its extent, is conformable with the underlying white member, but locally is unconformable and angular (Bohannon, 1983). The Baseline Sandstone is overlain by the Miocene Horse Spring Formation (Bohannon, 1983).

The age of Cretaceous strata in southern Nevada is well-constrained, although a minimum age has not been established. Fleck (1970) reported K-Ar ages from tuffs in the Willow Tank Formation of 98.4 and 96.4 Ma, on the Albian-Cenomanian boundary (97.5 Ma, from the DNAG time scale of Palmer, 1983). Similarly, the occurrence of the fern *Tempskya* suggests an Albian age (Ash and Read, 1976). Tuffs in the lower white member of the Baseline Sandstone have yielded K-Ar ages of 95.8+/-3.5 and 96.9+/-3.6 Ma, and an age of 93.1+/-3.4 Ma has been obtained from the overlying red member (biotite concentrates; Carpenter and Carpenter, 1987). All age data from the Baseline Sandstone indicate a Cenomanian age.

Northwest Arizona - Jacobs Ranch and Cottonwood Wash Formations.

Cretaceous(?) strata in the Virgin Mountains, northwest Arizona, include the Jacobs Ranch Formation and the Cretaceous(?) or Eocene(?) Cottonwood Wash Formation (Moore, 1972). The Jacobs Ranch Formation unconformably overlies the Navajo (Aztec) Sandstone and is up to 90 m thick. The formation comprises a 2- to 6-m-thick basal conglomerate overlain by interbedded sandstone, siltstone, and conglomerate. The Cottonwood Wash Formation lies unconformably on the Jacobs Ranch Formation and comprises up to 425 m of conglomerate, tuff, and carbonate (Moore, 1972). Locally the contact exhibits an angular discordance of up to 15°, and where the Cottonwood Wash Formation truncates the Jacobs Ranch Formation, it rests on Navajo Sandstone (Moore, 1972).

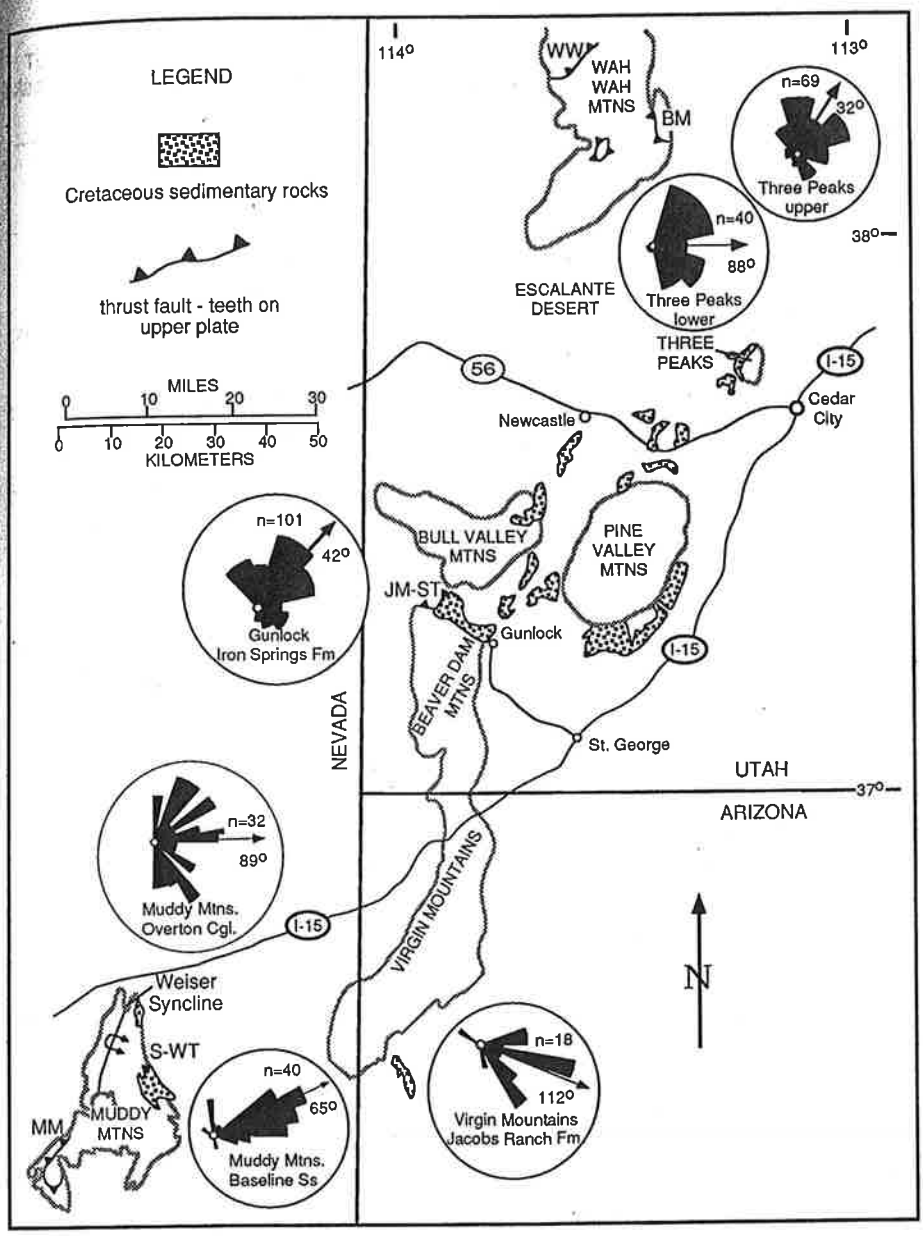

Figure 2. Map of the study area showing distribution of Cretaceous sedimentary rocks and thrust faults discussed in text. Rose diagrams show paleocurrent data with mean vector for each locality. WW: Wah Wah thrust; BM: Blue Mountain thrust; JM-ST: Jackson Mountain-Square Top thrust; S-WT: Summit-Willow Tank thrust; MM: Muddy Mountain thrust.

No age data are available for these strata, but based on stratigraphic location and lithologic character, Moore (1972) correlated the Jacobs Ranch Formation with the Willow Tank Formation and Baseline Sandstone in Nevada and the Iron Springs Formation in Utah. Moore (1972) correlated the Cottonwood Wash Formation with the Overton Conglomerate and the Horse Springs Formation in Nevada, and the Claron Formation in Utah. These correlations were made prior to the assignment of the Overton Conglomerate to the Baseline Sandstone and the establishment of a Miocene age for the Horse Spring Formation. Basal conglomerate of the Cottonwood Wash Formation is herein correlated with the Overton Conglomerate Member of the Baseline Sandstone based on stratigraphic, lithologic, and compositional similarities (Fig. 3). It is possible that the overlying tuff and carbonate is much younger than the basal conglomerate, and unrelated to foreland basin development.

METHODS

Interpretations of Late Cretaceous paleogeography reported in this paper are based on data obtained from detailed measured stratigraphic sections. Lithofacies analysis using facies associations and vertical successions are used to interpret depositional environments. Directional data from cross-stratification and clast imbrication are used to establish sediment dispersal patterns. These are used in conjunction with compositional data from modal analysis of thin-sectioned sandstone samples, and clast counts from conglomeratic units to determine the provenance of clastic facies.

Sandstone compositional data were obtained from point counts of 49 thin-sectioned Iron Springs Formation samples from the Three Peaks and Gunlock areas (Fillmore,

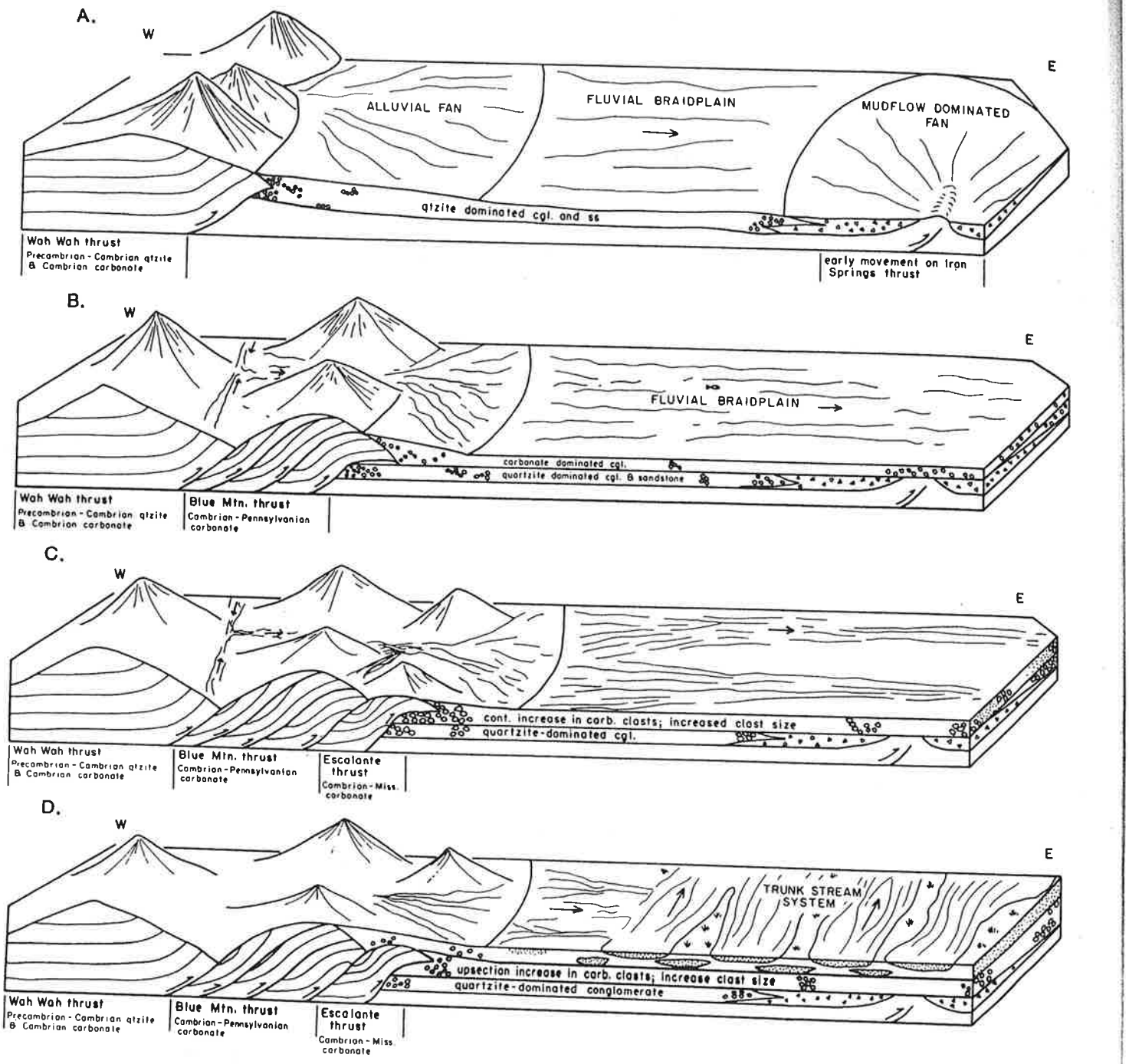

Figure 7. Tectonic evolution of thrust belt and depositional basin at Three Peaks. (A) Time 1: Uplift of the Wah Wah thrust producing quartzite conglomerate and subsurface movement on the incipient Iron Springs thrust, resulting in intrabasinal alluvial fan development. (B) Time 2: Ramping and erosion of the Blue Mountain thrust and influx of carbonate detritus into the basin. (C) Time 3: Escalante thrust as frontal expression of the thrust belt and coarsening of conglomerate due to eastward migration of tectonism. (D) Time 4: Development of trunk system in which flow parallels the strike of the Sevier mountain front (from Fillmore, 1991).

North America. We are incredibly fortunate that the rocks ... posed in the Grand Canyon record this time period like no other place on the continent. This great chasm is truly a unique "window into the past."

The Grand Canyon (Fig. 1) lies entirely in the northwestern part of Arizona. It extends nearly 278 miles (448 kilometers) between Lake Powell on its eastern end and Lake Mead to the west. In 1919, the region became a national park, which today encompasses approximately 1900 square miles (4921 square kilometers) of land. This most famous of all canyons was formed by swiftly flowing waters of the Colorado River cutting into rock layers of the southwestern Colorado Plateau, a vast uplifted tableland that includes a large portion of the Four Corners states: Arizona, Colorado, New Mexico, and Utah. The land surrounding the Grand Canyon includes six local plateaus and one low lying platform, all of which are bounded by faults or monoclines (Fig. 2). In a west-east cross section to the north of the canyon

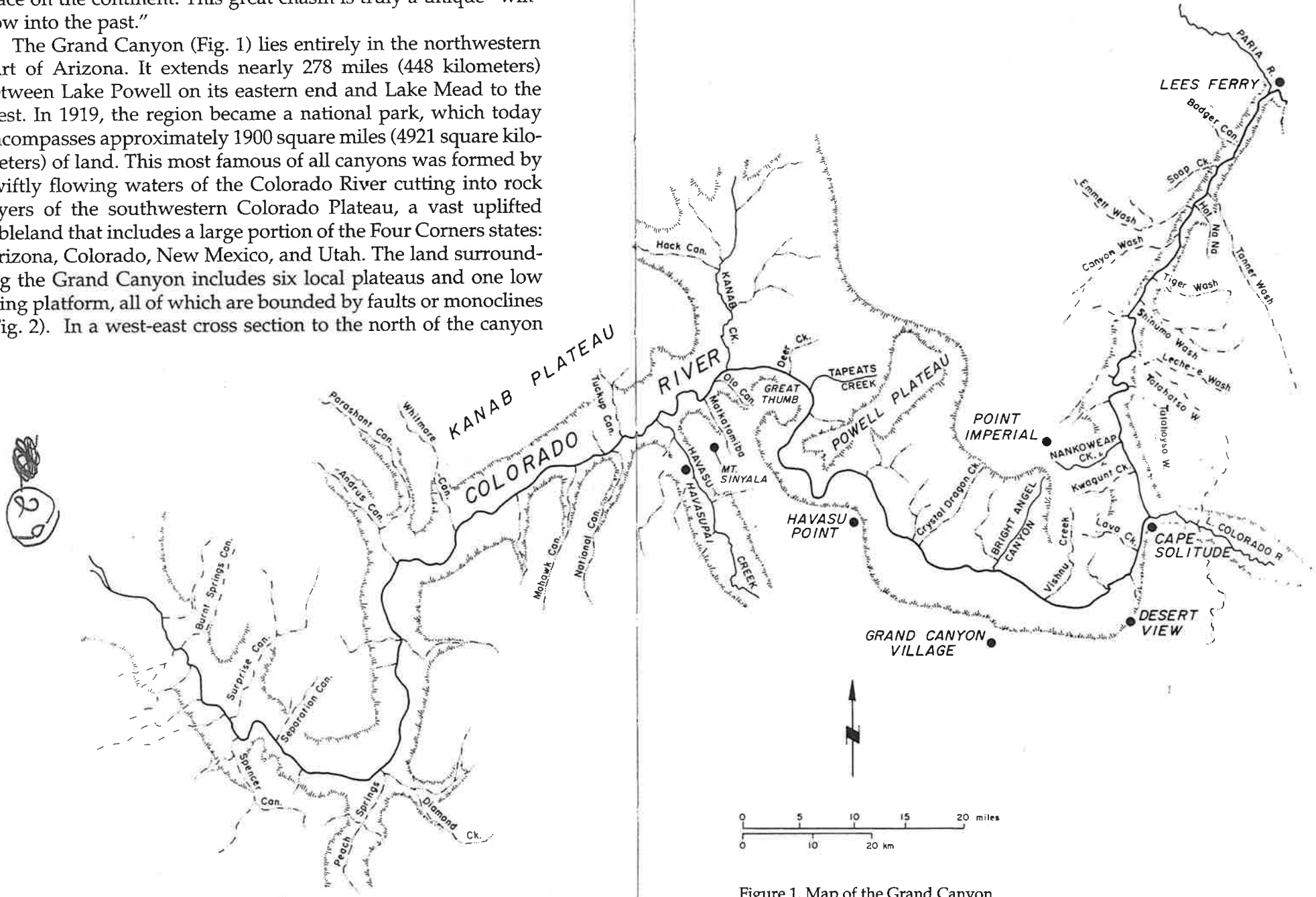

Figure 1. Map of the Grand Canyon

(Fig. 3), you can see how each of these blocks of land has been uplifted, downdropped, or tilted relative to its neighbor.

At its narrowest, the Grand Canyon is a little less than a mile (1.6 kilometers) across. Along the canyon's north and south rims, the relief is relatively gentle, except for incisions made by runoff waters flowing into the gorge. Within the canyon itself, however, the topography is quite varied and spectacular. The maximum depth of the canyon at any single place is about 6000 feet (1829 meters) from the rim to the floor. The maximum drop in elevation of the canyon as a whole, however, is approximately 6600 feet

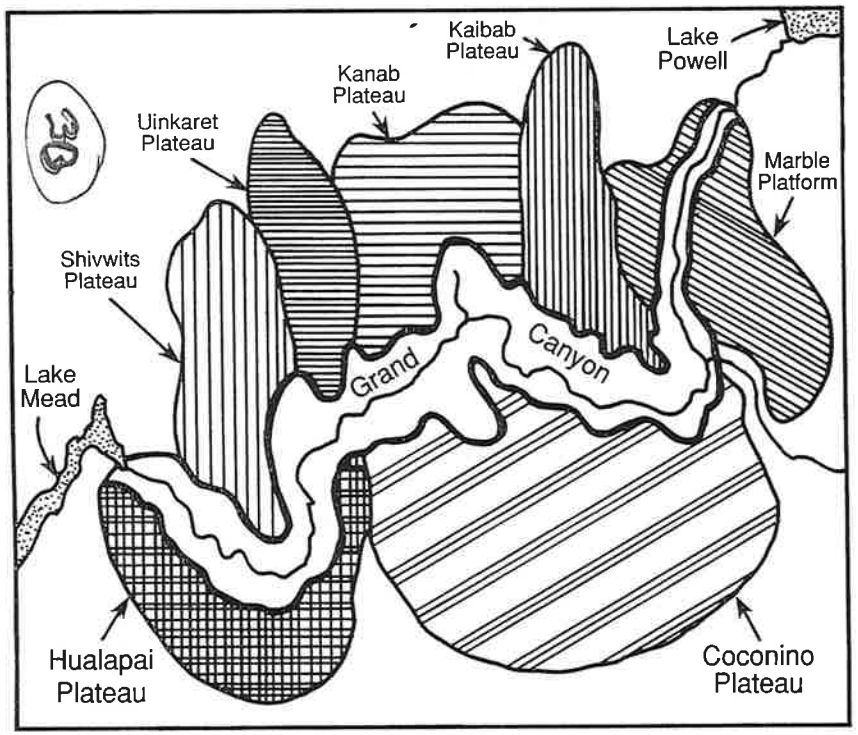

Figure 2. Generalized map of the area surrounding the Grand Canyon

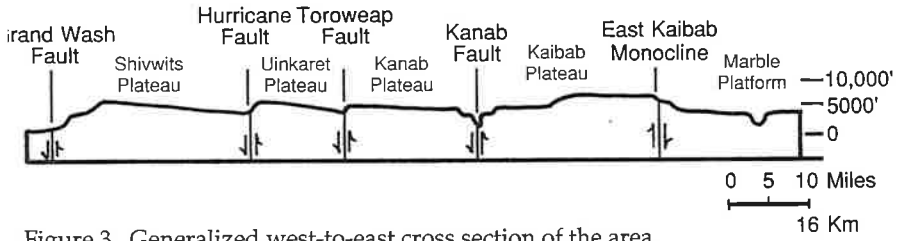

Figure 3. Generalized west-to-east cross section of the area just north of the Grand Canyon

(2012 meters) between Point Imperial on the north rim (8803 feet [2683 meters]) and the floor of the canyon near Lake Mead (1200 feet [366 meters]).

Many people are surprised to learn that there is a difference in elevation between the north and south rims. On the canyon's southern edge, the altitude ranges from 6000 to 7500 feet (1829 to 2286 meters) above sea level. The northern edge, however, is 1000 to 1200 feet (305 to 366 meters) higher even though both rims are capped by the same rock unit, the Kaibab Formation. The difference in height occurs because the various rock layers into which the canyon has been cut do not lie completely flat in this region. Instead, they arch or dome upward. The Colorado River carved the canyon through the southern flank of the dome, where the rock layers are tilted gently down to the south. Layers on the north rim, therefore, have been uplifted higher than the same layers on the south rim (Fig. 4).

Water that flows into and through the Grand Canyon comes primarily from four merging rivers—the Green, San Juan, Little Colorado, and Colorado—that drain hundreds of square miles of the Four Corners states (Fig. 5). As it courses through the canyon, the Colorado River drops about 2000 feet (610 meters) in elevation (Fig. 6). This steep gradient allows the river to continue its erosion of the chasm's floor.

Humans have been in the Grand Canyon for at least four thousand years, but the early records are sparse. Rare artifacts, remains of prehistoric dwellings, and the numerous mescal pits all attest to the early exploration and habitation by American Indians such as the Anasazi and the Cohonina. The first Euro-

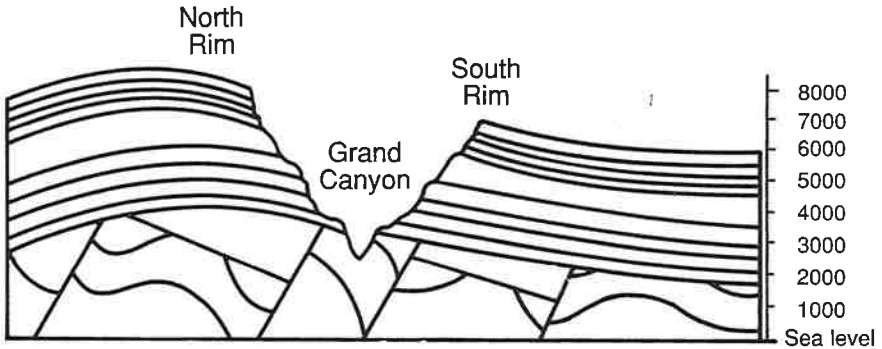

Figure 4. Generalized cross section through the Grand Canyon from the north rim to the south rim

Figure 5. Drainage area for runoff water that flows into and through the Grand Canyon

peans to see the canyon were a Spanish party of thirteen in search of the fabled lost cities of gold, under the command of Captain Don García López de Cárdenas. In 1540, Hopi Indian guides led them to the south rim in the eastern part of the Grand Canyon, but they were unable to reach the river below. In the next three

...uries, only ... visits to the region have been reliably recorded. In 1776, Father Francisco Tomás Garcés, a Spanish missionary, explored Havasu Canyon in the south-central part of the Grand Canyon. In the same year, two Spanish priests, Father Silvestre Vélez de Escalante and Father Francisco Domíngues, led an expedition to the region and discovered a ford across the Colorado River (Crossing of the Fathers).

Among the earliest geological reports of the Grand Canyon country are those of Jules Marcou (1856) and John Strong Newberry (1861), who described the region's Paleozoic stratigraphy from their explorations of the canyon and the land to the south. Newberry was a geologist in the War Department-sponsored Ives expedition of 1857-58. Ives' rather discouraging and, as it turned out, unprophetic statement about the Grand Canyon was:

> Ours has been the first, and will doubtless be the last party of whites to visit this profitless locality. It seems intended by nature that the Colorado River, along the greater portion of its lonely and majestic way, shall be forever unvisited and undisturbed.

In 1869, John Wesley Powell led a party of ten men (reduced later to nine and finally only six) on an epic journey by boat down a thousand miles of the Colorado River from Green River, Wyoming, across Utah, and finally through the Grand Canyon to the mouth of the Virgin River at what is today the north end of Lake Mead. Powell's work was followed up by a small group of outstanding scientists through the turn of the nineteenth century. These included G.K. Gilbert, who was the first to apply formal rock unit names to Grand Canyon rocks; C.E. Dutton, who wrote

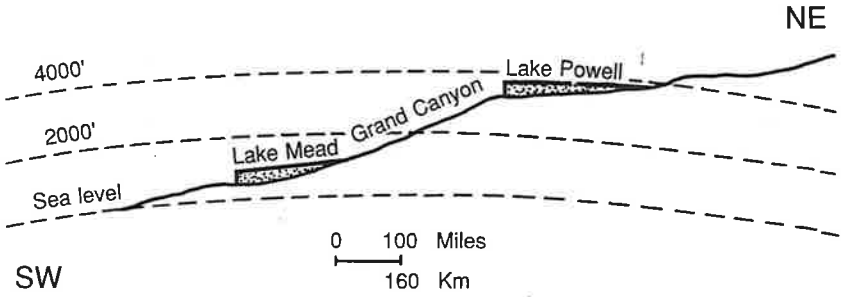

Figure 6. Diagrammatic profile of the Colorado River through the Grand Canyon, from Lake Powell to Lake Mead

the first monograph on the geology and geologic history of the Grand Canyon; A.R. Marvine, who participated in the U.S. Geographical Survey West of the 100th Meridian; and C.D. Walcott, who described both Paleozoic and Precambrian rocks in the canyon's central and eastern parts. These pioneer studies laid the groundwork for all subsequent research in the Grand Canyon.

Edwin D. McKee, to whom this book is dedicated, stands out as the premier research scientist of Grand Canyon geology in the twentieth century. Between 1933 and 1982, McKee either authored or coauthored five monographic publications on various Paleozoic rock units of the canyon—including the Redwall Limestone, Supai Group, Coconino Sandstone, the Toroweap and Kaibab formations, and Cambrian units. McKee also organized a special symposium in 1964 at the Museum of Northern Arizona to summarize the data and interpretations on the origin and evolution of the canyon. Much of our present understanding of the stratigraphy and age of Grand Canyon rocks (Fig. 7) is based on McKee's seminal work.

For more than a century, then, the Grand Canyon has attracted the extraordinary interest and effort of geologists to map its course, examine its rocks and fossils, and understand its record of earth history. In 1870, Powell wrote of the canyon country of the Colorado River:

> ... the thought grew in to my mind that the canyons of this region would be a Book of Revelations in the rock-leaved Bible of geology. The thought fructified and I determined to read the book.

Since then, several generations of earth scientists have searched the river and its canyon for answers to questions of when and how this part of our planet's crust developed. Although some questions have been answered, new ones are raised, and so the search goes on. This book is written for those who inquire about the revelations of the Grand Canyon. It is a compilation of the best efforts of a number of authors, all experts in their field, to summarize what is now known about the geology of the canyon. Much of the information presented here is an update and refinement of earlier works by pioneer scientists of the past. All of us who have written for this volume owe a great debt to those who preceded us in the search for the geologic secrets of the Grand Canyon.

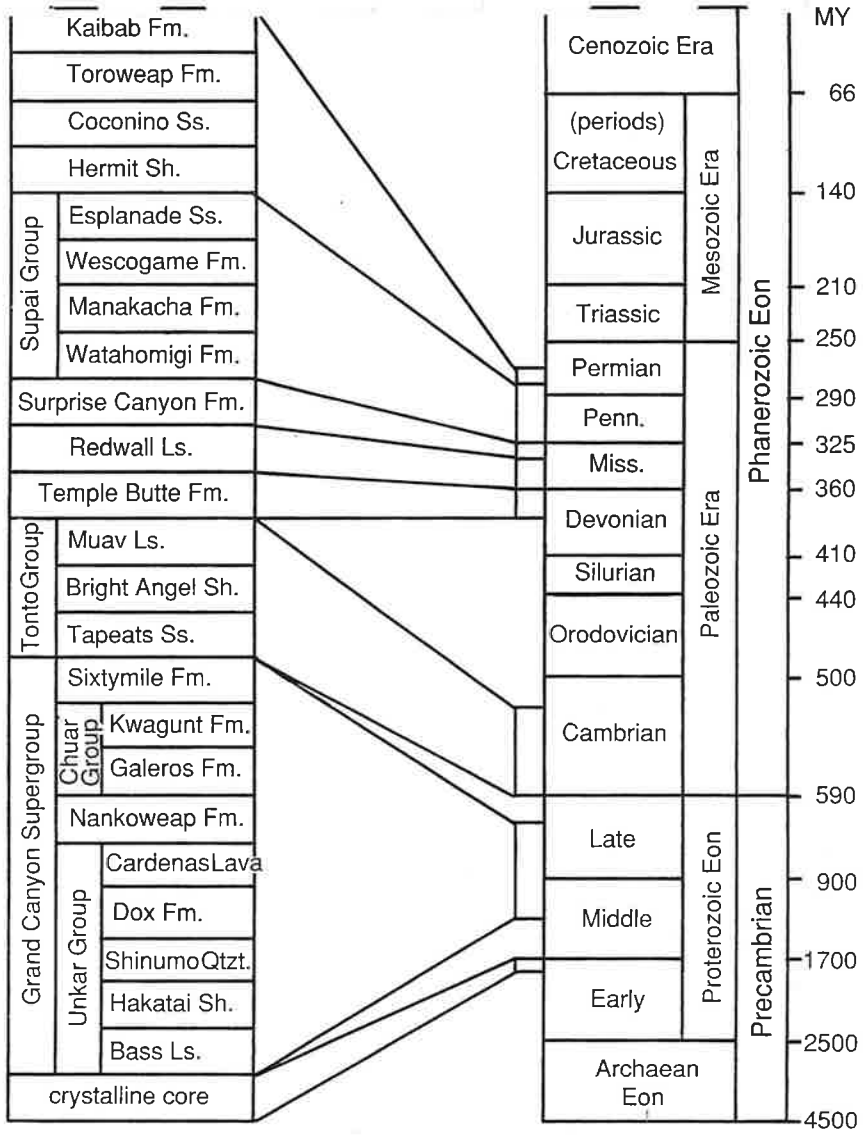

Figure 7. Comparison of the geologic column of the Grand Canyon with the Geologic Time Scale (After Haq and Van Eysinga, 1987)

Surprise Canyon Unconformity

The ... ion surface that developed on the Redwall Limestone during the Late Mississippian period, and on which the Surprise Canyon was deposited, must have been a relatively flat, resistant, limestone platform but with considerable local relief. Most of the Surprise Canyon outcrops occupy gently U-shaped or V-shaped notches cut into the top of the Redwall. By their nature and distribution, these notches appear to have been part of a major dendritic drainage system that flowed generally from east to west. They also appear to have been incised up to 400 feet deep (122 m) into the top of the Redwall Limestone near the western end. A preliminary reconstruction of the drainage pattern (Grover 1987) illustrates several major valleys that merge westward (Fig. 9). In addition, solution depressions and caves in the upper Redwall Limestone are filled locally with red mudstone of the Surprise Canyon Formation, indicating the development of a karst topography prior to Surprise Canyon deposition (Fig. 10). The time available for the development of this eroded and karsted topography on top of the Redwall is just a few million years—the interval between youngest Redwall (of middle Meramecian age) and oldest Surprise Canyon (of approximately middle or late Chesterian age). The depth of the stream valleys eroded into the top of the Redwall indicates an uplift or a several hundred foot (120 m) drop in sea level.

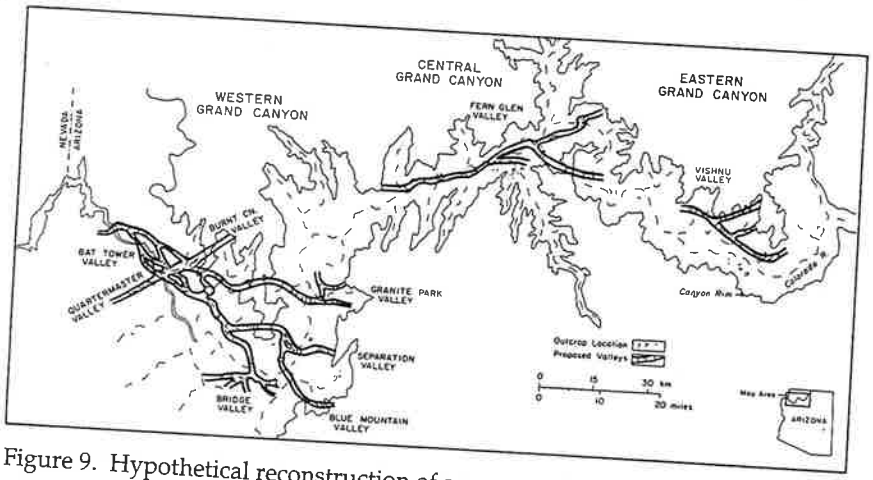

Figure 9. Hypothetical reconstruction of segments of the ancient valley system eroded into the Redwall Limestone in Late Mississippian time and into which the Surprise Canyon Formation was deposited

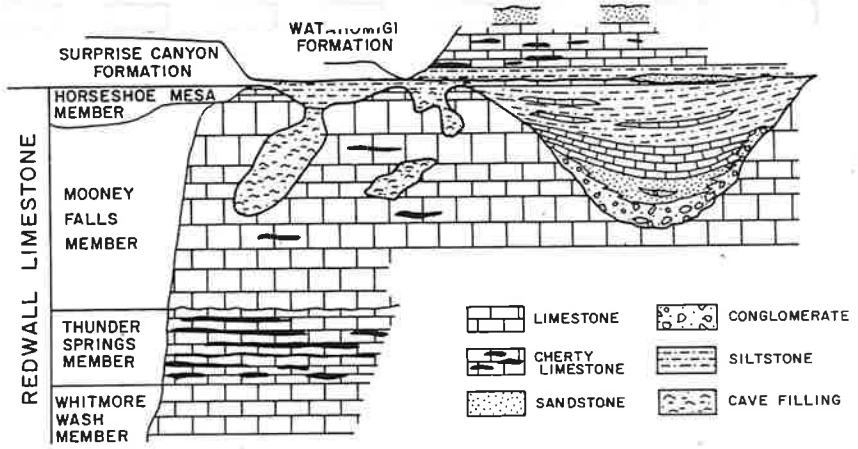

Figure 10. Cross section showing the stratigraphic relationship of the Surprise Canyon Formation to the underlying Redwall Limestone and overlying Watahomigi Formation of the Supai Group. Modified from Billingsley and Beus (1985, Fig. 3)

Stratigraphy and Lithology

The thicker sections of the Surprise Canyon Formation can be divided into three major rock units: 1) a lower conglomerate and sandstone, mainly of terrestrial origin; 2) a middle unit of skeletal limestone of marine origin; and 3) an upper, mainly marine unit of siltstone and silty, sandy, or algal limestone (Fig. 6). Since several lithofacies are included in each of the three units, the Surprise Canyon Formation exhibits a greater variety of sedimentary rock types than almost any other Paleozoic unit in the Grand Canyon.

The basal part of unit 1 in most sections consists of a ferruginous, pebble-to-cobble and local boulder conglomerate. Clasts are predominantly chert with minor limestone derived from the underlying Redwall Limestone. Some cobbles and boulders contain typical Redwall fossils. The clasts commonly are grain-supported and enclosed in a sandy matrix of nearly pure quartz grains and some hematite. Locally, the cobbles are sufficiently imbricated to indicate water current directions at the time of deposition (Fig. 11). In most sections, the conglomerate grades upward into a yellow or dark reddish brown or purple quartz sandstone or siltstone or, in some sections, a dark gray, carbonaceous shale. The sandstone beds commonly are flat bedded, but some

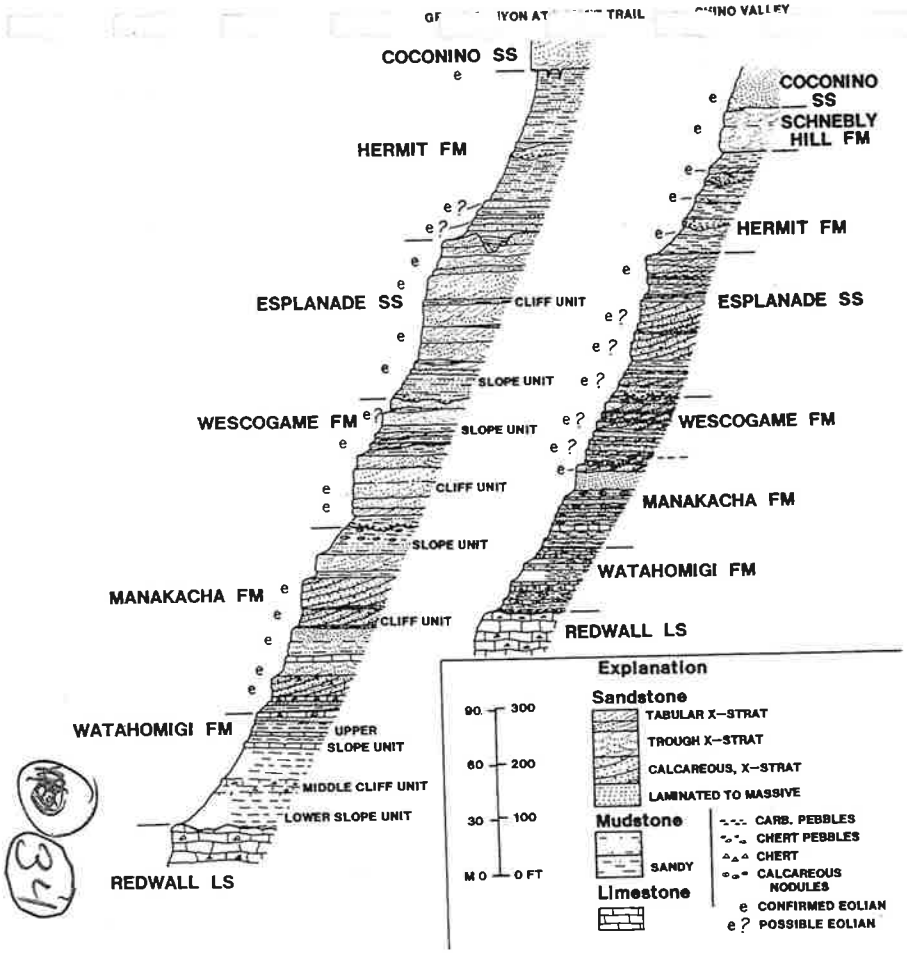

Figure 4. Columns of Supai Group and Hermit Formation and related strata showing distribution of known and suspected eolian strata

mudstone. The contact apparently occurs at the change from primarily slope below to steep slope or cliff above and, therefore, may not be a consistent stratigraphic level across the region.

The sharp increase in limestone west of a line paralleling the Hurricane Cliffs can be used to divide the Watahomigi Formation into an eastern redbed facies and a western carbonate facies (see McKee 1982, Fig. 6). The westward increase in thickness, carbonate content, and marine fossils is typical of many Paleozoic rock units in the Grand Canyon region.

Manakacha Formation

The Manakacha Formation marks an important change in the trend of Paleozoic depositional patterns in the Grand Canyon region. Following initial Cambrian sand deposition, the area was dominated by carbonates and minor mudstones from Middle Cambrian to Early Pennsylvanian time. The influx of quartz sand during the deposition of the Manakacha reflects a significant change across the western interior of the United States.

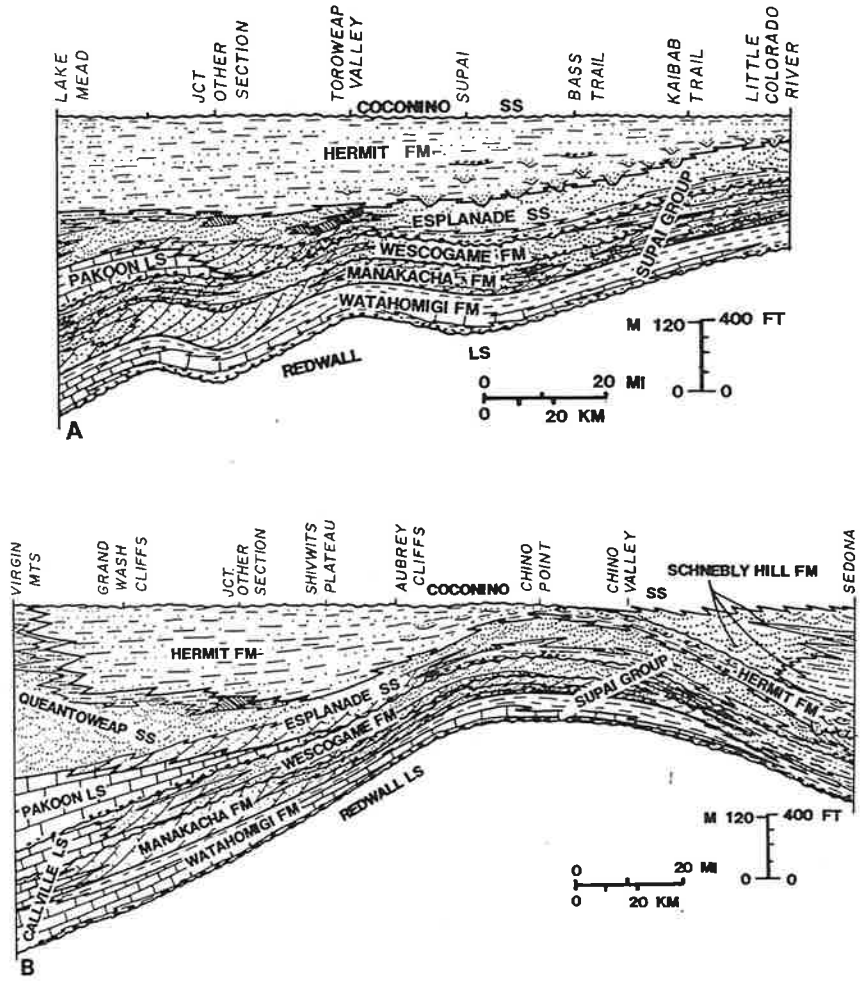

Figure 5. Restored stratigraphic cross section of Supai Group, Hermit Formation, and related strata. (a) West to east through Grand Canyon; (b) northwest to southeast from Virgin Mountains to Sedona

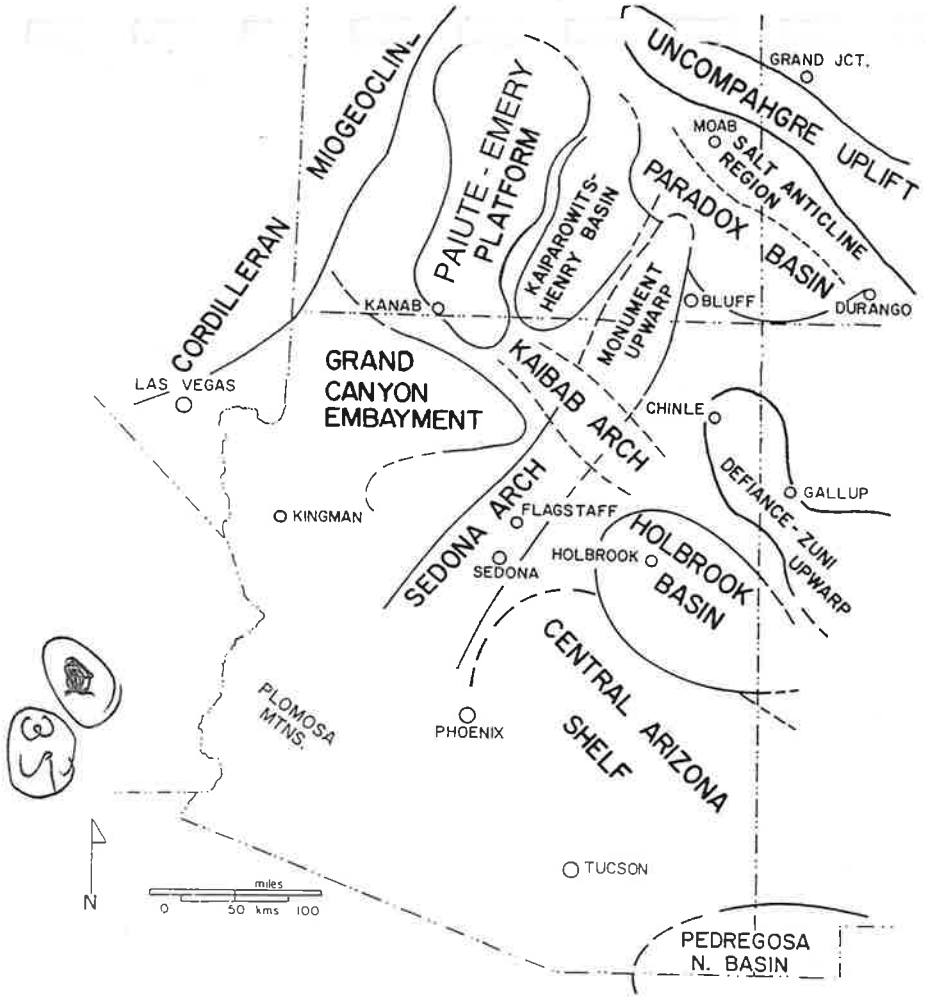

Figure 10. Map showing late Paleozoic tectonic elements of northern Arizona and vicinity. Note that Grand Canyon lies between more negative regions to the west and more positive areas to the east.

The influx of quartz sand into the Colorado Plateau region from the north also complicates the setting. The sand tended to accumulate between the arches and adjacent shelves or basins as extensive eolian deposits (Blakey 1988). When sea level was relatively low, eolian deposits became widespread, often expanding into basins and across shelves; when the sea level was high,

...n d... ...its, i... ...sent ...ec... ...ed t... row... ...s alc... ...he flanks of arches (Chan and Kocurek 1988).

The Grand Canyon and the western Mogollon Rim region lay in a somewhat intermediate position between more negative areas to the northwest and higher ones to the southeast. Not unexpectedly, the resulting sedimentation is intermediate in character; cyclic sedimentation with more continental aspects is present in the east while cyclic sedimentation with more marine aspects is present in the west.

The general structural grain of northwestern Arizona tended southwest-northeast during Supai and Hermit time. Shorelines and marine trends should have paralleled this pattern, and fluvial deposits should have flowed northwesterly, perpendicular to this grain. Indeed, marine and shoreline patterns do parallel the trend, but the sandstone bodies that McKee (1982) suggested might be of fluvial origin show a paleocurrent reading to the south and southeast; this is as much as 180° from the expected trend. We have not documented the trends of Hermit Formation sandstone bodies.

Any one of the above controls on deposition was sufficient to produce a complicated depositional pattern. Together, they combined to produce a heterolithic record that varies abruptly, both vertically and laterally. The summary presented below must be considered preliminary. We have much to learn about the depositional history of the Supai Group and the Hermit Formation.

Depositional Environments

Recent studies tend to confirm the long-standing belief that the Supai Group was deposited on a broad coastal plain. Individual depositional settings ranged from shallow marine to continental. However, the recent identification of eolian-deposited sandstone units throughout the section necessitates a reinterpretation of Supai depositional history. Most of our knowledge of the Supai is based on the work of McKee, who provided a general description of sandstone bodies in the Supai Group (1982, pp. 260, 261). He interpreted the large foresets planes in the Manakacha Formation as the fronts of large, subaqueous sand sheets or small Gilbert deltas in areas strongly affected by tides. Traditionally, geologists have interpreted sandstone bodies of the Wescogame Formation as having formed in a high-energy, fluvial environment. Marine bioclastic debris was thought to have been trapped in an estuarine setting.

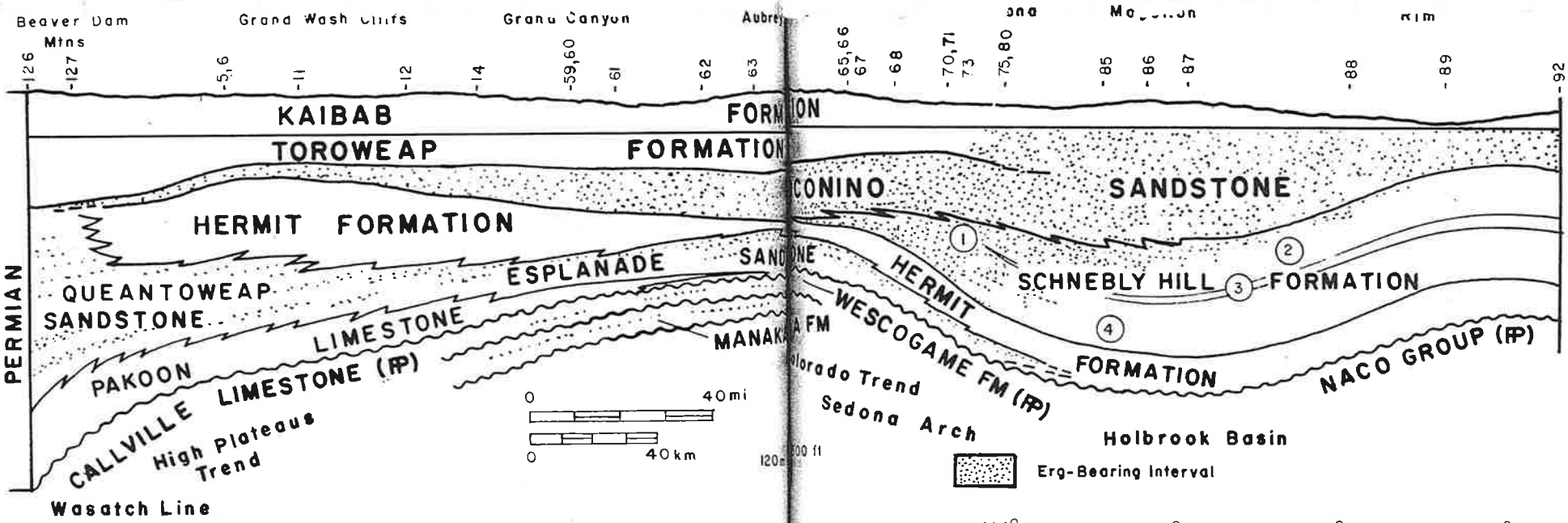

Figure 1. Regional stratigraphic relationships of Permian strata along the southern margin of the Colorado Plateau (after Blakey and Knepp)

In the 1940s, McKee conducted a series of experiments designed to duplicate the Coconino tracks. He filled a long trough with sand that formed a hill in the center. A variety of small vertebrates and invertebrates then were induced to walk along the sand and over the hill. By varying the slope of the hill and the moisture content of the sand, McKee was able to test the trace-forming capabilities of a variety of animals in a number of different environments. He tested the animals on a variety of surfaces—including dry sand, damp sand, saturated sand, and even sand that had been soaked and then allowed to dry. He found that only the largest animals tested (chuckwalla lizards) were able to make tracks in wet sand or crusted sand, and even then, the tracks were not as clear as those formed in dry sand. Smaller animals, such as millipedes and scorpions, were unable to make tracks in wet sediment and left clear traces only in dry, loose sand. He also found that at slopes below 27°, both uphill and downhill tracks were likely to be preserved. Avalanching, however, tended to destroy tracks on steep slopes.

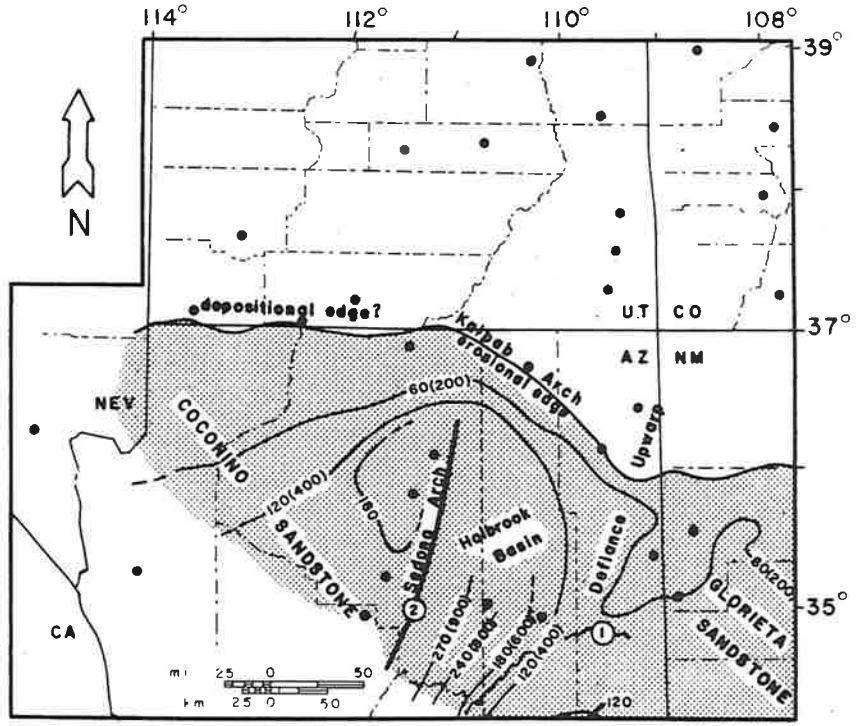

Figure 2. Isopach map of the Coconino Sandstone illustrating thinning away from the Sedona arch (after Blakey and Knepp)

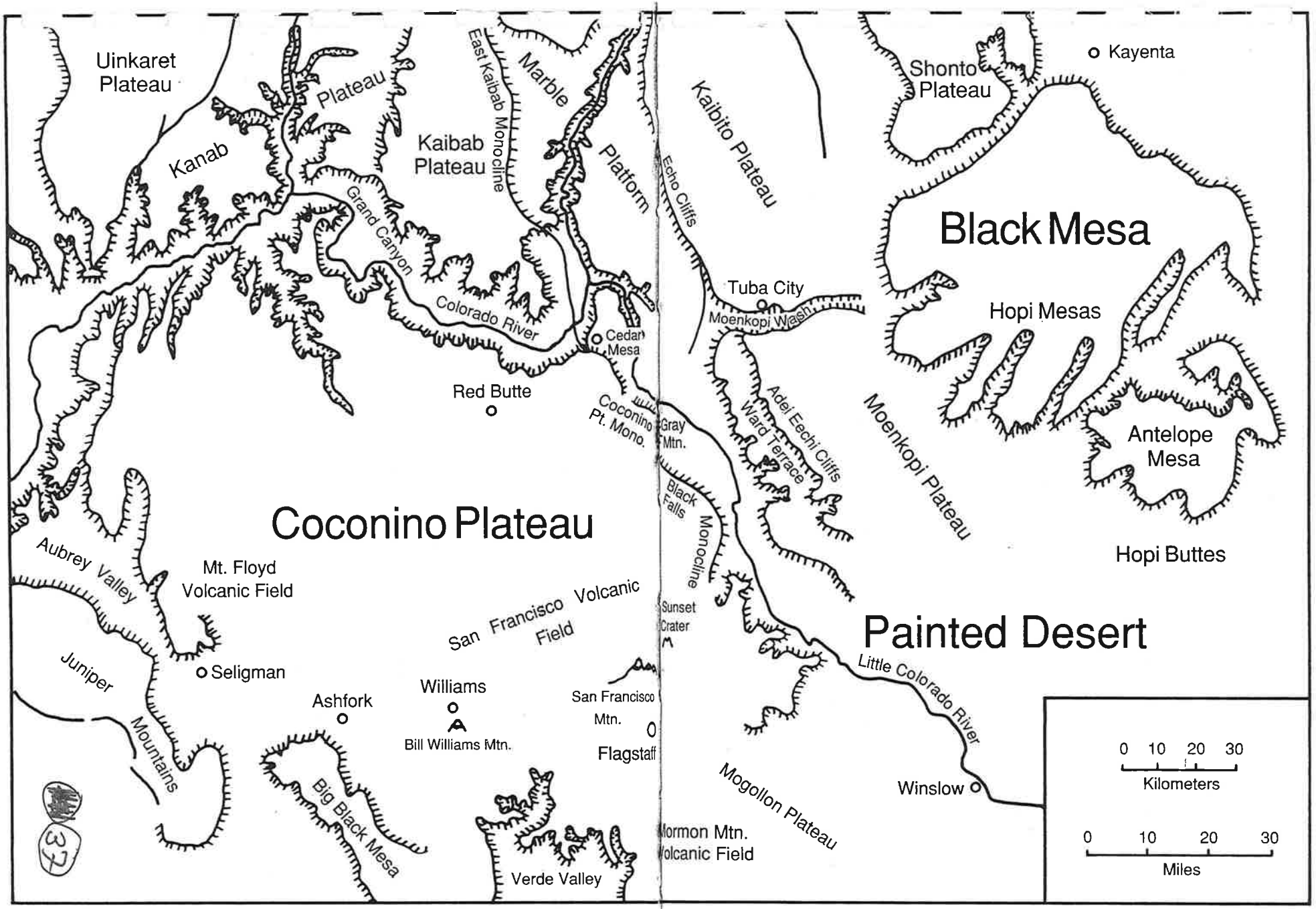

Figure 2. Physiographic map of the central and eastern Grand Canyon and surrounding areas (after Gregory 1950, Cooley and others 1969, King 1977, Billingsley and Hendricks 1989)

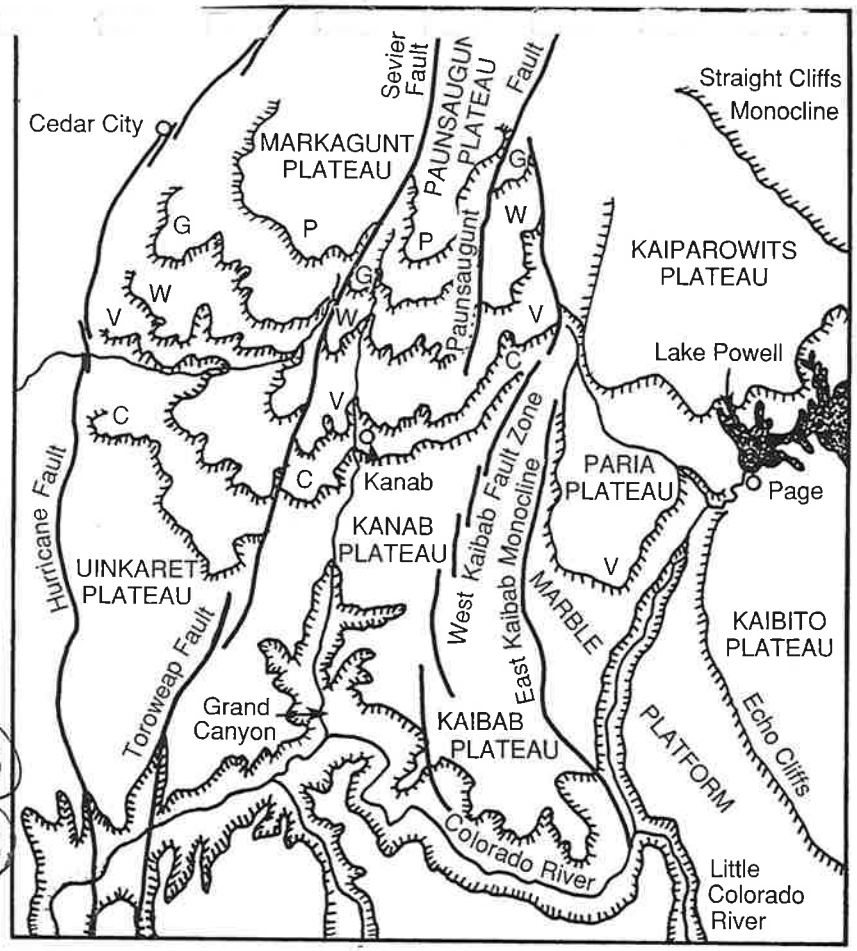

Figure 3. Physiographic map of the Grand Staircase section of the Colorado Plateau (after King 1977, Stokes 1986, Billingsley and Hendericks 1989)
C - Chocolate Cliffs; V - Vermilion Cliffs; W - White Cliffs; G - Gray Cliffs; P - Pink Cliffs; T - Terrace; Cyn - Canyon.

The first line of cliffs north of the Grand Canyon is the Chocolate Cliffs. The name is derived from the red-brown mudstone of the Lower and Middle Triassic Moenkopi Formation that forms the majority of the cliff profile. This escarpment sometimes is called the Shinarump Cliffs after sandstones and conglomerates of the Shinarump Member of the Upper Triassic Chinle Formation that cap the cliffs. Although the Chocolate Cliffs officially terminate at the northern end of Kaibab Plateau, the same rock units form a cliff and slope line along the southern

...gin ... ...ria ... ...eau. ...ere, ...ever, ... Mo...opi-...a-rump cliffs are not as well developed as the true Chocolate Cliffs. Erosional unconformities, which represent gaps in the rock/time record, separate the Moenkopi from the underlying Kaibab and overlying Chinle formations. The Moenkopi contains both marine and nonmarine sediments, whereas the Shinarump member of the Chinle is composed primarily of fluvial channel deposits. The flatlands and slopes above the Chocolate Cliffs, including Little Creek Terrace, Telegraph Flat, and related areas to the east, are formed by different fluvial and lacustrine members of the Chinle Formation.

The next step up the Grand Staircase is the very prominent Vermilion Cliffs. Starting at the base, red and purple deposits of the Chinle Formation, Wingate Sandstone, and the Moenave and Kayenta formations make up these cliffs, with the lower part of the Navajo Sandstone forming the caprock. The latter four formations comprise the Lower Jurassic Glen Canyon Group and are of

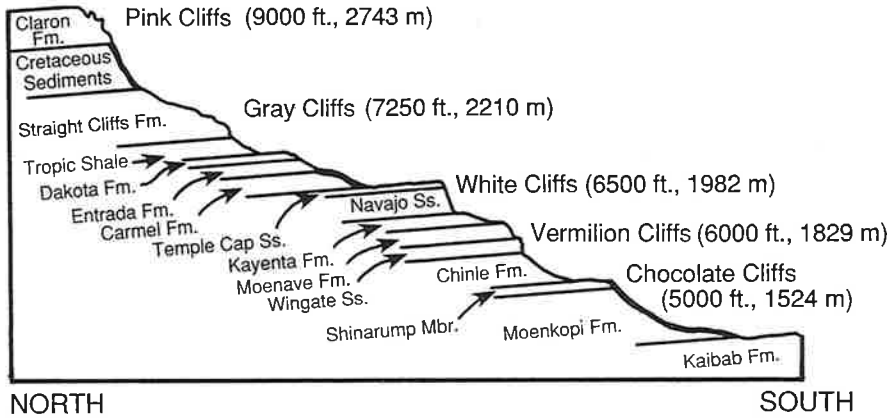

Figure 4. Diagrammatic cross section of the Grand Staircase—vertical scale greatly exaggerated (after King 1977, Stokes 1986, Hintze 1988, and Clemmeson and others 1989)

primarily eolian and fluvial origin. An unconformity separates the Wingate Sandstone from the underlying Chinle Formation; however, contacts between the other units are gradational to intertonguing. Above the Vermilion Cliffs, the Navajo Sandstone forms the bench that includes Moccasin Terrace, Wygaret Terrace, and their equivalents to the east.

The foregoing synopsis of Laramide events underscores the vast progress that has been made during the past century in deciphering the tectonic record preserved in the rocks of the Grand Canyon. Not only have we been able to map and date structures and deduce causative stresses, but we are beginning to weave these elements into the larger contexts of cordilleran tectonics, regional paleogeography, and sedimentation.

A number of important themes will be developed in this chapter. These include relating variations in the styles of deformation to different causative stress fields and documenting the overwhelming evidence for periodic reactivation of inherited fault zones by successive stress regimes. Another important theme is correlating uplift and subsidence to paleogeography, regional drainage patterns, and the movement of sediments into and out of the region.

Recent data indicate that most of the structures observed in the walls of the Grand Canyon vastly predate the Colorado River and its canyon. In fact, early Tertiary deformations are dated by sediments found in the remnants of Laramide, northward-draining canyons. Both these canyons and the sediments in them are ten times older than the Grand Canyon.

Even though late Cenozoic extensional faulting is spectacularly exposed, and exhibits an unprecedented record of recurrent activity here, the Grand Canyon still is best known in tectonic forums for its exceptional three-dimensional exposures of Laramide monoclines. The primary value of the Grand Canyon exposures is that the roots of the monoclines are unambiguously open to examination on the floor of the canyon.

The terms "Colorado Plateau region" and "Grand Canyon region" are used in this text for orientation purposes. However, recognize that the Colorado Plateau did not become fully defined until Miocene time, and erosion did not produce the Grand Canyon until Pliocene time. "Mogollon Highlands" refers to the general series of Mesozoic and Cenozoic uplifts occurring in the geographic regions south of the Colorado Plateau.

This chapter summarizes the work of many dozens of researchers spanning over a hundred years of effort. Detailed citations for each borrowed concept or fact lie beyond the scope of a work of this type. Consequently, the literature that is cited is designed to lead the interested reader to the most germane contributions or to sources that carefully develop important lines

of inquiry. A reading of this text will be facilitated greatly by having the following set of geologic maps close at hand: Huntoon and others (1981, 1982, 1986) and Billingsley and Huntoon (1983).

THE COLORADO PLATEAU

As Figure 1 shows, the Grand Canyon occupies a position on the southwest corner of the Colorado Plateau, a geologic province that is underlain by a thick continental crust that became slightly separated on the east from the continental craton during the Cenozoic Era. The plateau is ringed by zones of intense deforma-

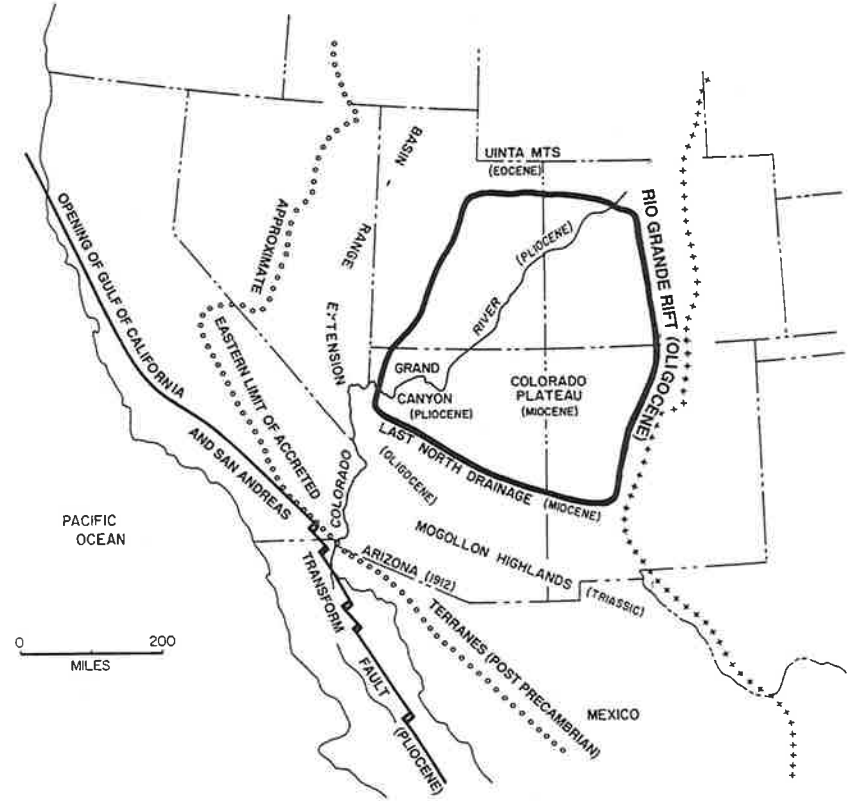

Figure 1. Selected tectonic elements in the western North American cordillera and the timing of their inception

...3 (10...n) c... rth-...neas ...d ti... atio... the ...-rado Plateau along right-lateral, strike-slip faults. The movement partially decoupled the Colorado Plateau from the North American continent along the future Rio Grande rift. The early Eocene reorganization of stresses within the plateau region appears to have resulted in minor development, or reactivation, of northwest-trending monoclines in the Grand Canyon region.

Chapin (1983) proposed that the northward crowding of the Colorado Plateau into the Wyoming province was accommodated by crustal shortening manifested as thrust faulting and regional folding. The result was the production of east-and southeast-trending basins and ranges in Wyoming. The southernmost of these was the east-trending Uinta uplift bounded both to the north and south by thrust faults dipping under the range. Bernaski (1985) summarizes data that reveals that the Uinta uplift began to rise in Early Eocene time. Thus, Laramide structures outlined the eastern and northern boundaries of the Colorado Plateau as we know it today. The eastern boundary, now the Rio Grande rift, became better defined and more strikingly decoupled from the North American craton as a result of extension beginning in Late Oligocene time.

Grand Canyon Monoclines

As Figure 4 shows, Laramide monoclines formed in the Paleozoic and Mesozoic sedimentary cover throughout the Grand Canyon region in response to reverse movement along favorably oriented, preexisting faults in the Precambrian basement. The reactivated basement faults most commonly were steeply west-dipping Precambrian normal faults that served as preexisting structural discontinuities within the Precambrian basement complex. Typical east-west spacings between the monoclines in the Grand Canyon region are fifteen to twenty miles (24-32 km). These spacings gradually increase toward the east across the Colorado Plateau. The total crustal shortening that resulted from deformation within the monoclines on the western Colorado Plateau was less than one percent. The reason for this low percentage is that spacings between the monoclines are large in comparison to local shortening across them.

Figures 5 and 6 demonstrate that the Grand Canyon provides the finest cross sections through monoclines found on the Colorado Plateau. The exposures into the Precambrian basement are

Lar...e fc...j ov...acti...d P...mbr...ault.
Precambrian fault was normal.

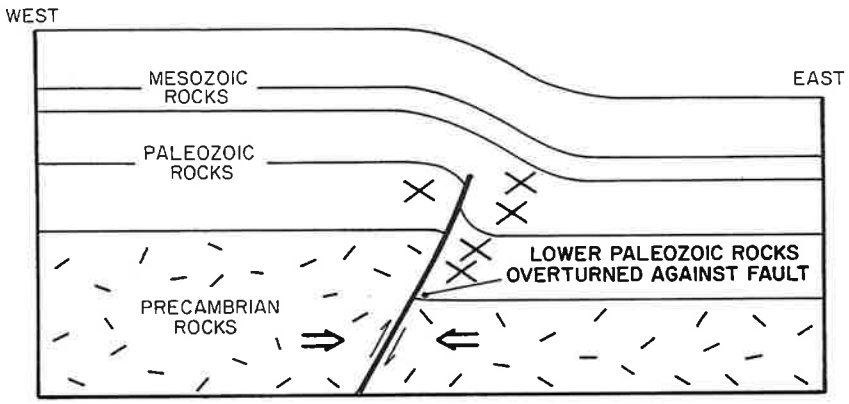

B. Late Cenozoic normal faulting.

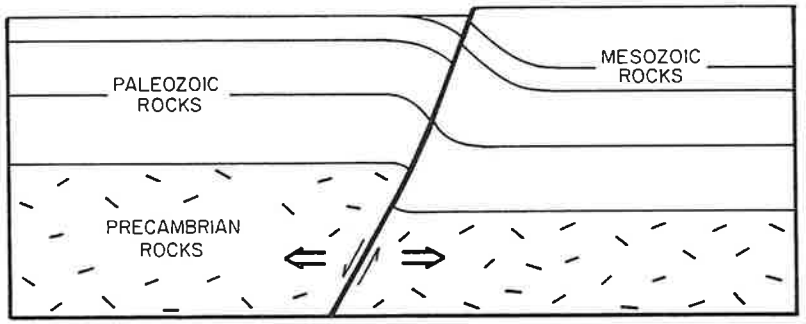

C. Late Cenozoic configuration after continued extension.

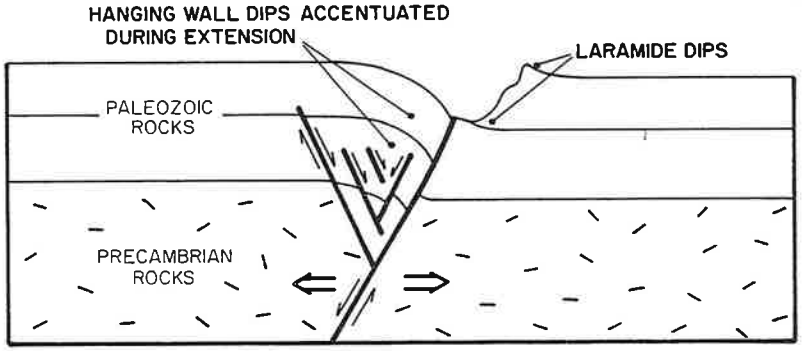

Figure 4. Stages in the development of a typical north-trending monocline-fault zone, Grand Canyon region, Arizona

tem... ...e re... wa... ...oles ... exte... w... the ... in-Range to the west and south of the Grand Canyon region during Late Oligocene through Middle Miocene time and east-west opening of the Rio Grande rift beginning in Late Oligocene time. The opening of the Rio Grande rift caused between two and four degrees of clockwise rotation of the Colorado Plateau. The plateau was fully defined as a structural entity by Middle Miocene time, and its modern style of tectonic deformation commenced. In addition, more than 3000 feet (900 m) of uplift occurred along the Grand Wash Cliffs at the mouth of the Grand Canyon in Pliocene time, indicating that rates of uplift in the region have accelerated during Late Cenozoic time.

The major phase of Basin-Range extension in the vicinity of the Whipple Mountains along the lower Colorado River southwest of the Colorado Plateau commenced in Late Oligocene time, considerably earlier than the first surface manifestations of normal faulting on the Colorado Plateau. Detachment faulting in the Whipple Mountains is characterized by east-northeast dipping, low-angle normal faults in which the upper plate glided downslope to the northeast on an unextended lower plate (Davis and others 1980). Although presently unproven, similar extension also may have been occurring during this period at middle and lower crustal levels under the southwestern part of the Colorado Plateau.

A speculative tectonic model accommodating Late Oligocene-Late Miocene extension at deep crustal levels under the Colorado Plateau and at shallower levels in the Basin-Range involves either a gently northeasterly dipping, crustal-penetrating normal fault or lateral extension within shear–bounded lenses, respectively illustrated in Figures 13D and 13C.

Figure 14 illustrates that northwest-striking blocks calving off the thin, trailing edge of the Colorado Plateau could account for tectonic erosion of the southwestern edge of the Colorado Plateau. These upper plate blocks now comprise the ranges in the area south and west of the plateau—including the Hualapai, Cerbat, Juniper, Aquarius, and Peacock ranges. In either scenario, the northeasterly tilted mountain blocks rest in tectonic contact on lower plate rocks, such as observed in similar environments in the Whipple Mountains. The detachment surface defining the base of the plateau appears to be spoon shaped and concaved upward, thus accounting for the southwestern bulge of the Colorado

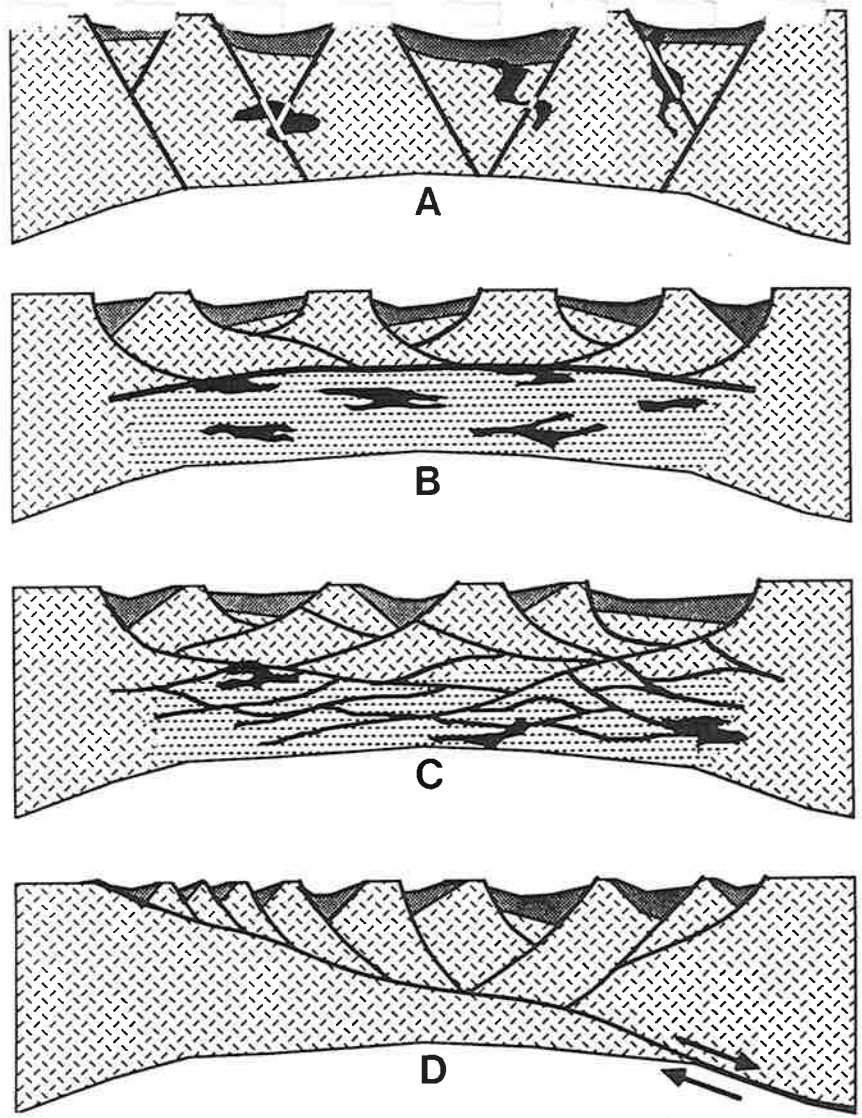

Figure 13. Summary of models used to explain extension in the Basin and Range Province southwest of the Colorado Plateau, Arizona (from Allmendinger and others 1987, Fig. 7). (A) Classic horst-graben model, (B) subhorizontal decoupling zone model, (C) shear zone bounded lense model, (D) crustal penetrating shear zone model. Either models C or D could have produced crustal thinning and subsidence along the southwestern Colorado Plateau in Late Oligocene-Early Miocene time.

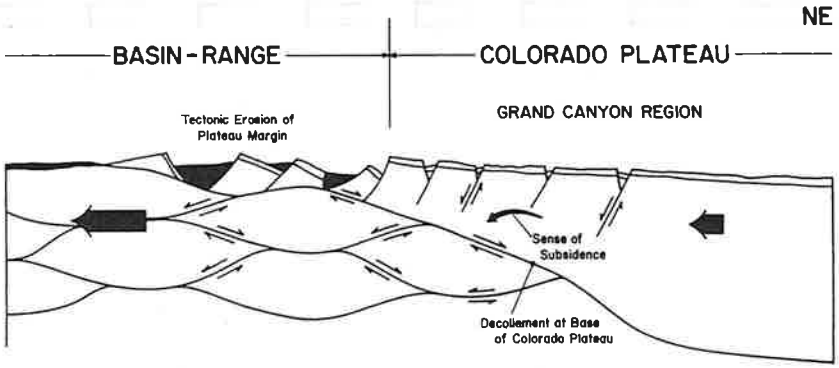

Figure 14. Cartoon illustrating tectonic erosion and subsidence along the southwestern edge of the Colorado Plateau over extending shear-bounded lenses in Late Oligocene-Early Miocene time. Lense concept from Hamilton (1982). Heavy arrows show absolute motions within the Basin-Range and Colorado Plateau provinces. Fine arrows show relative motions between shear surfaces. Notice that the relative motion between the lenses causes the crust to both thin and lengthen. Vertical scale greatly exaggerated, particularly at top

Plateau along the Hualapai Plateau over the thickened, northeasterly plunging axis of the upper plate.

Deep crustal extension probably was underway in Late Oligocene time. This allowed for (1) progressive tectonic erosion of the Colorado Plateau toward the northeast, (2) structural differentiation of the plateau from the Basin-Range in Miocene time, (3) thinning of the crust under the western part of the Colorado Plateau from about twenty-five to nineteen miles (40-30 km), and (4) nearly one degree of down to the southwest tilting of the southwestern edge of the Colorado Plateau. The latter easily accommodates sufficient subsidence of the Laramide erosion surface on the Colorado Plateau to force the abandonment of Laramide paleocanyons and to force the establishment of the west-flowing Colorado River in Late Miocene(?)-Pliocene time. Such subsidence also readily explains why early Tertiary rocks in the southern high plateaus of Utah now lie 2000 feet (600 m) or more above some of their source areas in the Grand Canyon region.

The relative motion of the Colorado Plateau above the decollement was down toward the northeast. Because such motion also corresponded to the opening of the Rio Grande rift, absolute regional motions had to include a slight clockwise rotation of the

...eau ...g. 15, ...l so... ...vest... ...l ex... ...on ... ...wer p...te rocks from under the plateau. This model implies that the Colorado Plateau was rotating into extensional space created within the Basin-Range Province, wherein the lower plate was moving into, and westward in concert with, the Basin-Range at a rate slightly greater than the upper plate carrying the Colorado Plateau. Thus, the entire Basin-Range Province was moving away from the Colorado Plateau to the southwest at all crustal levels.

By Miocene time, the western part of the Colorado Plateau was undergoing the first significant east-west crustal extension to affect the region since late Precambrian time. The Grand Canyon

Figure 15. Postulated clockwise rotation of the Colorado Plateau into extensional space created in the Basin-Range during Late Oligocene-Early Miocene time. Arrows in the Basin-Range schematically illustrate that all rocks within the province moved away from the Colorado Plateau at rates which increased to the west as the crust within the Basin-Range simultaneously extended.

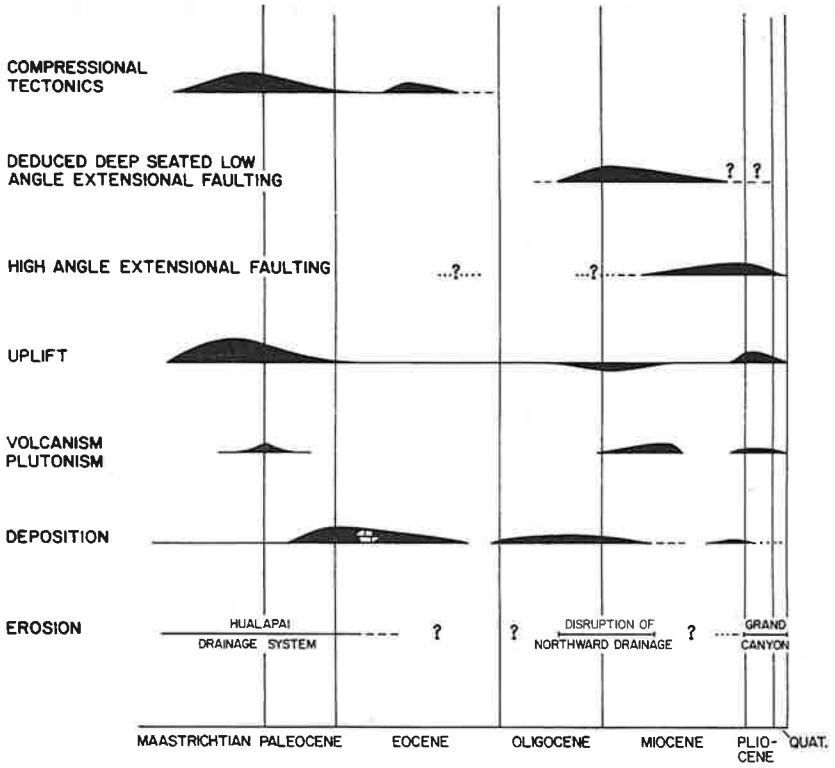

Figure 20. Temporal relationships between tectonics, sedimentation, and erosion in the Grand Canyon region, Arizona, during Laramide and post-Laramide time

velopment along the fault and the fact that the tuff is tilted on ranges that subsequently were partially buried by the Muddy Creek Formation. Therefore, major movement occurred along the Grand Wash fault after deposition of the Peach Springs Tuff, but prior to deposition of the upper part of the Muddy Creek Formation. These relationships bracket the major offsets across the fault between earliest Middle Miocene and latest Late Miocene time.

Some of the offsets along the Grand Wash fault probably were synchronous with deposition of the lower Muddy Creek Formation in the deepening Grand Wash trough, but relationships proving this remain buried. Minor post-Muddy Creek displacements along the Grand Wash fault appear to account for the folding of the Muddy Creek Formation in the vicinity of Lake Mead and for the faulting, by a few feet, of a gravel deposit located three and one-half miles (5.6 km) south of the Diamond Bar Ranch

(Lucchitta, 1967). Clearly, however, most of the activity along the Grand Wash fault in Arizona was finished by the beginning of Pliocene time.

The Hurricane fault is the southern, waning extension of the Wasatch fault zone that, in Utah, comprises the physiographic boundary between the Colorado Plateau and the Basin-Range Province. The province boundary steps westward to the Grand Wash fault in Arizona. Maximum late Tertiary offset across the Hurricane fault zone in the Grand Canyon is in excess of 3000 feet (900 m) at Granite Park.

The timing of the onset of late Cenozoic normal faulting along the Hurricane fault is difficult to determine. Young and Brennan (1974) point out that Truxton Valley and upper Peach Springs Canyon, which are aligned along the Hurricane fault, are unusually wide and filled with sediments that predate the Peach Springs Tuff. They conclude that the fault existed prior to eruption of the tuff, so erosion progressed more rapidly along the trend. Thus, they push the inception of faulting back in time. An alternative explanation is that erosion followed the coeval trend of a southern, now eroded, segment of the Laramide Hurricane monocline. This interpretation does not require such early faulting.

The Peach Springs Tuff and underlying Tertiary rocks are offset by the Hurricane fault near the head of Peach Springs Canyon. Unfortunately, the closest exposed offset Paleozoic rocks lie three miles (5 km) to the north, precluding accurate differentiation of pre- and post-Peach Springs Tuff faulting. The offset across the tuff is between 200 and 300 feet (60 and 90 m) as is the offset associated with the Paleozoic rocks to the north. Consequently, it is doubtful if there was pre-Peach Springs Tuff displacement in the area. However, the uncertainties in correlating the similar offsets between the two sites does not justify discounting the possibility of small pre-Peach Springs Tuff displacement.

If we assume that there was no faulting along the Hurricane fault prior to the eruption of the tuff, the inception of late Tertiary faulting is post ~17 m.y., which is post-earliest Middle Miocene in age. Gardner (1941) concluded from outcrops in southern Utah that 75 percent or more of the total offset across the fault occurred in Late-Miocene(?) and Pliocene time, an observation that commonly is cited to support a peaking in the rate of normal faulting in the region during Pliocene time.

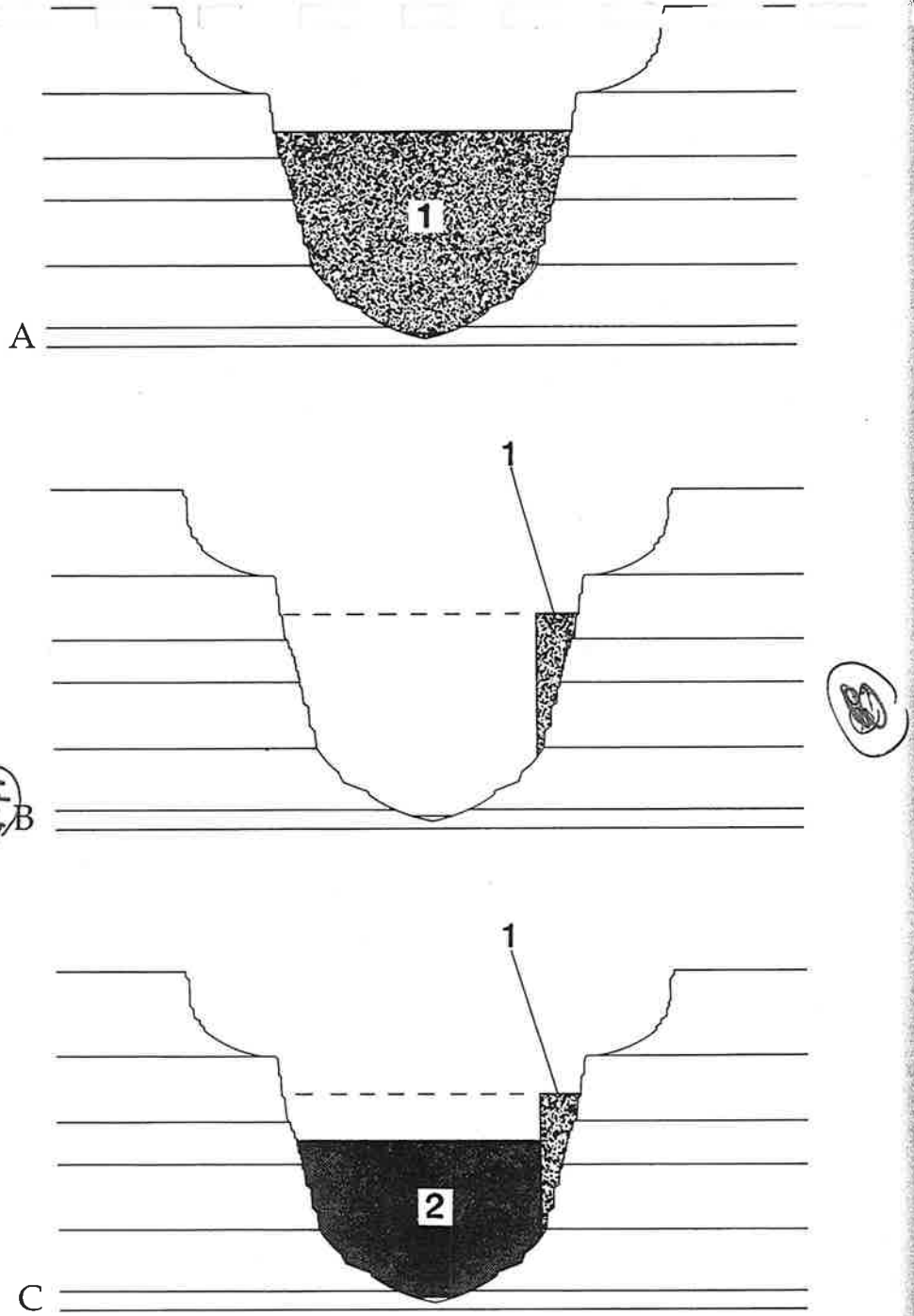

Figure 2. Diagrams showing the development of juxtaposed flows in the Grand Canyon. (A) Flow partly fills the canyon. (B) Erosion leaves small remnants of flow 1 adhering to the canyon wall. (C) Flow 2 refills the canyon. (D) Erosion removes most of flow 2, leaving remnants juxtaposed against flow 1 and against the canyon wall. (E) Flow 3 fills the canyon. (F) Erosion of flow 3 leaves remants of flows 1, 2, and 3 stacked side-by-side according to relative age.

ble 1

	DAM	ELEVATION	HEIGHT ABOVE RIVER	RADIOMETRIC DATE	VOLUME OF LAVA (mi 3)	LAKE LENGTH	WATER FILL TIME	SEDIMENT FILL TIME
1	Prospect	4000	2330		4.0		23 yrs.	3018 yrs.
2	Ponderosa	2800	1130		2.5		1.5 yrs.	163 yrs.
3	Toroweap	3093	1443	1.2 Ma	3.7		2.62 yrs.	345 yrs.
4	Esplanade	2600	960		1.8		287 days	92 yrs.
5	Buried Canyon	2480	850	0.89 Ma	1.7		231 days	87 yrs.
6	Whitmore	2500	900		3.0	100	240 days	88 yrs.
7	"D" Flows	2295	635	0.57 Ma	1.1	74	87 days	31 yrs.
8	Lava Falls	2260	600		1.2		86 days	30 yrs.
9	Black Ledge	2033	373		2.1	53	17 days	7 yrs.
10	Gray Ledge	1813	203		0.3	37	2 days	10.3 mos.
11	Layered Dbs.	1938	298	0.64 Ma	0.3	42	8 days	3 yrs.
12	Massive Dbs.	1826	226	0.14 Ma	0.2		5 days	1.4 yrs.

DEVELOPMENT AND DESTRUCTION OF LAVA DAMS

The hydrologic data from the Bureau of Land Management's Lake Mead Survey (1963 and 1964) provide the basic information from which we are able to calculate the rates at which the lakes behind the various lava dams were filled with water and, subsequently, sediment. These data also provide some indication of the time necessary for a lava dam to be eroded away completely (Table 1).

Rates of Formation of Dams

Although the formation of a lava dam in the Grand Canyon was a significant event that dramatically changed canyon morphology, the time needed to create a lava dam was remarkably short by any standard and certainly would be considered instantaneous in a geologic time frame. Observations of basaltic eruptions in historic times indicate that most basaltic extrusions occur in a matter of days or weeks. The major flows in the Grand Canyon, most of which were 100 to 200 feet (30 to 60 m) thick, probably moved tens of miles down the Colorado River in a matter of days.

This conclusion is supported by the fact that the upper colonnade and/or a clinkery upper surface of the flow often is preserved, essentially unmodified by erosion. This indicates that the flow was extruded in a period of time less than that required for the lake impounded behind the dam to overflow. If extrusion occurred during a longer period of time, the lake behind the dam would overflow, and erosion would modify the upper surface features of the basalts quickly.

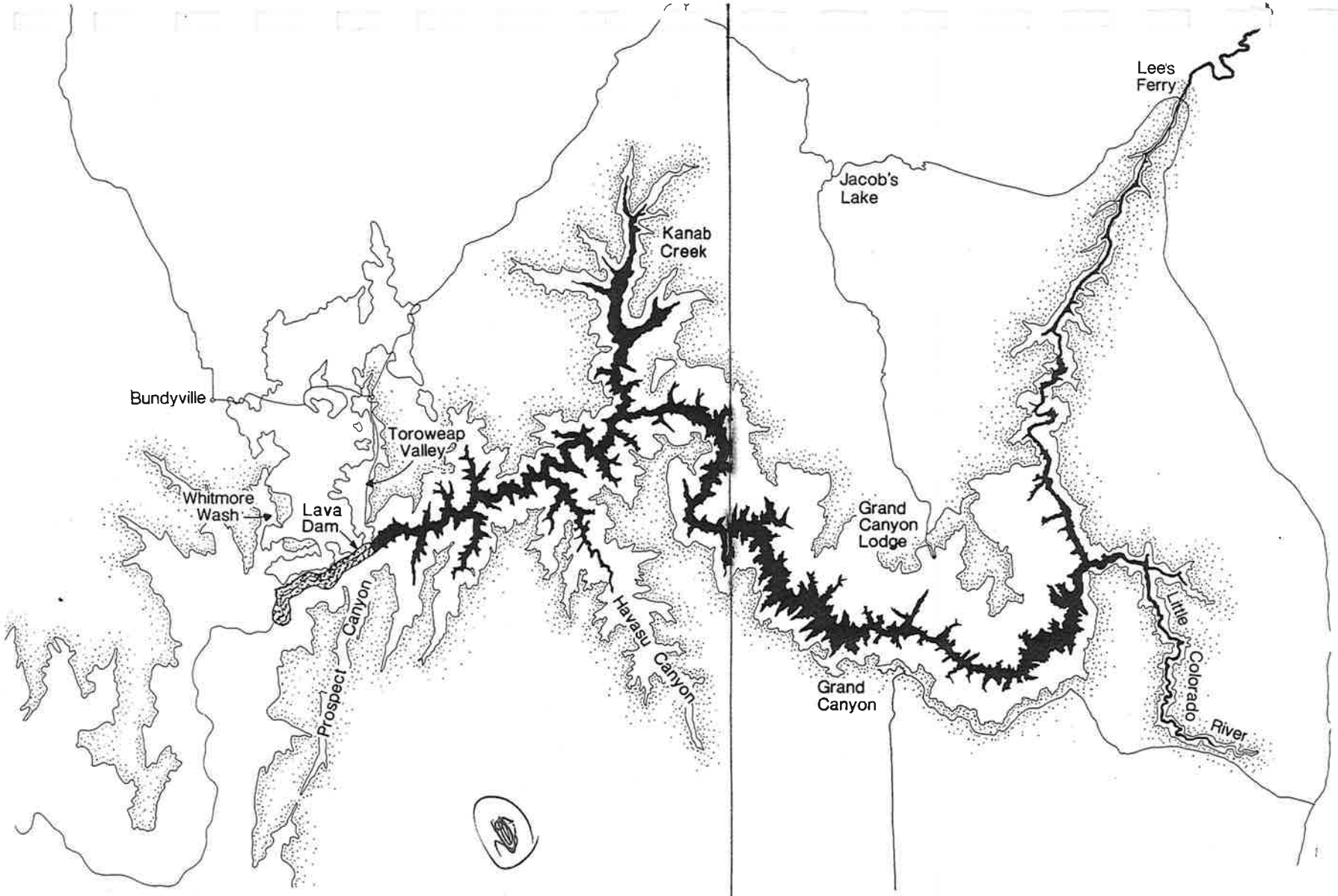

Figure 7. The Prospect Lake. The Prospect Dam was the highest lava dam formed across the Colorado River. The lake formed behind the dam that extended all the way through the Grand Canyon and up into Utah. It formed more than 1.2 million years ago.

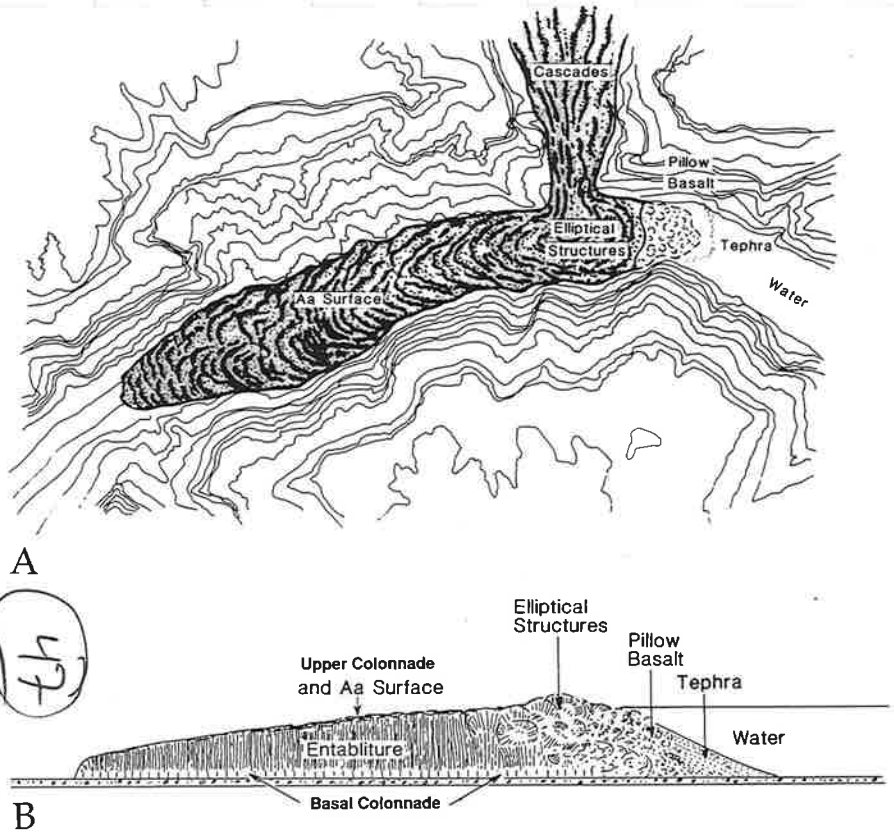

Figure 11. The structure of a hypothetical flow 200 feet thick in the Grand Canyon. Only the upstream margin of the flow would interact with water from the river. This would produce hydroexplosive tephra, which would be deposited at the upstream margin of the dam. Some pillow structures would be produced where lava came into direct contact with the river. Most of the flow would move downstream essentially dry until the backwater overflowed the barrier. The Colorado River would overflow the barrier of a simple flow within two days. It would flow over the top of the basalt and influence the cooling of the lava. The interaction of the river water with the lava would be most intense near the front of the dam and would form the elliptical structure. The overflow also may have had an effect on the development of the entablature in the downstream part of the flow.

Grand Canyon. It extended all the way through the present National Park Visitor's area and upstream into the vicinity of Lees Ferry (Fig. 12). Throughout much of the park region, the lake's

depth was approximately 750 feet (225 m). In the region of the visitor's center, the lake essentially flooded all of Granite Gorge—with the shoreline occurring very close to the vertical wall of the Tapeats Sandstone.

The gravel, sand, and silt that form the terrace deposits at Lees Ferry at an elevation of 3600 feet (1080 m) probably were deposited as a delta built by the Paria and Colorado rivers where they emptied into the Toroweap Lake. Likewise, the silt deposits that form the main floor of Havasu Canyon represent a major remnant of Toroweap Lake deposits.

If the Toroweap Dam formed instantaneously, the lake behind it would overflow in 2.6 years. It would be completely full of sediment in 345 years. Since the Toroweap Dam was constructed over a period of time, the lake undoubtedly was full of sediment by the time the dam was completed. After the extrusion that built the Toroweap Dam terminated, erosion by headwater migration of the waterfall and the downcutting of the stream channel probably destroyed the dam in less than 10,000 years.

The Esplanade Dam

On the north side of the river between Miles 181 and 182, a sequence of flows that formed a complex dam at an elevation of 2600 feet (780 m), or 960 feet (288 m) above river level, is preserved beneath the Esplanade Cascades (Fig. 13). These flows can be seen from viewpoints west of the present Toroweap Campground and resemble in some respects the Toroweap sequence. Both are preserved beneath major cascades.

The Esplanade sequence also is similar in some respects to that preserved in the Buried Canyon at Mile 184. These similarities have led some geologists to consider the Toroweap, Esplanade, and Buried Canyon lavas as part of a single complex lava dam. However, the stratigraphic sequence in each dam is distinctly different, and radiometric dates indicate three separate ages for the sequences.

Several small remnants of the Esplanade Dam are preserved in tributary canyons on the south wall of the inner gorge between Mile 183.5 and Mile 184. They provide important documentation concerning the height of the Esplanade Dam. All are preserved in "hanging valleys" at an elevation of 2600 feet (780 m).

The lake that formed behind the dam was similar to, but slightly smaller than, the Toroweap Lake and extended upstream

The enigmatic rise of the Colorado Plateau

Rebecca M. Flowers
Department of Geological Sciences, University of Colorado at Boulder, Boulder, Colorado 80309, USA

How and when the Colorado Plateau attained its current mean elevation of ~2 km has puzzled scientists for nearly 150 yr. This problem is most dramatically manifest when standing on the rim of the Grand Canyon, viewing the extraordinary 1500-m-deep gorge carved into nearly horizontal sedimentary rocks that were deposited during the 500 m.y. prior to plateau uplift when the region resided near sea level. What caused the elevation gain of this previously stable cratonic region in Cenozoic time? Did the source of buoyancy for plateau uplift arise from the crust, lithospheric mantle, or asthenosphere, or through some combination of the three? Why did this low-relief plateau escape significant upper crustal strain during uplift, in contrast to the Cenozoic surface deformation that is so strikingly apparent in the high-relief landscape of the surrounding Rocky Mountain, Rio Grande Rift, and Basin and Range provinces (Fig. 1)?

The answers to these contentious questions are significant for understanding how deep-seated processes control the elevation change and topographic evolution of Earth's surface. These relationships are particularly cryptic within continental interior settings like the Colorado Plateau. Although there is a first-order understanding of vertical motions in areas close to plate boundaries, there is comparatively little consensus on the causes of such motions distal from these margins. The Colorado Plateau exemplifies this problem. The protracted history of Cordilleran orogenesis affords numerous opportunities for how and when uplift of the Colorado Plateau might have occurred. The region is last known to have been at sea level in Late Cretaceous time, based on the widespread occurrence of marine sediments of this age. Elevation gain could have occurred in Early Tertiary time associated with Sevier-Laramide contraction, mid-Tertiary time synchronous with the proposed demise of the Laramide flat slab, or Late Tertiary time coeval with regional extensional tectonism in adjacent provinces. Hypothesized mechanisms include partial removal of the lithospheric mantle (e.g., Spencer, 1996), chemical alteration of the lithosphere owing to volatile addition or magma extraction (e.g., Humphreys et al., 2003; Roy et al., 2004), warming of heterogeneous lithosphere (Roy et al., 2009), hot upwelling within the asthenosphere (Parsons and McCarthy, 1995; Moucha et al., 2009), and crustal thickening (McQuarrie and Chase, 2000). It is clear that there is no shortage of mechanisms that could explain the plateau's origin. The core challenge is determining which mechanism, or combination of mechanisms, is indeed the cause.

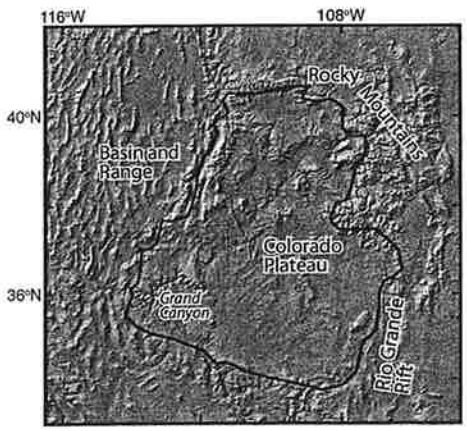

Figure 1. Topographic map of the Colorado Plateau and adjacent provinces.

Crucial for solving this problem are constraints on the plateau's elevation history, erosional evolution, magmatism patterns, and modern lithospheric structure. Liu and Gurnis (2010, p. 663 in this issue of *Geology*) and van Wijk et al. (2010, p. 611 in this issue of *Geology*) both present models for elevation gain of the plateau, and use such constraints from a variety of recent studies to better restrict and assess their models. Liu and Gurnis focus on an explanation for the Late Cretaceous through mid-Cenozoic uplift history of the southwestern plateau, whereas van Wijk et al. explore a mechanism for late Cenozoic elevation gain and differential uplift along the plateau edges.

In the first study, Liu and Gurnis employ an inverse mantle convection model to compute the changing dynamic topography, the vertical motion of Earth's surface in response to mantle flow. This model of dynamic uplift linked to Farallon slab evolution predicts an initial phase of subsidence associated with flat slab development, followed by two phases of uplift in Late Cretaceous and Eocene times due to progressive slab removal. Liu and Gurnis invoke mantle upwellings to induce the remainder of the plateau's uplift in the Oligocene. A distinctive result of the model is the prediction that the plateau was tilted to the northeast in Late Cretaceous–Early Tertiary time, with later differential elevation gain of the plateau interior that diminished or reversed this tilt. The authors note that their results compare favorably with the conclusions of two recent investigations on the southwestern plateau (Flowers et al., 2008; Huntington et al., 2010). In the second study, van Wijk et al. examine the consequences of late Cenozoic edge-driven convection along the plateau margins induced by a step in lithospheric thickness between the plateau and the adjacent Rio Grande Rift and Basin and Range provinces. The lithospheric thickness contrast is observed seismically and attributed to Cenozoic extension of the adjoining regions. This work finds that asthenospheric upwelling and lithospheric mantle removal along the plateau edges can account for Neogene–Quaternary patterns of magmatism, distinctive shallow mantle seismic anomalies, and several hundred meters of differential uplift along the plateau margins.

One question arising from these two studies is: are their conclusions compatible? The proposed dynamic topography model can account for ~1.2 km of uplift in the southwestern plateau in Late Cretaceous through Eocene time. This portion of the history does not preclude later uplift, although Liu and Gurnis propose mid-Tertiary mantle upwelling to account for much of the remaining elevation gain to generate the modern ~2 km plateau elevation. Van Wijk et al. can explain several hundred meters of differential plateau margin uplift by edge-driven convection in the late Cenozoic. Their results do not exclude earlier uplift. Thus, to first order, the results of these two studies do not appear to be mutually exclusive. When integrated, they would predict a complex spatio-temporal progression of uplift migrating from southwest to northeast in Late Cretaceous through mid-Cenozoic time, with a late Cenozoic uplift phase and development of differential topography along the plateau edges.

The other obvious question that emerges from these efforts is both more important and far more difficult to answer. Do the proposed models accurately describe the true origin and evolution of Colorado Plateau elevation? Both studies are significant in advancing potentially important and viable mechanisms to explain key features of the plateau. They are therefore serious contenders among the suite of competing models for plateau elevation gain. However, determining the extent to which these models

48

approximate reality must in part await additional constraints on the uplift history with which to further test the predictions of each study.

One reason why resolving the cause of plateau uplift is such a tough problem is that deciphering the paleoelevation of continents is extremely difficult, and the plateau's elevation history is critically important for isolating the correct uplift mechanism. Dated marine deposits can determine when an area was at sea level, but no direct, reliable proxy yet exists for the past altitude of an elevated region. Strategies for addressing this problem commonly involve estimating paleotemperature, constraining paleorelief, deciphering paleohydrology, and reconstructing erosional and depositional histories. Paleotemperature estimates for inferring paleoelevation are typically made by stable isotope and paleobotany studies. Application of the new clumped isotope thermometer on the Colorado Plateau (Huntington et al., 2010) and paleobotany efforts in the Rocky Mountain region (e.g., Wolfe et al., 1998) are noteworthy examples. The past amount of relief in a landscape imposes a minimum constraint on paleoelevation, and resolving the carving of the Grand Canyon is an obvious target for constraining Colorado Plateau paleorelief. Recent approaches to determine the history of canyon incision include U-Pb dating of carbonate cave deposits (Polyak et al., 2008), $^{40}Ar/^{39}Ar$ dating of canyon basalts (Karlstrom et al., 2008), and (U-Th)/He thermochronometry of plateau surface and canyon samples (Flowers et al., 2008). The reorganization of plateau paleodrainage systems in part reflects the plateau's topographic development; deciphering this history has been the target of numerous stratigraphic, geochronologic, and isotopic studies (e.g., Young, 1979; Davis et al., 2008; Pederson, 2008). Stratigraphic and thermochronologic efforts have been used to resolve the plateau's erosional and depositional evolution that is linked with its history of elevation change (e.g., Dumitru et al., 1994; Cather et al., 2008). A basalt vesicularity study differs from the investigations above in its attempt to directly constrain paleoatmospheric pressure, and therefore paleoelevation, from the size of vesicles in plateau lavas (Sahagian et al., 2002), but these results are widely debated (e.g., Libarkin and Chase, 2003). Not surprisingly, contradictory interpretations regarding the uplift history of the Colorado Plateau often arise from the diverse information yielded by the many studies in this region.

The two geodynamic studies in this issue of *Geology* underscore the probable complexity of the plateau's history. They especially highlight the unlikelihood of the entire plateau undergoing a single spatially uniform phase of surface uplift, and emphasize the potential for significant geographic and temporal heterogeneity in elevation gain. Such a history would only exacerbate the challenge of accurately reconstructing the plateau's evolution from the geological record. Perhaps some of the geological data that seemingly conflict in the context of simpler uplift models can be reconciled when evaluated in the framework of the more complex patterns of elevation gain predicted by these geodynamic studies. The inventive new approaches for deciphering the plateau's history coupled with testable predictions from geodynamic models are yielding fresh insights into the perplexing story behind the topographic rise of the Colorado Plateau.

REFERENCES CITED

Cather, S.M., Connell, S.D., Chamberlin, R.M., McIntosh, W.C., Jones, G.E., Potochnik, A.R., Lucas, S.G., and Johnson, P.S., 2008, The Chuska erg: Paleogeomorphic and paleoclimatic implications of an Oligocene sand sea on the Colorado Plateau: Geological Society of America Bulletin, v. 120, p. 13–33, doi: 10.1130/B26081.1.

Davis, S.J., Wiegand, B.A., Carroll, A.R., and Chamberlain, C.P., 2008, The effect of drainage reorganization on paleoaltimetry studies: An example from the Paleogene Laramide foreland: Earth and Planetary Science Letters, v. 275, p. 258–268, doi: 10.1016/j.epsl.2008.08.009.

Dumitru, T.A., Duddy, I.R., and Green, P.F., 1994, Mesozoic-Cenozoic burial, uplift and erosion history of the west-central Colorado Plateau: Geology, v. 22, p. 499–502, doi: 10.1130/0091-7613(1994)022<0499:MCBUAE>2.3.CO;2.

Flowers, R.M., Wernicke, B.P., and Farley, K.A., 2008, Unroofing, incision and uplift history of the southwestern Colorado Plateau from (U-Th)/He apatite thermochronometry: Geological Society of America Bulletin, v. 120, p. 571–587, doi: 10.1130/B26231.1.

Humphreys, E.D., Hessier, E., Dueker, K., Farmer, G.L., Erslev, E., and Atwater, T., 2003, How Laramide-age hydration of North American lithosphere by the Farallon slab controlled subsequent activity in the western United States: International Geology Review, v. 45, p. 575–594, doi: 10.2747/0020-6814.45.7.575.

Huntington, K.W., Wernicke, B.P., and Eiler, J.M., 2010, The influence of climate change and uplift on Colorado Plateau paleotemperatures from carbonate 'clumped isotope' thermometry: Tectonics, In press.

Karlstrom, K.E., Crow, R., Crossey, L.J., Coblentz, D., and van Wijk, J., 2008, Model for tectonically driven incision of the younger than 6 Ma Grand Canyon: Geology, v. 36, p. 835–838, doi: 10.1130/G25032A.1.

Libarkin, J.C., and Chase, C.G., 2003, Timing of Colorado Plateau uplift: Initial constraints from vesicular basalt-derived paleoelevations: Geology, v. 31, p. 191–192, doi: 10.1130/0091-7613(2003)031<0191:TOCPUI>2.0.CO;2.

Liu, L., and Gurnis, M., 2010, Dynamic subsidence and uplift of the Colorado Plateau: Geology, v. 38, p. 663–666, doi: 10.1130/G30368.1.

McQuarrie, N., and Chase, C.G., 2000, Raising the Colorado Plateau: Geology, v. 28, p. 91–94, doi: 10.1130/0091-7613(2000)028<0091:RTCP>2.0.CO;2.

Moucha, R., Forte, A.M., Rowley, D.B., Mitrovica, J.X., Simmons, N.A., and Grand, S.P., 2009, Deep mantle forces and the uplift of the Colorado Plateau: Geophysical Research Letters, v. 36, p. L19310, doi: 10.1029/2009GL039778.

Parsons, T., and McCarthy, J., 1995, The active southwest margin of the Colorado Plateau–Uplift of mantle origin: Geological Society of America Bulletin, v. 107, p. 139–147, doi: 10.1130/0016-7606(1995)107<0139:TASMOT>2.3.CO;2.

Pederson, J.L., 2008, The mystery of the pre-Grand Canyon Colorado River–Results from the Muddy Creek Formation: GSA Today, v. 18, no. 3, p. 4–10, doi: 10.1130/GSAT01803A.1.

Polyak, V., Hill, C., and Asmerom, Y., 2008, Age and evolution of the Grand Canyon revealed by U-Pb dating of water table-type speleothems: Science, v. 321, p. 1377–1380, doi: 10.1126/science.1151248.

Roy, M., Jordan, T.H., and Pederson, J., 2009, Colorado Plateau magmatism and uplift by warming of heterogeneous lithosphere: Nature, v. 459, p. 978–982, doi: 10.1038/nature08052.

Roy, M., Kelley, S.A., Pazzaglia, F.J., Cather, S.M., and House, M.A., 2004, Middle Tertiary buoyancy modification and its relationship to rock exhumation, cooling, and subsequent extension at the eastern margin of the Colorado Plateau: Geology, v. 32, p. 925–928, doi: 10.1130/G20561.1.

Sahagian, D., Proussevitch, A., and Carlson, W., 2002, Timing of Colorado Plateau uplift: Initial constraints from vesicular basalt-derived paleoelevations: Geology, v. 30, p. 807–810, doi: 10.1130/0091-7613(2002)030<0807:TOCPUI>2.0.CO;2.

Spencer, J.E., 1996, Uplift of the Colorado Plateau due to lithosphere attenuation during Laramide low angle subduction: Journal of Geophysical Research, v. 101, p. 13595–13609, doi: 10.1029/96JB00818.

van Wijk, J.W., Baldridge, W.S., van Hunen, J., Goes, S., Aster, R., Coblentz, D.D., Grand, S.P., and Ni, J., 2010, Small-scale convection at the edge of the Colorado Plateau: Implications for topography, magmatism, and evolution of Proterozoic lithosphere: Geology, v. 38, p. 611–614, doi: 10.1130/G31031.1.

Wolfe, J.A., Forest, C.E., and Molnar, P., 1998, Paleobotanical evidence of Eocene and Oligocene paleoaltitudes in midlatitude western North America: Geological Society of America Bulletin, v. 110, p. 664–678, doi: 10.1130/0016-7606(1998)110<0664:PEOEAO>2.3.CO;2.

Young, R.A., 1979, Laramide deformation, erosion and plutonism along the southwestern margin of the Colorado Plateau: Tectonophysics, v. 61, p. 25–47, doi: 10.1016/0040-1951(79)90290-7.

Printed in USA

49

Unroofing, incision, and uplift history of the southwestern Colorado Plateau from apatite (U-Th)/He thermochronometry

R.M. Flowers†
Division of Geological and Planetary Science, California Institute of Technology, Pasadena, California 91125, USA

B.P. Wernicke
K.A. Farley
Division of Geological and Planetary Science, California Institute of Technology, Pasadena, California 91125, USA

ABSTRACT

The source of buoyancy for the uplift of cratonic plateaus is a fundamental question in continental dynamics. The ~1.9 km uplift of the Colorado Plateau since the Late Cretaceous is a prime example of this problem. We used apatite (U-Th)/He thermochronometry (230 analyses; 36 samples) to provide the first single-system, regional-scale proxy for the unroofing history of the southwestern quadrant of the plateau. The results confirm overall southwest to northeast unroofing, from plateau margin to plateau interior. A single phase of unroofing along the plateau margin in Late Cretaceous to Early Tertiary (Sevier-Laramide) time contrasts with multiphase unroofing of the southwestern plateau interior in Early and mid- to Late Tertiary time. The Early Cretaceous was characterized by northeastward tilting and regional erosion, followed by aggradation of ≥1500 m of Upper Cretaceous sediments along the eroded plateau margin. Sevier-Laramide denudation affected the entire southwestern plateau, was concentrated along the plateau margin, and migrated from northwest to southeast. Following a period of relative stability of the landscape from ca. 50–30 Ma, significant unroofing of the southwestern plateau interior occurred between ca. 28 and 16 Ma. Additional denudation north of the Grand Canyon took place in latest Tertiary time.

Mid-Tertiary dates from the Grand Canyon basement at the bottom of the Upper Granite Gorge limit significant incision of the modern Grand Canyon below the Kaibab surface to <23 Ma. Modeling the age distributions of samples from the basement and Kaibab surface nearby suggests that the gorge and the plateau surface had similar Early to mid-Tertiary thermal histories, despite their >1500 m difference in vertical structural position. If these models are correct, they indicate that a "proto–Grand Canyon" of kilometer-scale depth had incised post-Paleozoic strata by the Early Eocene. Evidence for kilometer-scale mid-Tertiary relief in northeast-flowing drainages along the plateau margin, as well as the mid-Tertiary episode of plateau interior unroofing, imply that the southwestern plateau interior had attained substantial elevation by at least 25–20 Ma, if not much earlier. These observations are inconsistent with any model calling for exclusively Late Tertiary uplift of the southwestern plateau.

Sevier-Laramide plateau surface uplift and incision thus result from one or more processes that enhanced the buoyancy of the plateau lithosphere, expanding the Cordillera's orogenic highlands into its low-standing cratonic foreland. The onset of the Laramide slab's demise at ca. 40 Ma and the major pulse of extension in the Basin and Range from ca. 16–10 Ma appear to have had little influence on the denudation history of the southwestern plateau. In contrast, the post-Laramide unroofing episodes may be explained by drainage adjustments induced by rift-related lowering of regions adjacent to the plateau, without the need to otherwise modify the plateau lithosphere. Our data do not preclude a large component of post–Early Eocene elevation gain (or the geodynamic mechanisms it may imply), but they do point toward Laramide-age buoyancy sources as the initial cause of significant surface uplift, ending more than 500 m.y. of residence near sea level.

†E-mail: Rebecca.Flowers@colorado.edu
Present address: Department of Geological Sciences, University of Colorado, Boulder, Colorado 80309, USA

Keywords: Colorado Plateau, (U-Th)/He, Grand Canyon, unroofing, incision, uplift, thermochronometry.

INTRODUCTION

Like most of the North American craton, the Colorado Plateau remained near sea level for 500 m.y. during slow subsidence and deposition of Paleozoic and Mesozoic sediments (Hunt, 1956). However, unlike most of the craton, the plateau was uplifted to its current elevation of ~1.9 km with little internal upper crustal strain (<1%), requiring the acquisition of significant lithospheric buoyancy, sometime after widespread deposition of Upper Cretaceous marine sediments.

Models of how this buoyancy was acquired are numerous (e.g., McGetchin et al., 1980; Morgan and Swanberg, 1985), and can be broadly subdivided into three groups on the basis of the predicted timing of uplift. Late Cretaceous to Early Tertiary uplift mechanisms related to Sevier-Laramide contractional deformation (80–40 Ma) include crustal thickening due to channel flow (e.g., McQuarrie and Chase, 2000), convective removal of lithospheric mantle (England and Houseman, 1988), or chemical modification of the lithosphere by volatile addition from the Laramide flat slab (Humphreys et al., 2003). Mid-Tertiary buoyancy addition (40–20 Ma), perhaps driven by the demise of the Laramide flat slab, could be due to partial removal of the plateau lithosphere and replacement with hot asthenosphere (Spencer, 1996), or post-Laramide chemical modification through melt extraction along the plateau margins (Roy et al., 2004). Late Tertiary uplift models (post–20 Ma) associated with regional extensional tectonism involve heating the lithosphere from below (Thompson and Zoback, 1979) possibly aided by a mantle plume (Parsons and McCarthy,

GSA Bulletin; May/June 2008; v. 120; no. 5/6; p. 571–587; doi: 10.1130/B26231.1; 10 figures; 1 table; Data Repository Item 2008027.

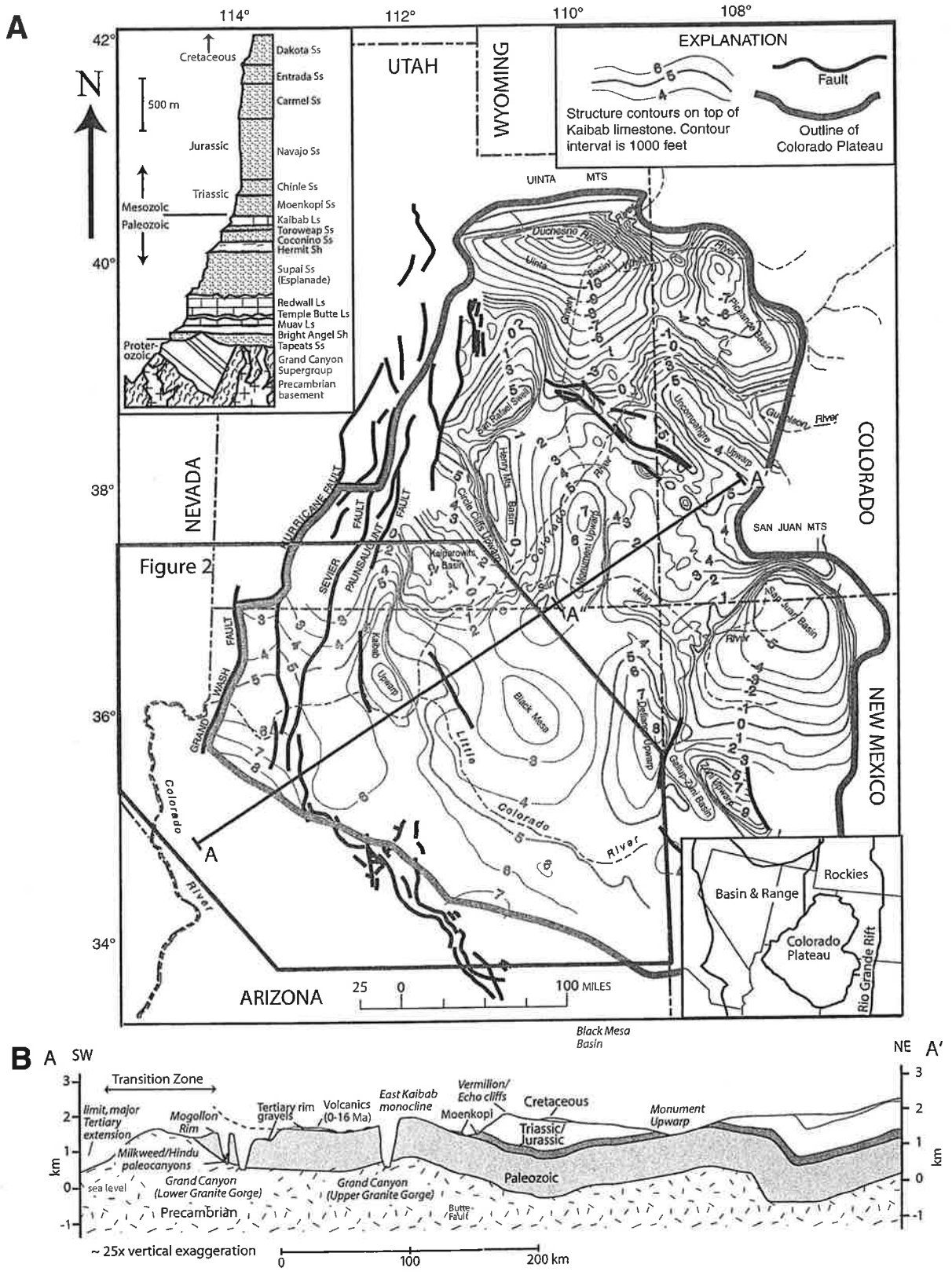

Figure 1. (A) Map from Hunt (1956) showing geomorphic outline of the Colorado Plateau and structure contours on top of the Permian Kaibab limestone and equivalents. Contour interval is 1000 ft. Location of map in Figure 2 is shown. A stratigraphic section for the southwestern plateau is included for reference. (B) Cross section through Colorado Plateau. Section line is A–A′ in (A). Section line A–A″ marks the location of the cross-sectional reconstructions in Figure 8. Features such as the Lower Granite Gorge are projected onto the cross-section line to more effectively depict the development and evolution of these features in our models.

51

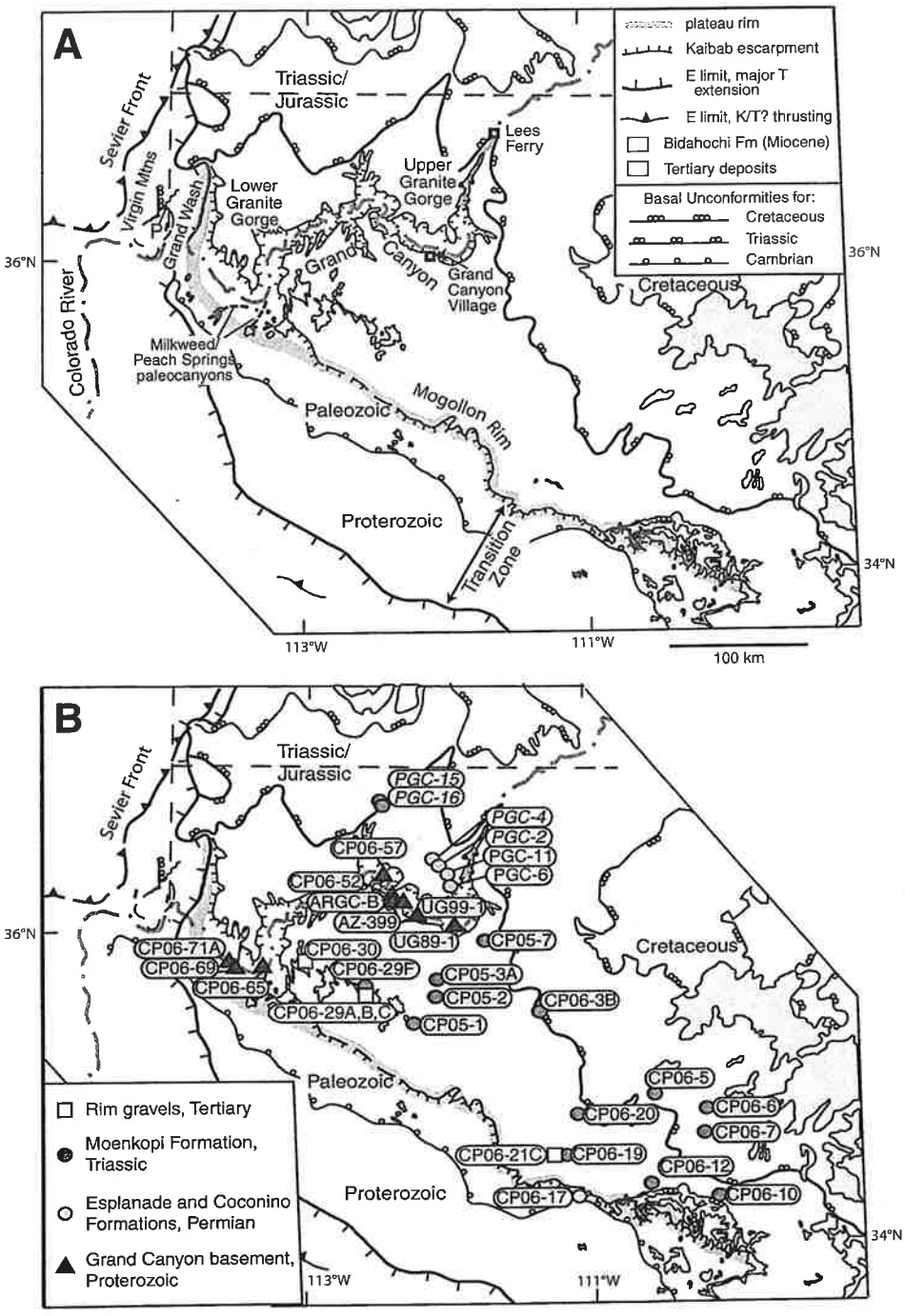

Figure 2. (A) Map showing selected tectonic elements of the southwestern Colorado Plateau. "P" indicates position of the southward pinchout of Mesozoic strata below sub-Oligocene unconformity in Virgin Mountains described in text. (B) Sample types, names, and locations.

reversal of drainage along the Mogollon Rim at 40–20 Ma induced by mid-Tertiary extension in central Arizona (e.g., Elston and Young, 1991), the abrupt truncation of the western plateau edge by extension from 16 to 11 Ma (e.g., Brady et al., 2000; Faulds et al., 2001), the appearance of the first Colorado River sediments in the Grand Wash trough after deposition of the Hualapai limestone near 6 Ma Hualapai limestone (e.g., Spencer et al., 2001), and the timing of incision of a Grand Canyon with kilometer-scale relief (e.g., Young, 1979; Lucchitta, 1979). A proposed marine origin for the upper Miocene Hualapai Limestone immediately west of the Grand Wash Cliffs and the Bouse Formation (preserved well downstream) along the lower reaches of the Colorado (Blair, 1978) suggested 800 m (the modern elevation of the youngest Hualapai Limestone) of plateau uplift since 6 Ma (Lucchitta, 1979). However, geochemical and physical evidence for a lacustrine origin of the Hualapai and Bouse makes this interpretation questionable (Spencer and Patchett, 1997; House et al., 2005). The only direct paleoaltimetry estimate for the southwestern portion of the plateau is based on the size distribution of vesicles in young basalts that suggests a general acceleration of uplift through the Tertiary (Sahagian et al., 2002), but this interpretation is also controversial (Libarkin and Chase, 2003; Sahagian et al., 2003). Thus, despite decades of debate, the timing of uplift of the southwestern Colorado Plateau is still only bracketed between ca. 80 Ma and the present, with little consensus on the details.

Timing Constraints on Incision

The timing and mechanisms of incision of the Grand Canyon, and the paleohydrology of the Colorado River, are highly controversial. From studies of the sedimentary record in the Grand Wash Trough where the Colorado River currently exits the western margin of the Colorado Plateau, it appears clear that the Colorado River did not become integrated into its modern course until after the 5.97 ± 0.07 Ma deposition of the Hualapai limestone (Longwell, 1946; Lucchitta, 1979, 1989; Faulds et al., 2001; Spencer et al., 2001). However, the course of the river from 16 to 5 Ma is problematic, resulting in a remarkable diversity of proposals for the pre-Pliocene paleohydrology of the southwestern plateau. A major topic of debate is whether lake spillover led to top-down river integration (e.g., Spencer and Pearthree, 2001; House et al., 2005) or headward erosion led to capture of an ancestral northward flowing Colorado River (e.g., Lucchitta 1979; Lucchitta et al., 2001). Another important uncertainty involves the role of pre-Pliocene paleocanyons in controlling the subsequent course of the river. The presence of the deeply incised Peach Springs and Salt River paleocanyons along the plateau margin, mentioned above, has led some workers to propose an extensive ancestral northeastward-flowing drainage system that may have included portions of the Grand Canyon (e.g., Potochnik, 2001; Young 2001, 2008). Quaternary Grand Canyon incision rates appear insufficient to carve the entire canyon in 6 m.y., indicating either that incision rates have decreased or that the modern river exploited paleocanyons that were present prior to river integration (e.g., Pederson et al. 2002; Karlstrom et al., 2007).

52

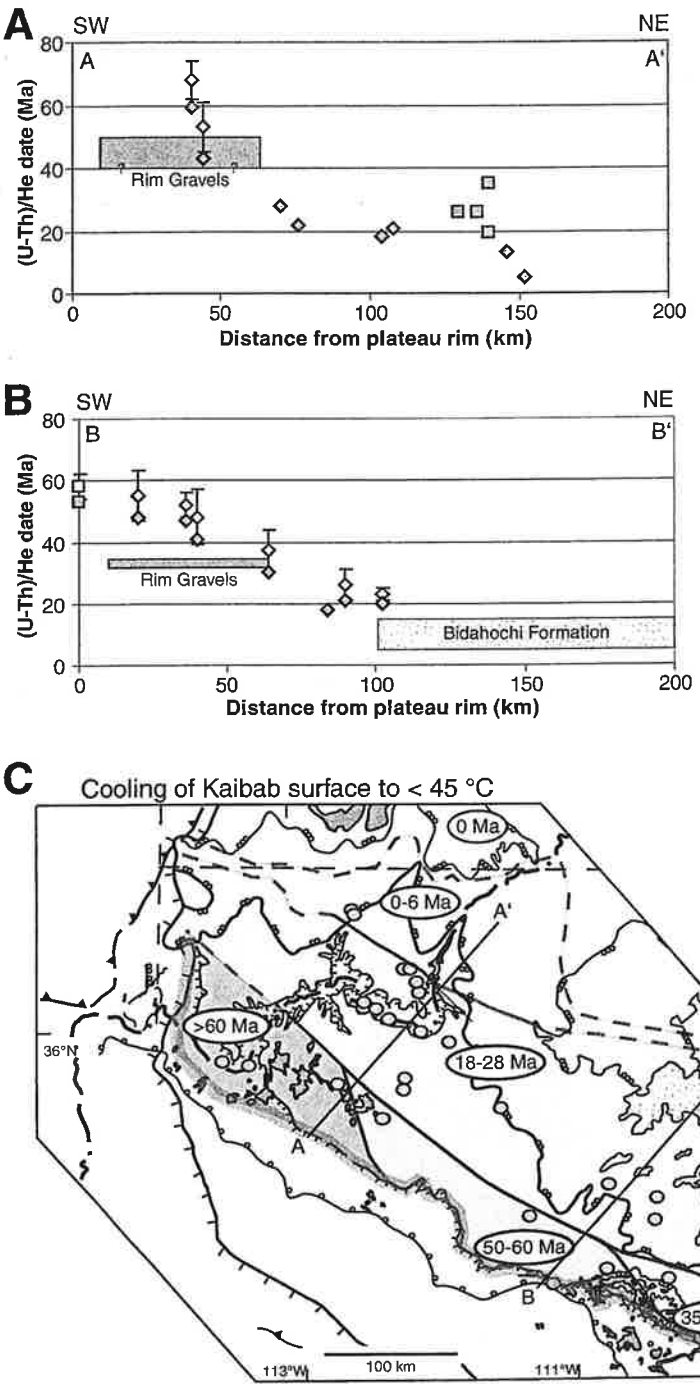

Figure 7. Apatite (U-Th)/He date versus distance from the plateau rim margin for cross sections through (A) northwestern study area, A–A′, and (B) southeastern study area, B–B′. Locations of cross-section lines indicated in (C) Diamonds represent data for Triassic Moenkopi sandstones, and squares represent data for Permian Esplanade and Coconino sandstones. For type A samples, the sample mean and standard deviation is plotted. For all samples, the youngest date is plotted (see text for additional explanation). The location and timing constraints for deposition of the Rim gravels and Bidahochi Formation are also shown. (C) Map showing the time at which the Kaibab surface is inferred to have cooled below 45 °C. Time periods not shown are intervals during which the landscape was relatively stable. Dashed lines indicate regions less constrained by data.

interior, confirming an overall pattern of southwest to northeast denudation. Second, models that reproduce the distributions of sample dates indicate a single dominant phase of Laramide unroofing along the plateau margin, in contrast to multiphase unroofing that denuded the southwestern plateau interior. Third, regional data patterns suggest significant differences in the migration of unroofing between Sevier-Laramide time and mid- to Late Tertiary time. Apatites from Lower Granite Gorge basement proximal to the plateau rim are older (Late Cretaceous) than those from Upper Granite Gorge basement samples from the southwestern plateau interior (mid-Tertiary), and the youngest apatite dates from the Triassic and Permian sandstones systematically young from the margin (Early Tertiary) to the interior (mid-Late Tertiary) (Fig. 7). The youngest apatite dates for the detrital sandstones are significant, because they have the lowest effective closure temperatures, and therefore yield dates that are most sensitive to the final removal of Mesozoic to Tertiary overburden. Although it is impossible to know whether we obtained the youngest date in each sample, the coherent regional pattern strongly supports the interpretation of southwest to northeast removal of overburden (Fig. 7). Toward the northwest, in northwestern Arizona (Figs. 3B and 7A), the data record (1) Sevier-Laramide unroofing along the plateau margin, with denudation to the Kaibab surface by the time of deposition of the Rim gravels at ca. 50 Ma, (2) mid-Tertiary unroofing (28–18 Ma) recorded both on the Kaibab surface and in the basement of the Grand Canyon, indicating this was a significant denudational phase, and (3) Late Tertiary unroofing (<16 Ma) north of the Grand Canyon. Toward the southeast, in east-central Arizona (Figs. 3B and 7B), the data indicate (1) Sevier-Laramide unroofing along the plateau margin, with denudation to the Kaibab surface by the time of deposition of the Rim gravels at 35 Ma, and (2) mid-Tertiary unroofing (28–18 Ma) to the Kaibab surface prior to the onset of deposition of the Bidahochi Formation at 16 Ma.

The temperature-time paths that best explain our data set imply that the entire Kaibab surface exposed in the study area cooled below 65–70 °C in Early Tertiary time. We constructed a map showing the inferred time at which the Kaibab surface cooled below 45 °C (Fig. 7C). We interpret a diachronous single phase of unroofing along the plateau margin, as implied by the uniform dates within individual samples that are younger southeastward along the plateau margin (Figs. 5 and 7). The northeastward advance of the second phase of unroofing within the southwestern plateau interior is inferred from our modeled distributions of sample dates (Figs. 6

53

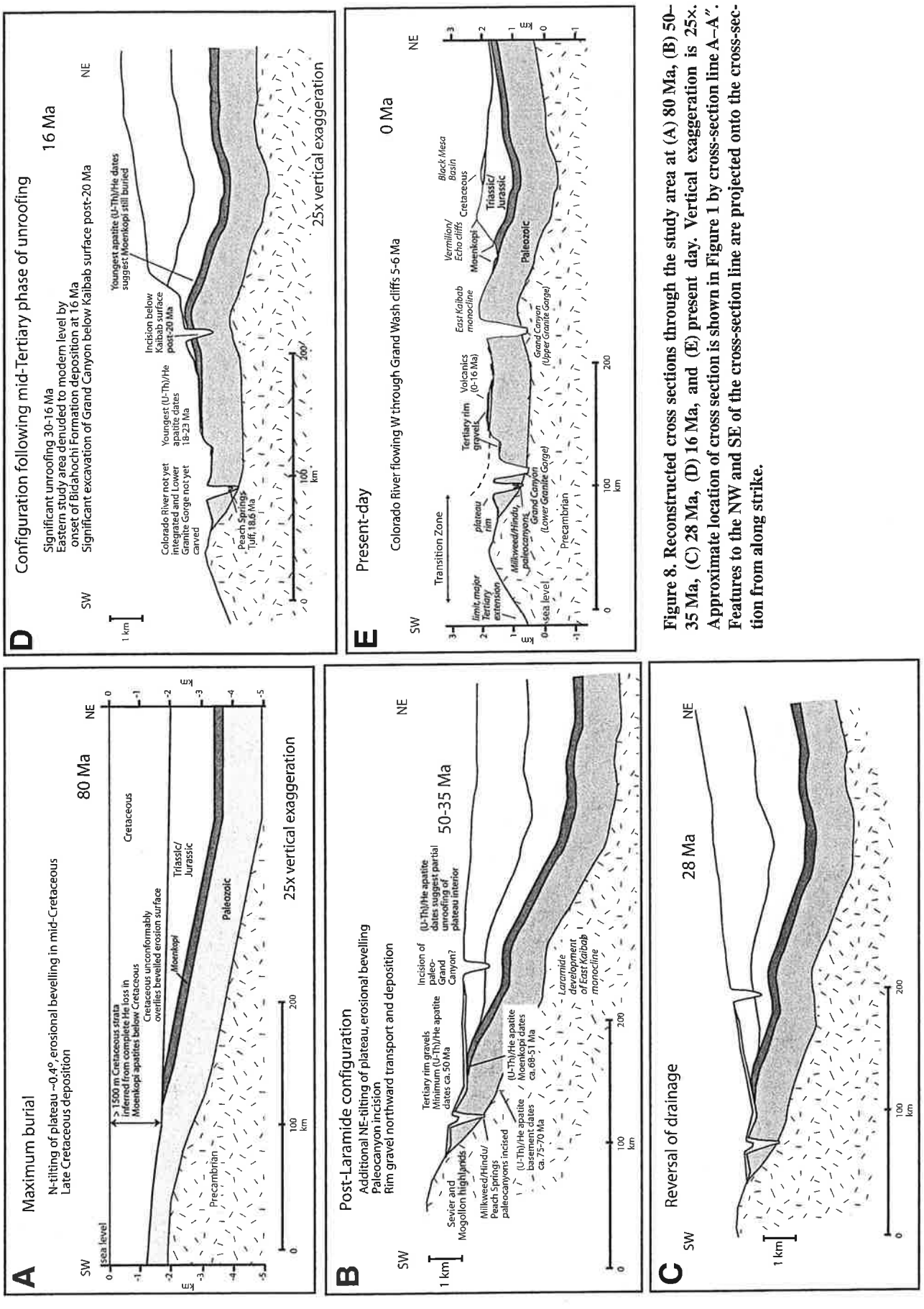

Figure 8. Reconstructed cross sections through the study area at (A) 80 Ma, (B) 50–35 Ma, (C) 28 Ma, (D) 16 Ma, and (E) present day. Vertical exaggeration is 25×. Approximate location of cross section is shown in Figure 1 by cross-section line A–A″. Features to the NW and SE of the cross-section line are projected onto the cross-section from along strike.

54

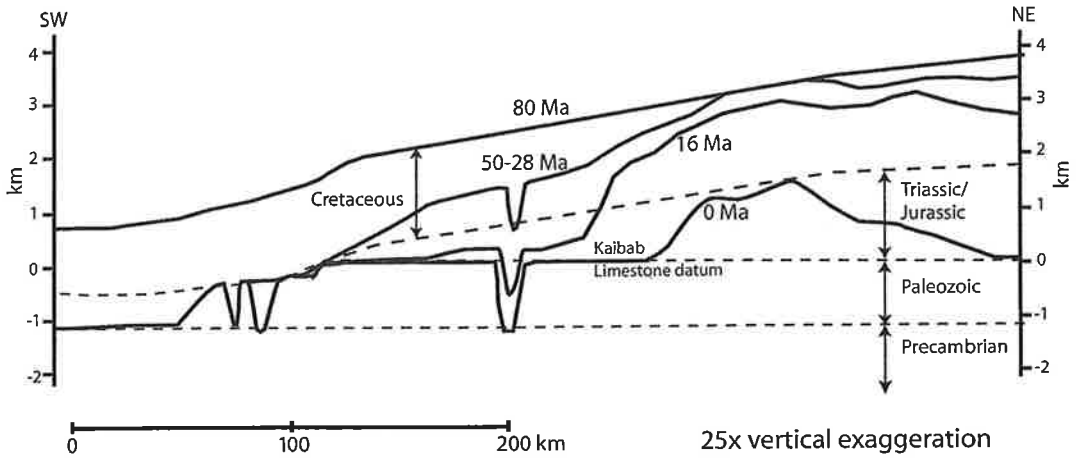

Figure 9. Reconstructed sedimentary thicknesses at the selected times depicted in the cross sections in Figure 9, relative to the horizontal Kaibab limestone datum. Dashed lines represent contacts between major rock packages of different age. Vertical exaggeration is 25×.

the cause of this migration, we note that the Sevier orogeny affected the western margin of the plateau well before the onset of the Laramide tectonism that affected the eastern margin, and therefore it seems likely that the diachronism in unroofing is in some way related to the diachronism in mountain building on either side of the plateau (Sevier versus Laramide). Denudation was followed by northeastward transport and aggradation of Rim gravels starting in the early Eocene in northwest Arizona, and starting in the late Eocene in east-central Arizona (Potochnik and Faulds, 1998). Assuming that the apatite (U-Th)/He apatite dates for the Music Mountain Formation reflect unroofing of their source regions, the youngest clast dates of ca. 50 Ma provide a maximum age for deposition, consistent with (1) apatite (U-Th)/He apatite dates from the underlying Moenkopi Formation as young as ca. 53 Ma, (2) a 64 Ma K-Ar date for the youngest dated volcanic clast at the base of the Long Point section (Elston et al., 1989), (3) the occurrence of upper Paleocene or lower Eocene freshwater gastropods in the Long Point section (Young, 2001), and (4) the identification of Eocene charophytes in the section (Young, 2006, personal commun.). Collectively, these data indicate that the plateau margin was topographically higher than the southwestern plateau interior, and had developed a net structural relief of at least 5500 m on the basal Cambrian unconformity by Early Tertiary time. According to our model, ca. 2300 m of this relief had developed by ca. 94 Ma (Late Cenomanian) (Fig. 8A), and an additional 3200 m developed at some time between ca. 80 and 50 Ma (Fig. 8B). Although we cannot constrain absolute elevations, evidence for kilometer-scale relief at the head of the Milkweed and Peach Springs paleocanyons and within the Upper Granite Gorge area imply that kilometer-scale uplift had affected both the plateau margin and at least a portion of the plateau interior by 50 Ma. If such a paleocanyon existed, then the Milkweed and Peach Springs drainages would presumably have been tributary to a northeast-flowing ancestral Colorado River.

We emphasize that our constraints on uplift and canyon incision are derived from samples from the Upper Granite Gorge in the eastern Grand Canyon, and need not apply to the western Grand Canyon or east central Arizona. In the westernmost segment of the Grand Canyon just downstream from the intersection of Peach Springs Wash and the Colorado, early Miocene basalts (19 Ma) appear to have flowed across a deeply incised southern tributary (Spencer Canyon), strongly suggesting this reach of the canyon was carved from a Miocene surface of low relief. An Early to mid-Tertiary proto–Grand Canyon may have extended from Peach Springs Canyon to the Upper Granite Gorge, but need not have had the precise form, course, or dimensions of the modern canyon. Rather an ancestral canyon may have been modified and subsequently exploited during the integration of the modern river post–6 Ma (e.g., Potochnik, 2001; Young, 2001), perhaps accounting for the inadequacy of Quaternary incision rates to carve the entire canyon in 6 m.y. (Pederson et al., 2002; Karlstrom et al., 2007).

Drainage Reversal and Unroofing in Mid-Tertiary Time

The southwestern plateau appears to have been characterized by a relatively stable landscape (Figs. 8B–8C) with either slow erosion or aggradation from ca. 50–30 Ma. In the mid-Tertiary (28–16 Ma), a significant phase of unroofing coincides with the initiation of major extensional tectonism in the Basin and Range province, which is presumably the cause of drainage reversal across the Mogollon Rim recorded in the Salt River region (Potochnik, 2001) (Figs. 8C–8D). Relatively little is known about this time interval on the plateau from geological relationships, because there are few preserved deposits of this age. Toward the southeast (Fig. 7B), (U-Th)/He dates of ca. 26–18 Ma for Moenkopi samples record unroofing at this time, prior to the onset of aggradation of the Bidahochi Formation at 16 Ma. Toward the northwest (Fig. 7A), the youngest (U-Th)/He dates from the Moenkopi samples on the Kaibab surface, Coconino and Esplanade samples from the Kaibab uplift, and crystalline basement samples from the Grand Canyon are 28–19 Ma. The dates in this range are laterally persistent in a northwest-trending band ~75 km wide (Fig. 7A), suggesting a pulse of erosion of the plateau interior at this time. The youngest dates of ca. 23 Ma from the Grand Canyon basement indicate that significant incision of the Upper Granite Gorge below the Kaibab surface could not have begun until after this time. Our model maintains kilometer-scale relief in the Upper Granite Gorge area from 25 Ma to 16 Ma, with the bottom of the channel cut in Lower Jurassic strata at 25 Ma and Mississippian strata at 16 Ma (Figs. 8C–8D). Our data do not allow us to determine whether relief increased or decreased through this interval in the Upper Granite Gorge area. However, in contrast to the westernmost portion of the canyon below Peach Springs Canyon, the data do not support carving of the Upper Granite Gorge into a surface of low relief cut on or near the Kaibab Formation.

Unroofing in Late Tertiary Time

Substantial post-Laramide unroofing of the southwestern plateau interior north of the Grand Canyon occurred in latest Miocene to Pliocene time, recorded by samples containing (U-Th)/He dates <18 Ma, and as young as 5 Ma (Figs. 7A and 8E). These youngest dates are consistent with apatite (U-Th)/He apatite results even farther north in southern Utah suggesting accelerated erosion <10 Ma (Stockli, 2005). On the basis of widespread Pliocene river gravels along

the lower part of the Colorado River derived in part from central Utah, there is strong consensus that a through-going Colorado River existed at least as far back as 5 Ma (e.g., Spencer et al., 2001). Rapid, young denudation of the interior portions of the southwestern plateau supports the hypothesis that river integration induced the latest phase of plateau unroofing by providing a mechanism to efficiently remove large sediment volumes from the plateau interior (Pederson et al., 2002).

Implications for the Relationship between Unroofing, Incision, and Surface Uplift in the Upper Granite Gorge Region

Our new results impose important constraints on the controversial timing of uplift and incision of the southwestern Colorado Plateau, especially in the Upper Granite Gorge region of the plateau interior. In this section, we describe and evaluate two endmember models for the relationship between these processes (Fig. 10). We note that although these endmembers echo the views of many geologists since the time of John Wesley Powell's exploration of the canyon, neither precisely describes the views of any particular investigator or period of investigation. Concise, modern overviews of the complex evolution of ideas relating to this topic may be found in Ranney (2005) and Powell (2005). In one endmember, regional unroofing to the Kaibab surface occurred prior to Late Tertiary incision of the Grand Canyon and coeval uplift of the plateau, implying that regional unroofing of the Mesozoic (Dutton's Great Denudation) is genetically unrelated to uplift and incision of the Grand Canyon (Dutton's Great Erosion) (Fig. 10, model #1). In the opposite endmember, canyon incision and plateau uplift in Early Tertiary time preceded regional unroofing, such that regional unroofing is a direct consequence of these processes (Fig. 10, model #2). In this extreme, a high-relief Early Tertiary "equilibrium" landscape lowers itself largely unchanged onto the present landscape, such that the carving of the modern Grand Canyon from Kaibab down to basement was accompanied by equivalent lowering of the plateaus on the canyon's rim from Cretaceous down to Permian.

In support of the general viability of the low-relief denudation of model #1, we cite the pre-mid Cretaceous erosion of ~1500 m of Lower Triassic through Upper Jurassic units (~0.03 mm/yr for ~56 m.y.), followed by deposition of Late Cretaceous marine sediments (Fig. 8A). Deposition on either side of the low-relief, basal Cretaceous erosion surface occurred at or near sea level (e.g., Blakely, 1989), and therefore it is difficult to envisage the growth and demise of kilometer-scale topographic relief during this erosional event. This particular example does not specifically support either of the models in Figure 10, which apply only to post–mid-Cretaceous unroofing. Rather, it cautions us not to presume that unroofing is a direct proxy for surface uplift, or that erosional unroofing at moderate rates requires the development of kilometer-scale relief.

Our data indicate significant denudation of the southwestern plateau interior during the mid-Tertiary (28–16 Ma), most likely due to drainage reversal across the plateau rim. The question of whether this unroofing was associated with elevation gain of the plateau interior is difficult to address on the evidence for unroofing alone. Along the plateau margin, substantial topographic relief had developed by the mid-Tertiary in the Salt River Canyon (850–1400 m) and along the Mogollon Rim (~600 m). Because regional drainage had reversed such that the plateau interior was now the source region for gravels deposited in these areas, the southwestern plateau interior presumably had attained significant elevation by this time (Peirce et al., 1979; Potochnik, 2001). Uplift of at least a portion of the plateau interior may have occurred as early as the Early Tertiary, when the plateau margin was topographically higher than the plateau interior and the area had developed a net structural relief of >5500 m. If our models for the thermal histories of samples from the Upper Granite Gorge region are correct, they would imply that a significant proto–Grand Canyon had incised post-Paleozoic strata by the early Eocene, therefore indicating kilometer-scale elevation gain of at least this part of the plateau during Sevier-Laramide time. These results are inconsistent with models for the rise of the entire plateau from near sea level during Late Tertiary time (Fig. 10, model #1), and indicate that at least part of the uplift was decoupled from the integration of a southwest-flowing Colorado River in latest Miocene time. Rather, the data suggest a scenario more similar to model #2 (Figs. 9 and 10), in which canyon incision and substantial plateau uplift in Early Tertiary time preceded the mid- and Late Tertiary unroofing episodes that denuded the plateau interior. Clearly, however, our data do not preclude a significant component of elevation

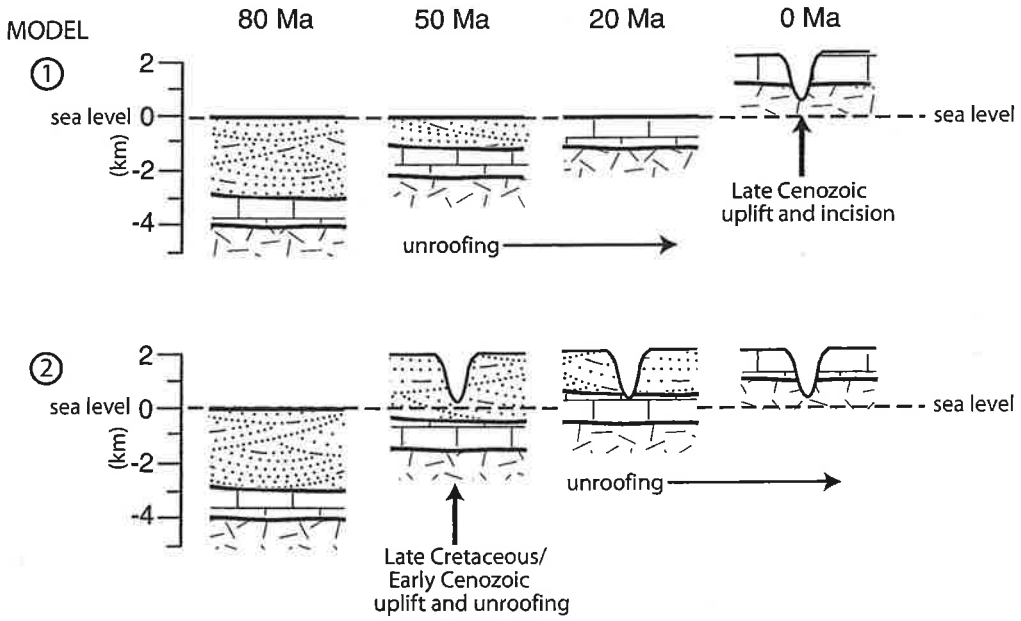

Figure 10. Endmember models for the uplift, incision, and unroofing history of the plateau interior in the Upper Granite Gorge region of the Grand Canyon.

Displacement rates on the Toroweap and Hurricane faults: Implications for Quaternary downcutting in the Grand Canyon, Arizona

Cassandra R. Fenton* Department of Geology and Geophysics, University of Utah, Salt Lake City, Utah 84112, USA
Robert H. Webb U.S. Geological Survey, 1675 W. Anklam Road, Tucson, Arizona 85745, USA
Philip A. Pearthree Arizona Geological Survey, 416 W. Congress Street, Tucson, Arizona 85701, USA
Thure E. Cerling Department of Geology and Geophysics, University of Utah, Salt Lake City, Utah 84112, USA
Robert J. Poreda Department of Earth and Environmental Sciences, University of Rochester, Rochester, New York 14627, USA

ABSTRACT

The Toroweap and Hurricane faults, considered to be the most active in Arizona, cross the Uinkaret volcanic field in the western Grand Canyon. These normal faults are downthrown to the west, and the Colorado River crosses these faults as it flows west in the Grand Canyon. Cosmogenic ^{3}He (^3He_c) dates on basalt flows and related landforms are used to calculate vertical displacement rates for these faults. The two faults cross unruptured alluvial fans dated as 3 ka (Toroweap) and 8 ka (Hurricane), and 10 other landforms that range in age from 30 to 400 ka are displaced. Middle and late Quaternary displacement rates of the Toroweap and Hurricane faults are 70–180 and 70–170 m/m.y., respectively. On the basis of these rates, the combined displacement of 580 m on these faults could have occurred in the past 3 to 5 m.y. All ^3He_c dates are younger than existing K-Ar dates and are consistent with new $^{40}Ar/^{39}Ar$ dates and existing thermoluminescence (TL) dates on basalt flows. These different dating techniques may be combined in an analysis of displacement rates. Downcutting rates for the Colorado River in the eastern Grand Canyon (400 m/m.y.) are at least double the downcutting rates west of the faults (70–160 m/m.y.). Faulting probably increased downcutting in the eastern Grand Canyon relative to downcutting in the western Grand Canyon during the late Quaternary.

Keywords: cosmogenic elements, Colorado River, normal faults.

INTRODUCTION

The Hurricane and Toroweap faults are the most active faults in northwestern Arizona (Jackson, 1990; Stenner et al., 1999). These north-south–trending normal faults cross the southwestward-flowing Colorado River near river miles 179 and 191 (Fig. 1A) and are in the structural transition zone between the Great Basin and Colorado Plateau physiographic provinces (Stenner et al., 1999). The faults are downthrown to the west and have a combined vertical displacement of 580 m in Paleozoic rocks (Fig. 1B). Quaternary landforms in the Uinkaret volcanic field have been displaced by Toroweap and Hurricane faults. Dates of volcanism near the rim of the Grand Canyon range from 1 ka (Fig. 1A) to 3.7 Ma at Mount Trumbull (Wenrich et al., 1995), although most lava flows are younger than 600 ka (Dalrymple and Hamblin, 1998). At various times basalt flows have dammed the Colorado River (Hamblin, 1994).

Previous estimates of displacement rates on the Toroweap fault are 20 m/m.y., 56 m/m.y., and 110 m/m.y. in the time periods from 10 Ma to 600 ka, 600 to 40 ka, and 40 to 3 ka, respectively (Jackson, 1990). Holmes et al. (1978) reported displacement estimates of 60 to 75 m/m.y. for the interval 300 to 200 ka. Jackson inferred that either the rate of displacement increased significantly during the Quaternary or that faulting began more recently than previously thought. Previous estimates for the displacement rate on the Hurricane fault from 200 to 90 in the vicinity of Grand Canyon range from 30–70 m/m.y. (Pearthree et al., 1983) to 125–250 m/m.y. (Holmes et al., 1978).

In this paper we report new displacement rates based on ^3He_c ages for surfaces younger than 400 ka crossed by the Toroweap and Hurricane faults. We linearly extrapolate these rates to estimate that the combined total vertical displacement on both faults could have occurred in the past 3 to 5 m.y. We suggest that these displacement rates probably differentially affected downcutting rates of the Colorado River in the eastern versus western Grand Canyon.

AGE DATING OF BASALT FLOWS AND ASSOCIATED LANDFORMS

The age of volcanism in the Uinkaret volcanic field has been previously estimated using K-Ar (Dalrymple and Hamblin, 1998) and thermoluminescence (TL) dating (Holmes et al., 1978). K-Ar dating in this volcanic field is known to be problematic owing to excess ^{40}Ar incorporated into large phenocrysts from the magmatic environment (Damon et al., 1967) and abundant glassy groundmass (Dalrymple and Hamblin, 1998). $^{39}Ar/^{40}Ar$ dating is more precise than K-Ar analysis and has been used to accurately date young basalt flows (Laughlin et al., 1994). However, hydration and alteration of abundant glassy groundmass in Uinkaret basalts can contribute atmospheric Ar to analyses and can cause large uncertainties in $^{39}Ar/^{40}Ar$ ages. In the Uinkaret volcanic field, ^3He_c dating provides an alternative to K-Ar dating and, in certain cases to $^{39}Ar/^{40}Ar$ dating, particularly for relatively young (<200 ka) basalt flows with abundant olivine and/or pyroxene phenocrysts (Fenton et al., 2001). Samples collected from the Uinkaret volcanic field were analyzed in accordance with techniques described in Cerling et al. (1999).

Most of the ^3He_c ages on surfaces in the Uinkaret volcanic field differ significantly from existing K-Ar ages (Table 1; for details see Table DR1[1]). Damon et al. (1967) reported a K-Ar age of 10 ka for Vulcan's Throne (Fig. 1A), noting that it is only an order of magnitude estimate because of a high atmospheric Ar correction. We believe our ^3He_c age of 73 ± 4 ka is fairly accurate, although it is a minimum age because Vulcan's Throne, a cinder cone, is more erodible than nearby basalt flows. Damon (quoted in Hamblin, 1994) reported a K-Ar age of 993 ± 97 ka for Hamblin's (1994) Whitmore Dam basalt, but Dalrymple and Hamblin (1998) concluded that this date may not be reliable, on the basis of stratigraphic relations.

Fenton et al. (2001) concluded that their Whitmore Cascade basalt is correlative with the Whitmore Dam basalt (Fig. 1A) and reported a ^3He_c age of 177 ± 9 ka for the flow. This age is bracketed by TL dates of the same flow (Table 1; Holmes et al., 1978). The Whitmore Cascade contains abundant glass that may contribute to an anomalously old K-Ar

*E-mail: crfenton@mines.utah.edu.

[1]GSA Data Repository item 2001119, ^3He_c exposure ages of landforms in the Uinkaret volcanic field, is available on request from Documents Secretary, GSA, P.O. Box 9140, Boulder, CO 80301-9140, editing@geosociety.org, or at www.geosociety.org/pubs/ft2001.htm.

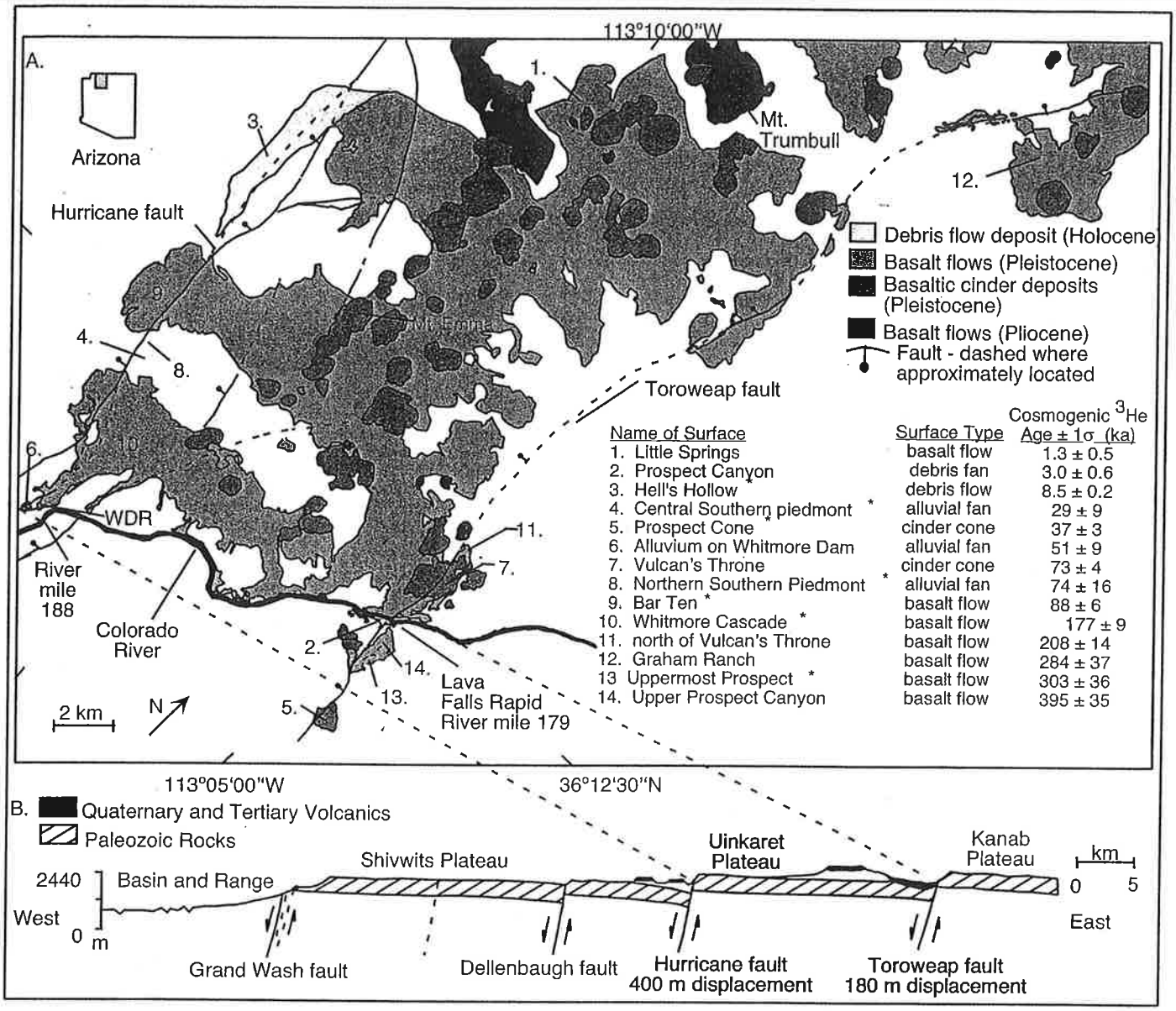

Figure 1. A: Map of Quaternary basalt flows in Uinkaret volcanic field and Hurricane and Toroweap faults, western Grand Canyon, Arizona (adapted from Wenrich et al., 1997). Details of analyses in Table DR1 (see text footnote 1). Hurricane and Toroweap faults do not displace Hell's Hollow and Prospect Canyon debris flows, respectively. Little Springs basalt flow (Billingsley, 1997) is not crossed by either fault, but is reported to show range in age of volcanic activity in region. Names with asterisk are informal. WDR—Whitmore Dam remnant (Hamblin, 1994). B: East-west cross section of western Grand Canyon from Grand Wash fault to Toroweap fault (adapted from Jackson, 1990).

age. ^3He_c ages of the Whitmore Cascade and Bar Ten basalt flows are consistent with middle to late Quaternary age $^{39}Ar/^{40}Ar$ and TL age estimates of these flows (Table 1). Large analytical uncertainties render the $^{39}Ar/^{40}Ar$ ages essentially useless in calculating late Quaternary slip rates.

Three basalt flows with the oldest ^3He_c ages are found along the Toroweap fault. A lava flow adjacent to and north of Vulcan's Throne has identical TL and ^3He_c ages of 201 ± 14 ka and 208 ± 14 ka, respectively (Table 1). The K-Ar (500 ± 47 ka; Dalrymple and Hamblin, 1998) and ^3He_c (395 ± 35 ka) ages of Hamblin's (1994) Upper Prospect basalt flow overlap within two standard deviations (Table 1). The ^3He_c age may be younger due to minimal flow-surface weathering. In contrast, the K-Ar age may be older because of the presence of excess Ar. The Graham Ranch flow in Toroweap Valley (Fig. 1A) has reported K-Ar and TL ages of 635 ± 24 ka (Jackson, 1990) and 284 ± 48 ka (Holmes et al., 1978). We obtained a ^3He_c age of 284 ± 37 ka for that flow. The ^3He_c age of the Graham Ranch flow may be younger than the reported K-Ar age because the flow is weathered, but it is likely that the ^3He_c and TL ages are more accurate than the K-Ar age.

TOROWEAP AND HURRICANE FAULTS

An alluvial fan at the mouth of Prospect Valley (Fig. 1A) composed of debris-flow deposits delineates the Holocene displacement history on the Toroweap fault. The debris flow covering the surface was emplaced 3.0 ± 0.6 ka, and the fault does not rupture this surface (Cerling et al., 1999). An estimated displacement of 2.2 m occurred during a magnitude 7 earthquake on the Toroweap fault at 3.1 ± 1.6 ka, on the basis of morphologic fault-scarp analysis in Prospect Valley, south of the Colorado River (Jackson, 1990). This earthquake must have occurred before 2.4 ka, the minimum age of the surface of the fan.

Using ^3He_c ages of volcanic landforms along the Toroweap fault and published displacements (Jackson, 1990; Wenrich et al., 1997), we estimate a range in displacement rates of 70–180 m/m.y. for the past 300 k.y.

TABLE 1. DISPLACEMENT RATES FOR THE TOROWEAP AND HURRICANE FAULTS

Fault	Site	Average ^3He_c age ±1σ* (ka)	K-Ar or $^{39}Ar/^{40}Ar$ age (ka)	TL age (ka)	Displacement (m)	Average Displacement rate (m/m.y.)
Toroweap	Prospect Canyon debris fan	3.0 ± 0.6	—	—	0	0
Toroweap	Prospect Cone	37 ± 3	—	—	7	180
Toroweap	Vulcan's Throne	73 ± 4	10	—	5	70
Toroweap	Basalt flow north of Vulcan's Throne	208 ± 14	—	201 ± 34	14	70
Toroweap	Graham Ranch basalt flow	284 ± 37	635 ± 24	284 ± 48	36	130
Toroweap	Upper Prospect basalt flow	395 ± 35	500 ± 47	—	46	120
Hurricane	Hell's Hollow debris flow	8.5 ± 0.2	—	—	0	0
Hurricane	Northern alluvial fan of southern piedmont	74 ± 16	—	—	7	90
Hurricane	Central alluvial fan of southern piedmont	29 ± 9	—	—	3	100
Hurricane	Alluvium overlying Whitmore Dam remnant	51 ± 9	—	—	4*	80
Hurricane	Bar Ten basalt flow	88 ± 6	190 ± 390†	108 ± 29	10 ± 3	110
Hurricane	Whitmore Cascade basalt flow (north end)	177 ± 9	220 ± 120† 150 ± 220†	203 ± 24 88 ± 15	15 ± 3	80
Hurricane	Whitmore Cascade basalt flow (south end)	177 ± 9	220 ± 120† 150 ± 220† 993 ± 97	203 ± 24 88 ± 15	12	70

Note: Rates calculated using average ^3He_c ages of displaced lava flows, cinder cones, and alluvial deposits in the Uinkaret volcanic field. Details of analysis in Table 2 (see text footnote 1). —= no date. Documented K-Ar and TL (thermoluminescence) ages are listed for comparison and are referenced in the text. Displacements other than those produced by the authors are referenced in the text. Uppermost Prospect flow is not listed in this table because the vertical displacement of this flow has not been measured.

*Scarp profile measured by authors using laser range finder and displacement calculated using far-field slopes.

†$^{39}Ar/^{40}Ar$ ages analyzed at the New Mexico Geochronological Research Laboratory; Samples 97-AZ-318-WDA and 97-AZ-321-WCB were collected from the Whitmore Cascade and sample 97-AZ-329-BT came from the Bar Ten basalt flow. Large uncertainties likely result from alteration of glass in the groundmass.

for the Toroweap fault (Table 1). Two cinder cones—Prospect Cone and Vulcan's Throne—are displaced 7 and 5 m, respectively (Table 1). If we use ^3He_c ages of 37 ± 3 and 73 ± 4 ka for Prospect Cone and Vulcan's Throne (Fig. 1A), the displacement rates are 180 and 70 m/m.y., respectively. The basalt flow dated at 208 ± 14 ka (^3He_c) and located north of Vulcan's Throne has a displacement of 13–15 m (Jackson, 1990), yielding a vertical slip rate of 70 m/m.y.

If we use a displacement of 36 m and a K-Ar age of 635 ka, the Graham Ranch basalt flow has a minimum displacement rate of 56 m/m.y. (Jackson, 1990). Using the same displacement and our minimum ^3He_c age of 284 ± 37 ka, we calculate a maximum displacement rate of 130 m/m.y. Huntoon (1977) mentioned a 46 m displacement on "older lava flows that fill Prospect Valley" ~2.5 km south of the Colorado River. On the basis of field evidence, we conclude that Huntoon's flow is Hamblin's Upper Prospect Canyon flow (Fig. 1A), which has a cosmogenic ^3He age of 395 ± 35 ka; the displacement rate is 120 m/m.y., which agrees with a linear displacement rate (Fig. 2). Jackson (1990) concluded that the displacement rate on the Toroweap fault increases from 56 m/m.y. to 110 m/m.y. ca. 40 ka. Our data show that the displacement rate on the Toroweap fault has been linear over the past 400 k.y. (Fig. 2).

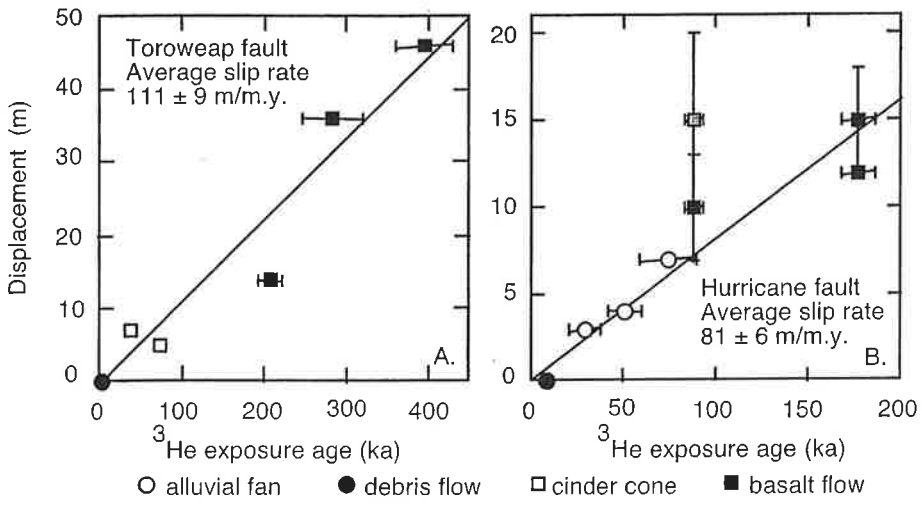

Figure. 2. Vertical displacement rates of (A) Toroweap and (B) Hurricane faults based on ^3He_c ages of displaced landforms in Uinkaret volcanic field. Average slip rates on faults, 111 ± 9 m/m.y. for Toroweap and 81 ± 6 m/m.y., for Hurricane, are based on linear regressions (R^2 = 0.966 and 0.970 for Toroweap and Hurricane faults). Gray square in B is maximum average displacement on Bar Ten flow. It is not included in average slip rate of Hurricane fault (see text for details).

On the Hurricane fault, alluvial fans provide data on displacements <100 k.y. old. The Hell's Hollow debris flow, which is not ruptured, yielded a ^3He_c age of 8.5 ± 0.2 ka, providing a datum on the age of youngest displacement (Fig. 1A). Our age agrees with morphologic analyses of fault scarps that suggest that the youngest displacement in Whitmore Wash, which resulted in 2–3 m of offset, occurred between 5 and 15 ka (Pearthree et al., 1983). A suite of alluvial fans, called the southern piedmont by Stenner et al. (1999), lies between the Bar Ten and Whitmore Cascade lava flows (Fig. 1A). Varnished basalt boulders in the alluvium yielded average ^3He_c ages of 74 ± 16 and 29 ± 9 ka for the northern and central fans, respectively, in the piedmont. These surfaces are displaced 7 and 3 m by the Hurricane fault (Stenner et al., 1999), and the resulting displacement rates are 90 and 100 m/m.y. Alluvium overlying Hamblin's (1994) Whitmore Dam remnant at the mouth of Whitmore Canyon (Fig. 1A) has a 4 m displacement (Table 1), and varnished basalt boulders yield a ^3He_c age of 51 ± 9 ka for a displacement rate of 80 m/m.y.

In Whitmore Canyon, the Bar Ten basalt flow, which has an ^3He_c age of 88 ± 6 ka, has an average vertical displacement of 15 ± 6 m (Stenner et al., 1999; Fig. 2). The flow surface is steep and irregular, and the displacement varies by at least 100% in short distances along strike. The higher displacements may reflect buried bedrock scarps over which the Bar Ten basalt flowed. Excluding the highest two or three scarps results in estimated displacements of 12 ± 4 and 10 ± 3 m for the Bar Ten flow; given the agreement in linear displacement of nearby alluvial fans and in the Whitmore Cascade (Fig.

2), we believe the lesser of the displacement values of 10 m on the Bar Ten flow is more reasonable. If this figure is used, the displacement rate is 110 m/m.y.

The Whitmore Cascade has an average total displacement of 15 ± 3 m at the north end of the basalt flow (Stenner et al., 1999) and a displacement of 12 m near the Colorado River (Wenrich et al., 1997). Given an average ^3He_c age of 177 ± 9 ka, the displacement rate for this basalt flow is between 70 and 80 m/m.y. Using these age and displacement data, we estimate a late Quaternary displacement rate for the Hurricane fault of between 70 and 170 m/m.y., but it is likely that the displacement rate is between 80 and 110 m/m.y. (Fig. 2). We conclude that the displacement rates for the Toroweap and Hurricane faults have been linear for the past 400 k.y. and 200 k.y., respectively, and we find no evidence to support Jackson's (1990) conclusion that displacement rates have increased in the past 40 k.y.

The Toroweap fault has 150–265 m of total vertical displacement along its length (Jackson, 1990); displacement in the vicinity of the Grand Canyon is 180 m (Wenrich et al., 1997). The total vertical displacement on the Hurricane fault is 400 m at the Colorado River (Wenrich et al., 1997), but published maps show the fault concealed by a 600 ka lava flow (Hamblin, 1994). Our field inspection indicates that the Hurricane fault lies east of the path mapped by Wenrich et al. (1997) and that the fault does not directly interact with the lava flow on the south side of the Colorado River. Instead, there is substantial Quaternary displacement in an alluvial fan just south of the river in 192 Mile Canyon. The displacement south of the river indicates that the Hurricane fault crosses the Colorado River with possibly the same activity it shows north of the river (Fig. 2B).

The Hurricane and Toroweap faults have a combined vertical displacement of 580 m. This is 68% of the depth of the Inner Gorge from Toroweap Overlook to Lava Falls Rapid (850 m) just upstream of the Toroweap fault. By extrapolation of the displacement rates (Fig. 2) on both faults through the Quaternary, we calculate that the Toroweap and Hurricane faults could have accommodated all of their vertical displacement in the past 1.5 and 5 m.y., respectively. Billingsley and Workman (2000) reported that all of the faults on the Uinkaret plateau probably became active at 3.5 to 2 Ma and that extension on the Hurricane fault began after emplacement of the Bundyville basalt (3.6 ± 0.18 Ma). Thus, the fault may have decelerated from approximately 115 m/m.y. to 80 m/m.y. between 3.5 Ma and 180 ka. The combined Quaternary vertical displacement on both faults is 380 m (45% the depth of the Inner Gorge), suggesting that 65% of the combined displacement on the Toroweap and Hurricane faults may have occurred in the past 2 m.y.

IMPLICATIONS FOR QUATERNARY DOWNCUTTING OF THE COLORADO RIVER

Displacements on the Toroweap and Hurricane faults probably induced differential downcutting rates of the Colorado River in the Grand Canyon east versus west of the faults. Vertical displacements on these faults result in local base-level fall, as evidenced by the west sides of these faults being downdropped relative to the eastern Grand Canyon. A river responding to base-level fall will incise upstream to reduce the gradient to its previous level and it can maintain a steady longitudinal profile as long as stream power of the river is large enough to allow downcutting to occur at a rate equal to that of the uplift (Merritts et al., 1994). The Colorado River has sufficient power to quickly downcut through material (Lucchitta et al., 2000) that is uplifted during individual fault movements of 3 m or less, and we would expect no discrete knickpoints in the channel profile related to faulting. Thus, the effects of this downcutting would be expressed in increased downcutting rates on the Colorado River and its tributaries in the eastern Grand Canyon, and perhaps an overall increase in the steepness of hillslopes in that part of the Grand Canyon.

Quaternary displacement on the Hurricane and Toroweap faults can help account for variations in downcutting rates reported for various locations in the Grand Canyon. Lucchitta et al. (2000) estimated downcutting rates of 70–160 m/m.y. and 400 m/m.y. for the Grand Canyon west and east, respectively, of these faults for the past 500–600 ka. Therefore, the fluvial incision rate in the eastern Grand Canyon is at least double that west of the faults, and displacement across the Toroweap and Hurricane faults is probably responsible for this difference. These faults likely played a major role in the development of the eastern Grand Canyon. Obviously, variations in lithology through the Grand Canyon influence the morphology of the canyon, but we propose that much of the development of the narrow, steep-sided Inner Gorge of the Grand Canyon just upstream of the Toroweap fault has been driven by displacement on these faults.

ACKNOWLEDGMENTS

Clair Roberts, Ben Passey, Dave Marchetti, Heidi Stenner, Jeanne Klawon, Tom Biggs, Jon Pelletier, Andy Hunt, Joel Pederson, and George Billingsley helped with field work, laboratory analyses, and technical discussions. David Fastovsky and Thomas Gardner critically reviewed the manuscript. Funding was provided by the National Science Foundation, U.S. Geological Survey, Geological Society of America, and Sigma Xi. We thank the Grand Canyon Monitoring and Research Center for logistical support.

REFERENCES CITED

Billingsley, G.H., 1997, Geologic map of the Mount Logan Quadrangle, northern Mohave County, Arizona: U.S. Geological Survey Open-File Report 97-426, scale 1: 24 000, 21 p. text.

Billingsley, G.H., and Workman, J.B., 2000, Geologic map of the Littlefield 30′ × 60′ Quadrangle, Mohave County, northwestern Arizona: U.S. Geological Survey Geologic Investigations Map I-2628, 1 sheet, scale 1:48 000, 25 p. text.

Cerling, T.E., Webb, R.H., Poreda, R.J., Rigby, A.D., and Melis, T.S., 1999, Cosmogenic ^3He ages and frequency of late Holocene debris flows from Prospect Canyon, Grand Canyon, U.S.A.: Geomorphology, v. 27, p. 93–111.

Dalrymple, G.B., and Hamblin, W.K., 1998, K-Ar of Pleistocene lava dams in the Grand Canyon in Arizona: National Academy of Science Proceedings, v. 95, p. 9744–9749.

Damon, P.E., Laughlin, A.W., and Percious, J.K., 1967, The problem of excess argon-40 in volcanic rocks, *in* Proceedings of the symposium Radioactive Dating and Methods of Low-Level Counting, Monaco, 1967: Vienna, International Atomic Energy Agency, 24 p.

Fenton, C.R., Webb, R.H., Cerling, T.E., Poreda, R.J., and Nash, B.P., 2001, Cosmogenic ^3He ages and geochemical discrimination of lava-dam outburst-flood deposits in western Grand Canyon, Arizona, *in* House, K., et al., eds., Ancient floods and modern hazards, principles and applications of paleoflood hydrology: Washington, D.C., American Geophysical Union, Water Science and Application Series, v. 4 (in press).

Hamblin, W.K., 1994, Late Cenozoic lava dams in the western Grand Canyon: Geological Society of America Memoir 183, 135 p.

Holmes, R.D., Best, M.G., and Hamblin, W.K., 1978, Calculated strain rates and their implications for the development of the Hurricane and Toroweap faults, Utah and northern Arizona: U.S. Geological Survey Technical Report Summaries, Earthquake Hazards Reduction Program, v. VII, p. 44–50.

Huntoon, P.W., 1977, Holocene faulting in the western Grand Canyon, Arizona: Geological Society of America Bulletin, v. 88, p. 1619–1622.

Jackson, G.W., 1990, Tectonic geomorphology of the Toroweap fault, western Grand Canyon, Arizona: Implications for transgression of faulting on the Colorado Plateau: Arizona Geological Survey Open-File Report, v. 90-4, p. 1–66.

Laughlin, A.W., Poths, J., Healey, H.A., Reneau, S., and WoldeGabriel, G., 1994, Dating of Quaternary basalts using the cosmogenic ^3He and ^{14}C methods with implications for excess ^{40}Ar: Geology, v. 22, p. 135–138.

Lucchitta, I., Curtis, G.H., Davis, M.E., Davis, S.W., and Turrin, B., 2000, Cyclic aggradation and downcutting, fluvial response to volcanic activity, and calibration of soil-carbonate stages in the western Grand Canyon, Arizona: Quaternary Research, v. 53, p. 23–33.

Merritts, D., Vincent, K.R., and Wohl, E.E., 1994, Long river profiles, tectonism, and eustasy: A guide to interpreting fluvial terraces: Journal of Geophysical Research, v. 99, p. 14 031–14 050.

Pearthree, P.A., Menges, C.M., and Mayer, L., 1983, Distribution, recurrence, and possible tectonic implications of late Quaternary faulting in Arizona: Arizona Bureau of Geology and Mineral Technology Open-File Report 83-20, 51 p.

Stenner, H.D., Lund, W.R., Pearthree, P.A., and Everitt, B.L., 1999, Paleoseismologic investigations of the Hurricane fault in northwestern Arizona and southwestern Utah: Arizona Geological Survey Open-File Report 99-8, 137 p.

Wenrich, K.J., Billingsley, G.H., and Blackerby, B.A., 1995, Spatial migration and compositional changes of Miocene-Quaternary magmatism in the western Grand Canyon: Journal of Geophysical Research, v. 100, p. 10 417–10 440.

Wenrich, K.J., Billingsley, G.H., and Huntoon, P.W., 1997, Breccia-pipe and geologic map of the northeastern part of the Hualapai Indian reservation and vicinity, Arizona: U.S. Geological Survey Miscellaneous Investigations Map I-2440, scale 1:48 000, 19 p. text.

Manuscript received January 4, 2001
Revised manuscript received June 29, 2001
Manuscript accepted July 20, 2001

Printed in USA

Geological Society of America
Field Guide 6
2005

Paleoseismology and geomorphology of the Hurricane Fault and Escarpment

Lee Amoroso
U.S. Geological Survey, 2255 North Gemini Drive, Flagstaff, Arizona 86001, USA

Jason Raucci
Department of Geology, Northern Arizona University, Flagstaff, Arizona 86011, USA

ABSTRACT

The Hurricane Fault is one of the longest and most active late Cenozoic normal faults in southwestern Utah and northwestern Arizona. This fault shows evidence of tectonic activity during the late Tertiary and Quaternary, neotectonism involving the Hurricane Fault as well as the Toroweap Fault imply encroaching Basin and Range extension onto the Colorado Plateau. Paleoseismology investigations suggest that the Hurricane Fault poses a seismic hazard to the southwestern Utah area. During the trip, we will examine evidence of late Pleistocene and earliest Holocene(?) surface-rupturing faulting along the Shivwits and Whitmore Canyon sections of the fault. The Hurricane Fault separates the Uinkaret and Shivwits plateaus and displacement along the fault produced the spectacular Hurricane Escarpment. We will see late Quaternary landforms related to back-wasting and mass movement along the Hurricane Escarpment and look at evidence of the style and age estimates of late Pleistocene fan deposition.

Keywords: Hurricane Fault, paleoseismology, neotectonism, alluvial fan, colluvium.

INTRODUCTION

The Hurricane Fault (Fig. 1) is the longest and most active of the late Cenozoic down-to-the-west normal faults in southwestern Utah and northwestern Arizona. The Hurricane Fault crosses the Arizona Strip between the Utah border and Grand Canyon in close proximity to St. George, Utah (Fig. 1). Although the Arizona portion of the Hurricane Fault crosses sparsely populated terrain, much of populous southwestern Utah lies within 75 km of the Shivwits section. Two significant, historic seismic events have occurred in the region. An ~M6 earthquake occurred in the Pine Valley, Utah, area in 1902 (Williams and Tapper, 1953). A M5.8 earthquake in the St. George area in 1992 caused minor structural damage in southwestern Utah, triggered a large landslide near the entrance to Zion National Park 45 km from the epicenter (Christensen, 1995), and caused numerous rockfalls along the Hurricane cliffs (G.H. Billingsley, 2000, personal commun.).

Several recent paleoseismic investigations have addressed the potential for larger earthquakes than those of the historic record. These workers have suggested that the threshold magnitude for surface rupture along faults within the Intermountain Seismic Belt (ISB; Fig. 1) in Utah is $6 < M < 6.5$ (Arabasz et al., 1992; Doser, 1985; Smith and Arabasz, 1991). Fault scarps and other evidence of Quaternary faulting suggest that there is potential for $M > 7$ earthquakes along the Hurricane Fault (Stewart et al., 1997; Stenner and Pearthree, 1999; Amoroso et al., 2004). This field trip guide introduces evidence for late Quaternary ruptures on the Hurricane Fault in Arizona, considers the neotectonics implications, and places the late Quaternary deformation within the context of the encroachment of Basin-and-Range style

Amoroso, L., and Raucci, J., 2005, Paleoseismology and geomorphology of the Hurricane Fault and Escarpment, *in* Pederson, J., and Dehler, C.M., eds., Interior Western United States: Geological Society of America Field Guide 6, p. 449–477, doi: 10.1130/2005.fld006(20).

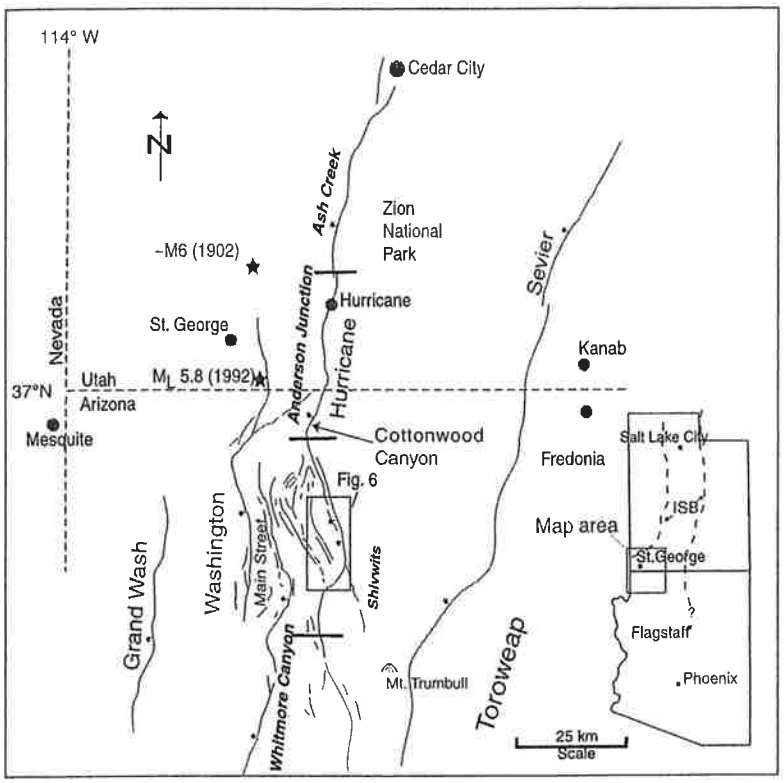

Figure 1. (A). Quaternary normal faults in northwestern Arizona and southwestern Utah, compilation adapted from Scarborough et al. (1986), Hecker (1993), and Pearthree and Bausch (1999). Significant recent earthquake epicenters (stars) and the sections (bold font) of the Hurricane Fault (Pearthree, 1998) are shown. Cottonwood Canyon, the site of recent seismic hazard assessment work on the Hurricane Fault in Arizona, is located north of the Shivwits-Anderson Junction boundary (Stenner et al., 1998). The Intermountain Seismic Belt (ISB) is a zone of earthquake activity extending through the Intermountain West from northwestern Montana south to Utah, southern Nevada and northern Arizona. The approximate boundaries of the ISB are shown in the inset.

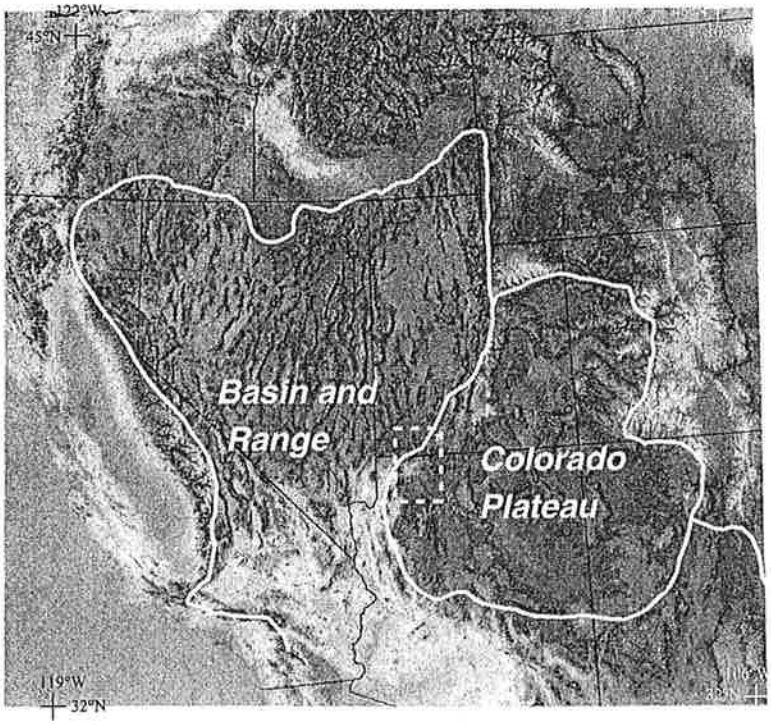

Figure 2. Digital elevation model/hillshade map of the southwestern United States showing the Colorado Plateau and Basin and Range physiographic provinces. The dashed white box shows the extent of Figure 1.

in the Fossil Mountain Member of the Kaibab Formation. Lower slopes on the cliffs consist of the Woods Ranch and Seligman Members of the Toroweap Formation, which bracket the cliff-forming Brady Canyon Member. Coarse, very poorly sorted colluvium covers much of the slope-forming units, especially the Seligman Member. Because of the structural complexity of the Hurricane Fault zone immediately across the valley from this vantage point, you may see all or parts of this sequence repeated several times.

Most of the Shivwits segment is a large structural embayment between two prominent convex fault bends. On the hanging wall at the northern end of the Shivwits segment, you can see a prominent east-sloping butte (mentioned at road-log mile 39.3), where beds of the Triassic Moenkopi Formation are capped with late Tertiary basalt and all are tilted toward the Hurricane Fault. This butte is at a major convex bend in the trace of the Hurricane Fault similar to the State Line geometric bend (Stewart and Taylor, 1996). Immediately northeast of our overlook, the gravel road of the Navajo Trail can be traced up to the Hurricane Escarpment, where it ascends the surface of a ruptured relay ramp between overlapping strands of the Hurricane Fault. The Grandstand, seen south of the Navajo Trail, is a zone of multiple fault strands associated with a left stepover. To the southeast, we can see the Moriah Knoll basalt where it flowed across the escarpment (Fig. 6). This is discussed at Stop 2.

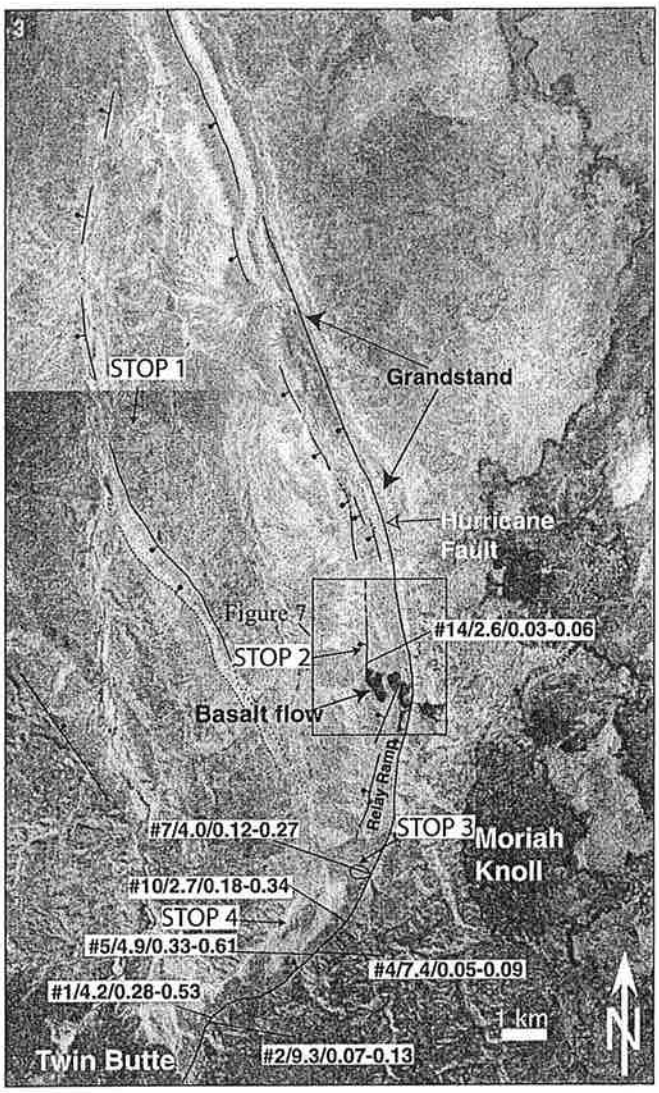

Figure 6. Mosaic of NASA high-altitude aerial photography of the central part of the Shivwits section of the Hurricane Fault showing fault traces, slip-rate estimates, and field trip stops. The fault strands are from Billingsley (1994a and 1994b) and field reconnaissance. Faults are dashed where approximate or inferred, dotted where concealed. The relay ramp, south of the basalt flow, is evidence that fault linkage had occurred on this portion of the fault (Peacock and Sanderson, 1994). Shown is a compilation of the vertical surface displacement observations (the format is profile #/surface offset in m/slip-rate range in mm/yr). Profile #7 is the Boulder Fan (outlined) trench site. The basalt flow displaced by the Hurricane Fault originated from Moriah Knoll.

Neotectonics of the Hurricane Fault

The Hurricane Fault provides excellent exposures of displaced Quaternary alluvium and basalt flows for the evaluation of seismic hazard and discerning its neotectonic history. Lund and Everitt (1999) and Stenner and Pearthree (1999) all have identified displaced basalt and alluvium that indicate that the Hurricane Fault has been active throughout the Quaternary. Paleoseismic investigations of the Anderson Junction section (Fig. 1) discovered evidence of several Pleistocene and Holocene surface-rupturing earthquakes. Stenner and others identified a latest Pleistocene to early Holocene surface-rupturing most-recent event (MRE) at Cottonwood Canyon on the Anderson Junction section (just south of the Utah border, Fig. 1) with 0.6 m of vertical displacement (Stenner et al., 1998). Further trenching investigations at Rock Canyon, 4 km north of Cottonwood Canyon, revealed that the last three events had variable amounts of slip per event (Stenner et al., 2003). The MRE had an estimated 0.3–0.4 m net vertical slip, whereas the penultimate and pre-penultimate events together had ~2.7–3.7 m of vertical slip. Possible scenarios to explain the lower MRE offset at Cottonwood and Rock Canyons include the rupture of the Shivwits that propagated north into the adjacent southern Anderson Junction sections, or a separate rupture in the boundary between the two sections. The size of older fault scarps at Cottonwood and Rock canyons, along with estimates of earthquake recurrence intervals (5–100 ka) in the Basin and Range province (Stenner et al., 1998), suggest that larger slip-per-event (more than 0.6 m) is typical along this part of the Hurricane Fault.

A paleoseismic investigation here along the Shivwits section of the Hurricane Fault revealed evidence of surface-rupturing late Quaternary events (Amoroso et al., 2004). Mapping did not show any evidence of surface rupture of Holocene deposits; the only convincing evidence of tectonic displacement was found in late to middle(?) Pleistocene alluvial fans. Results using displacement of the Moriah Knoll basalt (Fig. 7), topographic profiling, surface dating, morphologic modeling of fault scarps, and observations

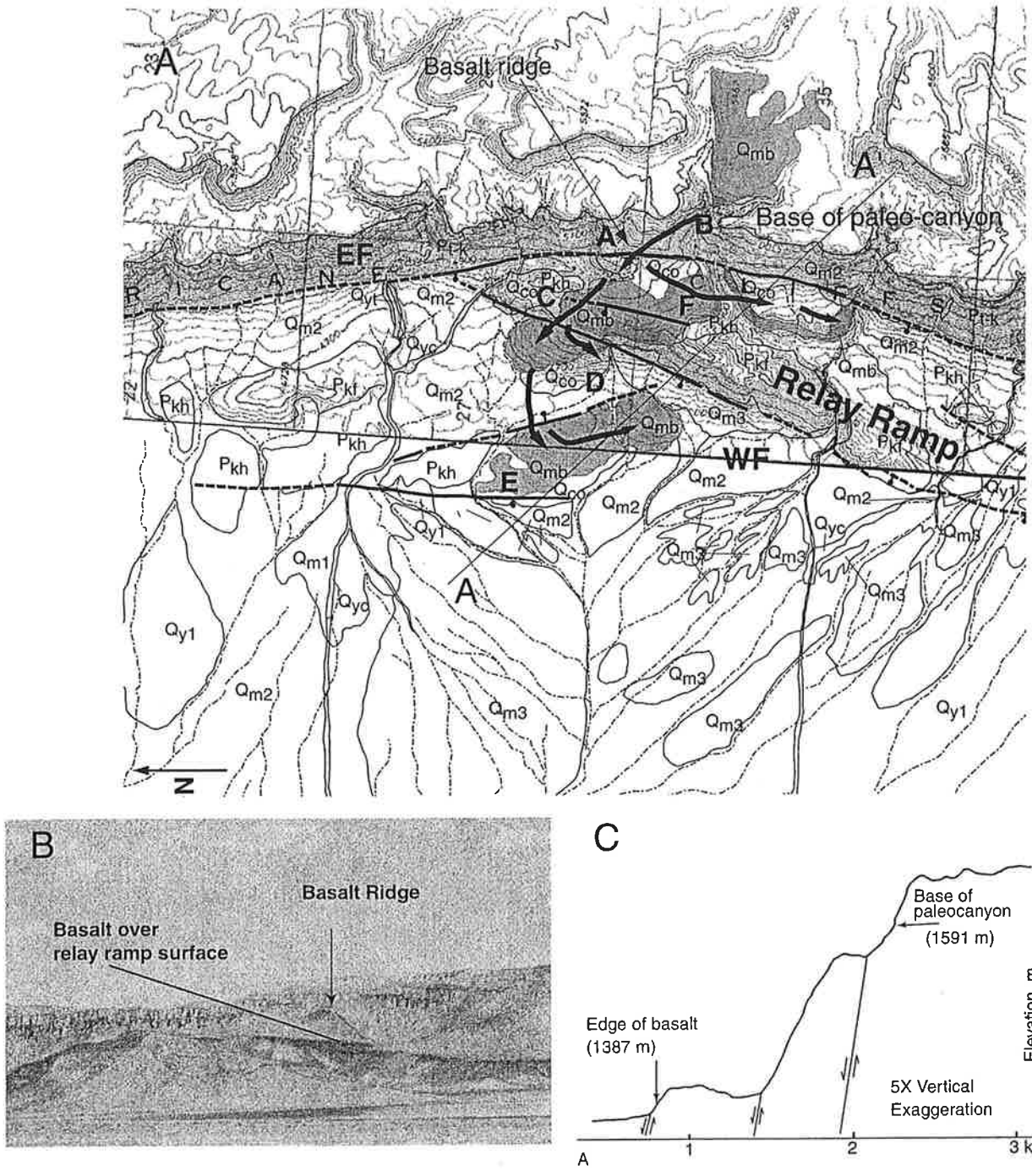

Figure 7. (A) Geologic map showing the relation of the faults to the Moriah Knoll basalt (Qmb) and the mapped flow directions (heavy black arrows). Mapped surficial units: Pkh, Harrisburg Member of the Kaibab Formation; Pt-k, Permian Toroweap and Kaibab Formations undifferentiated; Qm1–3, from mid to late Pleistocene alluvium; Qy1, Holocene alluvium; Qco, Quaternary colluvium. The basalt flowed through a paleo-canyon, crossed the fault, and covered the relay ramp surface between the escarpment and the Pkf western ridge of the relay ramp until the ridge was overtopped and the basalt flowed further northwest (B). The basalt flow directions, estimated from flow thickness, are shown by heavy black arrows. A–A′ is the location of the cross-section C. The letters on the map (A through F, EF, WF) refer to locations discussed in the text. (B) Photograph looking NE toward the Hurricane Cliffs, note the relay ramp and basalt flow that crossed the escarpment, flowed across the relay ramp, to the valley floor. (C) Cross section A–A′ showing the estimation of maximum vertical displacement of the Moriah Knoll basalt.